BAND STRUCTURE OF SILVER CHLORIDE AND SILVER BROMIDE BY THE

AUGMENTED PLANE WAVE METHOD

by

PETER MICHAEL SCOP

B. S., Massachusetts Institute of Technology
(1959)

SUBMITTED IN PARTIAL FULFILLMENT

OF THE REQUIREMENTS FOR THE

DEGREE OF DOCTOR OF

PHILOSOPHY

at the

MASSACHUSETTS INSTITUTE OF TECHNOLOGY

June 1964

Signature of Author. . . . .
[Signature redacted]
Department of Physics, May 15, 1964

Certified by. . . . .
[Signature redacted]
Thesis Supervisor

Accepted by. . . . .
[Signature redacted]
Chairman, Departmental Committee
on Graduate Students

Abstract

Title: Band Structure of Silver Chloride and Silver Bromide by the
Augmented Plane Wave Method.

Author: Peter Michael Scop

The energy of silver chloride and silver bromide crystals has
been calculated using the augmented plane wave method.

In this method one solves Schroedinger's equation for a
periodic one electron potential in the crystal. In the augmented
plane wave method, this potential is assumed to be ionic-like and
spherically symmetric within spheres surrounding the ions, and con-
stant in the region between spheres. Consequently, the wave function
is expanded in a sum of free-ion functions within spheres and plane
waves outside of the spheres. By varying the relative value of the
constant potential between spheres, the size of the direct band gap
at k = 0 has been fit to the experimental value.

After considering non-spherical cubic field effects within the
spheres and relativistic effects (including spin-orbit coupling), the
calculated magnitude of the indirect band gap is found to agree quite
well with experiment. The indirect band gap arises from electronic
transitions from the highest point in the valence band (the point L_3
at $k = \frac{\pi}{a}$ (1,1,1) for both crystals) to the lowest point in the con-
duction band at k = 0.

Selection rules for both direct and indirect transitions (with
and without spin) have been derived.

Thesis Supervisor: Professor John H. Wood
Title: Assistant Professor of Physics

Table of Contents

List of Figures and Tables

Acknowledgments

Chapter I

APW Calculations

I-1. Introduction.

The Augmented Plane Wave Method (henceforth abbreviated APW) was employed in calculating the electronic band structure of silver chloride and silver bromide crystals. This method was originally proposed by Slater[1] and later used by Wood[2] in his calculation of the band structure of iron. More recently, Switendick[3] has extended the method to deal with problems involving two atoms per unit cell in his band calculations of nickel oxide. This APW calculation of the band structure of silver chloride and silver bromide has been performed using the programs written by Wood and Switendick for the IBM 709 computer.

Briefly, the APW method takes advantage of the fact that the one-electron wave function is ionic-like near an ionic site and plane wave-like far from ionic sites. Consequently one inscribes spheres about each ion in the crystal; within each sphere we assume a spherically symmetric potential appropriate for the corresponding ion. In the region between spheres, we assume that the potential is equal to a constant, V_o. Corresponding to this choice of potential, the one electron wave function is expanded in APW's; that is, functions that are ionic-like inside the ionic spheres and plane wave-like outside of the spheres. Finally, the secular equation is obtained and, after taking advantage of the cubic symmetry, one obtains the eigenvalues.

Since the APW functions are constructed to correspond to the assumed potential, the convergence (the number of APW's needed to adequately represent a particular state) will be fairly rapid. However,

one must face some serious questions about the validity of the assumed potential.

The general form of this potential is sensible from physical reasoning, but the problem of choosing the various parameters entering into the calculations is a difficult one. Specifically, one must determine the sizes of the APW sphere radii and the constant value of the potential between spheres, V_0. In addition, the ionic potentials themselves usually depend on several parameters, especially the "ionicity" (the limit of $\frac{r}{2}$ times the ionic potential, for large r).

If one attempts to choose these parameters by physical reasoning, the results may be quite confusing. For example, in a real ionic crystal the previous simple definition of ionicity cannot even be applied since an electron never experiences a single ionic potential far from ionic sites. In addition, the concept of sphere radii may be misleading if there is any covalent bonding in the crystal.

In order to avoid these (and other) physical arguments, the present author has chosen the parameters in a rather arbitrary manner, and then varied one of them in order to obtain some agreement with experimental results.

I-2. Details of the calculations for AgBr and AgCl

AgBr and AgCl both have the NaCl structure; that is, two
displaced face centered cubic lattices. One lattice composed of
silver ions, the other containing the halogen ion.

In Figure I-1 we show the AgCl lattice. The silver ion is lo-
cated at the origin of coordinates. The six neighboring chlorine ions
are located at the points $\pm \frac{a}{2} (1,0,0)$, $\pm \frac{a}{2} (0,1,0)$, $\pm \frac{a}{2} (0,0,1)$. There are
twelve nearest neighbor silver ions located at $\pm \frac{a}{2} (1,1,0)$, $\pm \frac{a}{2} (1,-1,0)$,
$\pm \frac{a}{2} (0,1,1)$, $\pm \frac{a}{2} (0,1,-1)$, $\pm \frac{a}{2} (1,0,1)$, $\pm \frac{a}{2} (1,0,-1)$. All translations which
leave the lattice invariant are given by $T_n = n_1\vec{a_1} + n_2\vec{a_2} + n_3\vec{a_3}$
(n_1, n_2, n_3 are integers) where $\vec{a_1}$, $\vec{a_2}$, $\vec{a_3}$ are three primitive trans-
lations:

$$\vec{a_1} = \frac{a}{2} (0,1,1)$$

$$\vec{a_2} = \frac{a}{2} (1,0,1)$$

$$\vec{a_3} = \frac{a}{2} (1,1,0)$$

For AgCl $\frac{a}{2}$ = 5.23 atomic units.

AgBr $\frac{a}{2}$ = 5.463 atomic units.

The ionic potentials used are those determined by the
Hartree-Fock-Slater equations and calculated using programs described
by F. Herman and S. Skillman.[4] That is, for a particular ion,

Figure I-1

SILVER CHLORIDE LATTICE
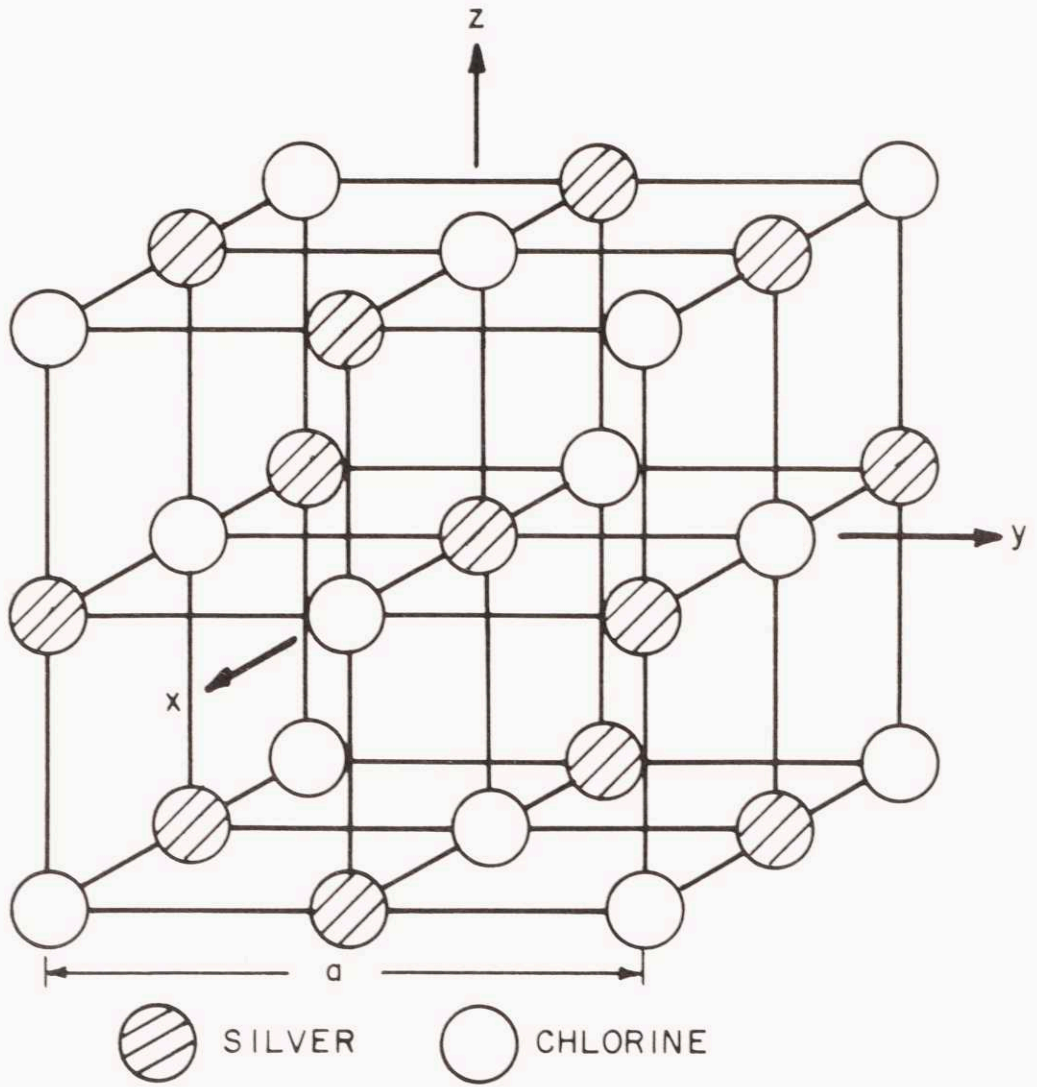
$$V(r) = \frac{-2Z}{r} - \frac{2}{r}\int_0^r \sigma(t)dt - 2\int_r^\infty \frac{\sigma(t)}{t}dt - 6\left[\frac{-3}{8\pi}\wp(r)\right]^{\frac{1}{3}}$$

where $\quad \wp(r) = \frac{\sigma(r)}{4\pi r^2}$, $\quad \sigma(r) = -\sum_{n,\ell} \omega_{n\ell}[P_{n\ell}(r)]^2$

$$\omega_{n\ell} = \text{occupation number for the orbital } (n,\ell)$$
$$= 2(2\ell+1) \text{ for a closed shell}$$

The total number of electrons is $N = \sum_{n,\ell}\omega_{n\ell}$, and the ionicity is $Z - N$.

The $P_{n\ell}$'s are normalized solutions of the radial Schroedinger equation:

$$\left\{\frac{-d^2}{dr^2} + \frac{\ell(\ell+1)}{r^2} + V(r)\right\}P_{n\ell}(r) = E_{n\ell}P_{n\ell}(r)$$

i.e. $\quad P_{n\ell}(r) = r R_{n\ell}(r)$

The ionicity parameters were chosen in accordance with the ordinary ideas of chemical valence (i.e. ionicity of Ag^+ = +1, ionicity of Cl^- = ionicity of Br^- = -1).

The potentials within each sphere are modified by adding (or subtracting) the Madelung potential $V_M = \pm\frac{2\alpha}{a/2} = \pm\frac{4\alpha}{a}$ where α is the Madelung constant for an NaCl structure (α = 1.747558) and "a" is the cube edge (see Figure I-1). That is:

about silver sites $\quad V(r) = (V_{\text{Herman-Skillman}})Ag^+ + V_M$

about halogen sites $\quad V(r) = (V_{\text{Herman-Skillman}})^{\text{halogen}} - V_M$

The choice of the sphere radii and the initial determination of V_O was made in the following way. First the Herman-Skillman ionic potentials for Ag^+ and Cl^- were superimposed and plotted in the (100) direction (Figure I-2-a). Then these potentials were corrected by adding or subtracting the Madelung potential. The point where the Madelung corrected potentials cross defines the sphere radii and the first determination of V_O (Figure I-2-b). This scheme has the desirable effect of insuring that $V(\vec{r})$ is continuous throughout the crystal. Finally we choose the zero of potential to be V_O on the APW scale. The net result of the Madelung correction and change of the zero of energy is that the Herman-Skillman potentials have been altered by different amounts called V_{SHIFT}.

$$\text{for } Ag^+ \qquad V_{SHIFT} = V_O + V_M$$

$$\text{for halogen} \qquad V_{SHIFT} = V_O - V_M$$

and our corrected potentials become:

$$Ag^+: \qquad V(r) = (V_{Herman-Skillman})_{Ag^+} + (V_{SHIFT})_{Ag^+}$$

$$\text{halogen}: \qquad V(r) = (V_{Herman-Skillman})_{halogen} + (V_{SHIFT})_{halogen}$$

This potential is shown in Figures I-2-c and I-2-d for the (100) and (110) directions.

Figure I-2

DETERMINATION OF V_O AND SPHERE RADII

UNCORRECTED POTENTIAL ALONG (100) DIRECTION
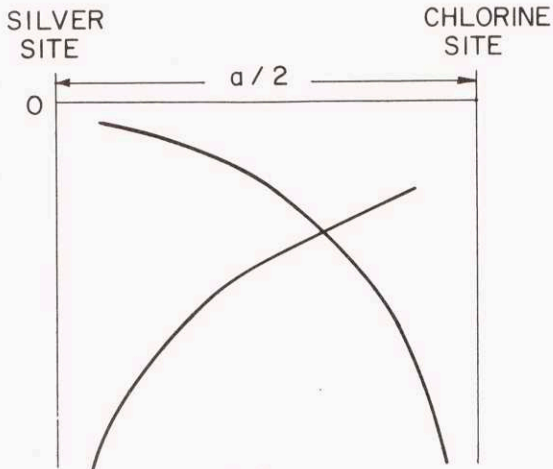
(a)

WITH MADELUNG CORRECTION (100) DIRECTION
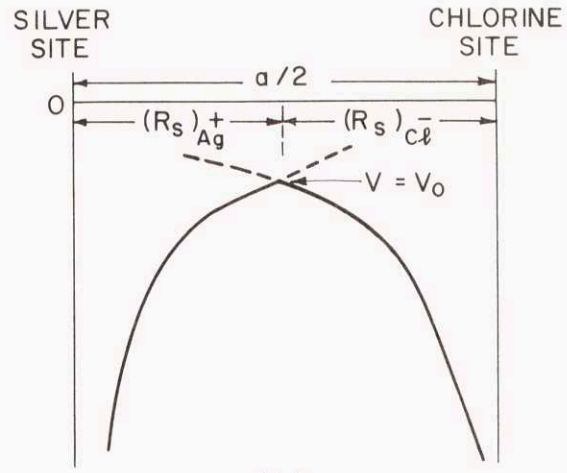
(b)

WITH MADELUNG CORRECTION AND SHIFT BY V_O, (100) DIRECTION
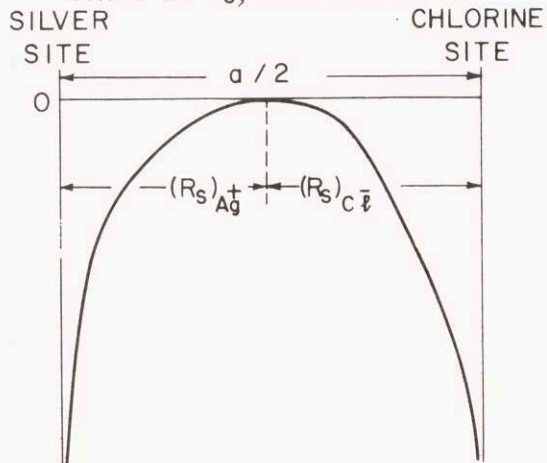
(c)

WITH MADELUNG CORRECTION AND SHIFT BY V_O, (110) DIRECTION
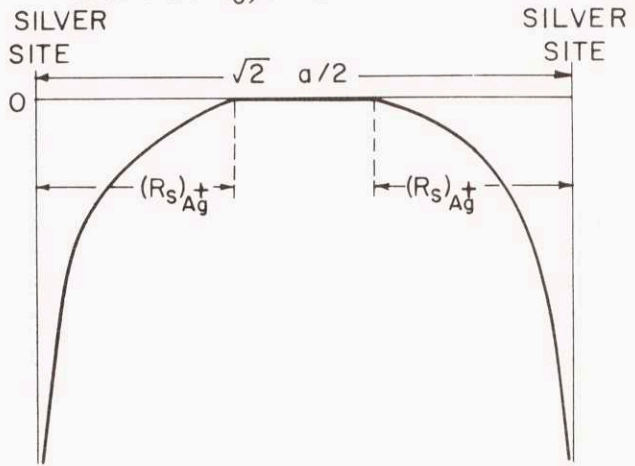
(d)

FINAL POTENTIAL WITH V_O ADJUSTED TO FIT Eg, (100) DIRECTION
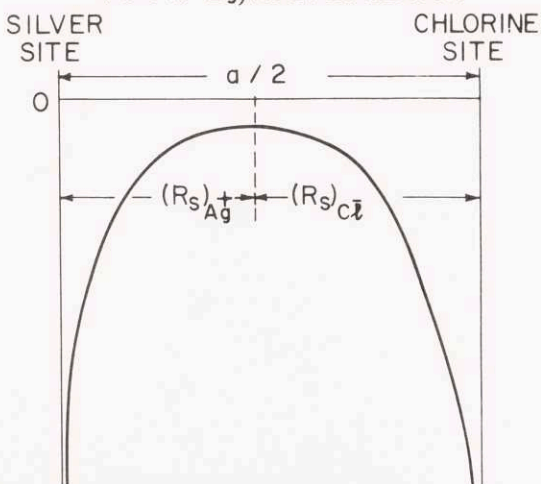
(e)

FINAL POTENTIAL WITH V_O ADJUSTED TO FIT Eg, (110) DIRECTION
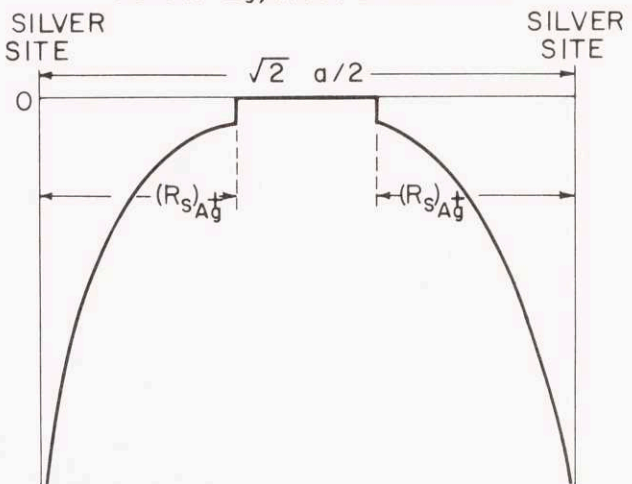
(f)

Unfortunately, when the above scheme is used in determining the sphere radii and V_O, the bands subsequently found do not agree with experimental facts. Specifically, the band gap at $\vec{k} = o$ is too small for both AgCl and AgBr. This discrepancy may be resolved by varying the magnitude of V_O until agreement with experiment is obtained. For both AgCl and AgBr the experimental band gap at $\vec{k} = o$, E_g, was duplicated when the magnitude of V_O was reduced. This final potential is shown in Figures I-2-e and I-2-f for the (100) and (110) directions, respectively.

There are two reasons why this corrected potential should be more representative of the actual crystalline potential than that shown in Figures I-2-c and I-2-d. Along the line joining the APW sphere centers (x, y, or z directions) the ionic potentials employed will have some value V at the sphere radii. However, in some other direction the actual crystalline potential just beyond either of the APW spheres will not be equal to V as in Figure I-2-d, but will have some larger value as in our corrected potential (Figure I-2-f). Also, the valence p and d states as well as the core electrons should be fairly insensitive to the value of the potential between spheres.

Although the size of the band gap at $\vec{k} = o$ depends in a critical way on the value of the potential between spheres, the relative spacing of core states is almost independent of V_O. In fact, changing V_O by as much as a few tenths of a Rydberg only changed the relative spacings of valence bands by less than .01 Rydbergs, and left their

qualitative features virtually unchanged.

The Brillouin zone for the FCC lattice is shown in Figure I-3, and the APW bands for AgCl and AgBr are shown in Figures I-4 and I-5 respectively. Values for the sphere radii, V_o, V_{SHIFT}, V_M, the ionic potentials as functions of r, the starting values of the wave functions, and the points in the Brillouin zone actually calculated for the bands in Figures I-4 and I-5 are given in Appendix One.

At this point it should be mentioned that because our basis functions are located on different sites on the unit cell, the symmetry properties of certain eigenstates of the Hamiltonian depend on which ion is located at the origin of coordinates. Switendick[5] has shown that within the Brillouin zone it makes no difference which ion is at the origin; but on the surface of the Brillouin zone, the representation matrices for the ion located at $\vec{R}_n = \frac{a}{2}(1,0,0)$ must be multiplied by the factor $e^{i(R\vec{K}_\ell - \vec{K}_\ell)\cdot\vec{R}_n}$ (here R is an operation of the group under consideration, and $\vec{K}_\ell$ is a vector of the reciprocal lattice). One finds that the symmetries at L, W, and Q are affected. The results are shown below in Table 1-1.

center A at origin	center B at $\frac{a}{2}$ (010)
L_1	L_2'
L_2	L_1'
L_3	L_3'
L_1'	L_2
L_2'	L_1
L_3'	L_3

Table I-1 (continued)

center A at origin	center B at $\frac{a}{2}(0,1,0)$
W_1	W_2'
W_2	W_1'
W_1'	W_2
W_2'	W_1
W_3	W_3
Q_+	Q_-
Q_-	Q_+

After solving the secular equations and obtaining eigenvalues, the eigenfunctions may also be determined. For points of major interest in the Brillouin zone, we have obtained the radial charge densities, $P^2_{n\ell}(r)$, within each APW sphere. The total amount of charge in each sphere associated with a given "ℓ" value, q_ℓ, and the amount of plane-wave charge (between spheres) has been calculated and is also tabulated in Appendix One. Here the total amounts of charge are normalized to unity; i.e.

$$\sum_{\ell=0}^{L_{max}=12} (q_\ell)_{Ag^+ \text{ sphere}} + \sum_{\ell=0}^{L_{max}=12} (q_\ell)_{\text{Halogen sphere}} + \text{plane wave charge} = 1$$

However, in Appendix One these quantities are tabulated for only the first three ℓ values ($\ell = 0$, $\ell = 1$, $\ell = 2$).

Since the group of the wave vector at $\vec{k} = 0$ (point group O_h) contains the inversion, the bands are parity eigenstates at Γ. By examining the charge within each APW sphere (Appendix One) the valence bands at this point are seen to arise predominately from either p or

Figure I-3

BRILLOUIN ZONE FOR FCC LATTICE
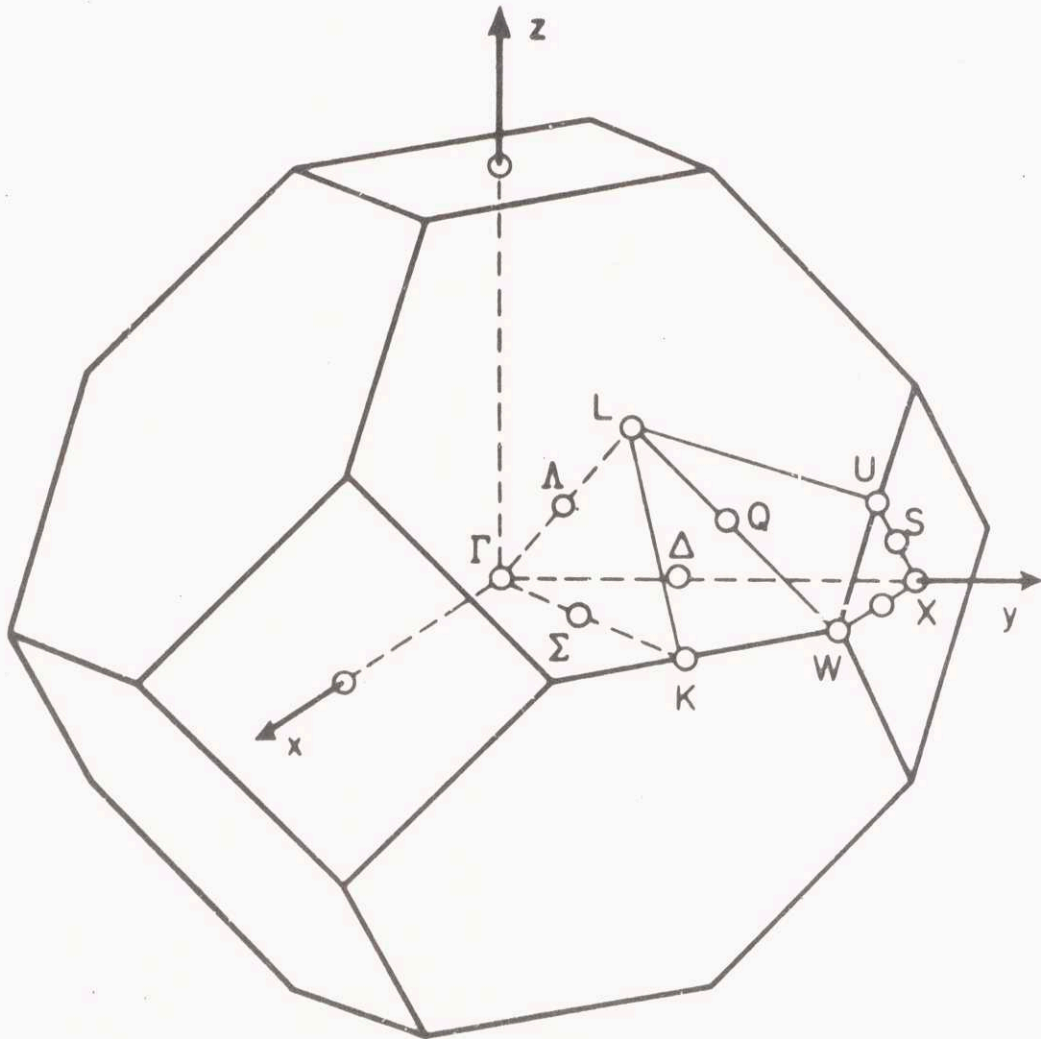
Figure I-4

BAND STRUCTURE OF SILVER CHLORIDE
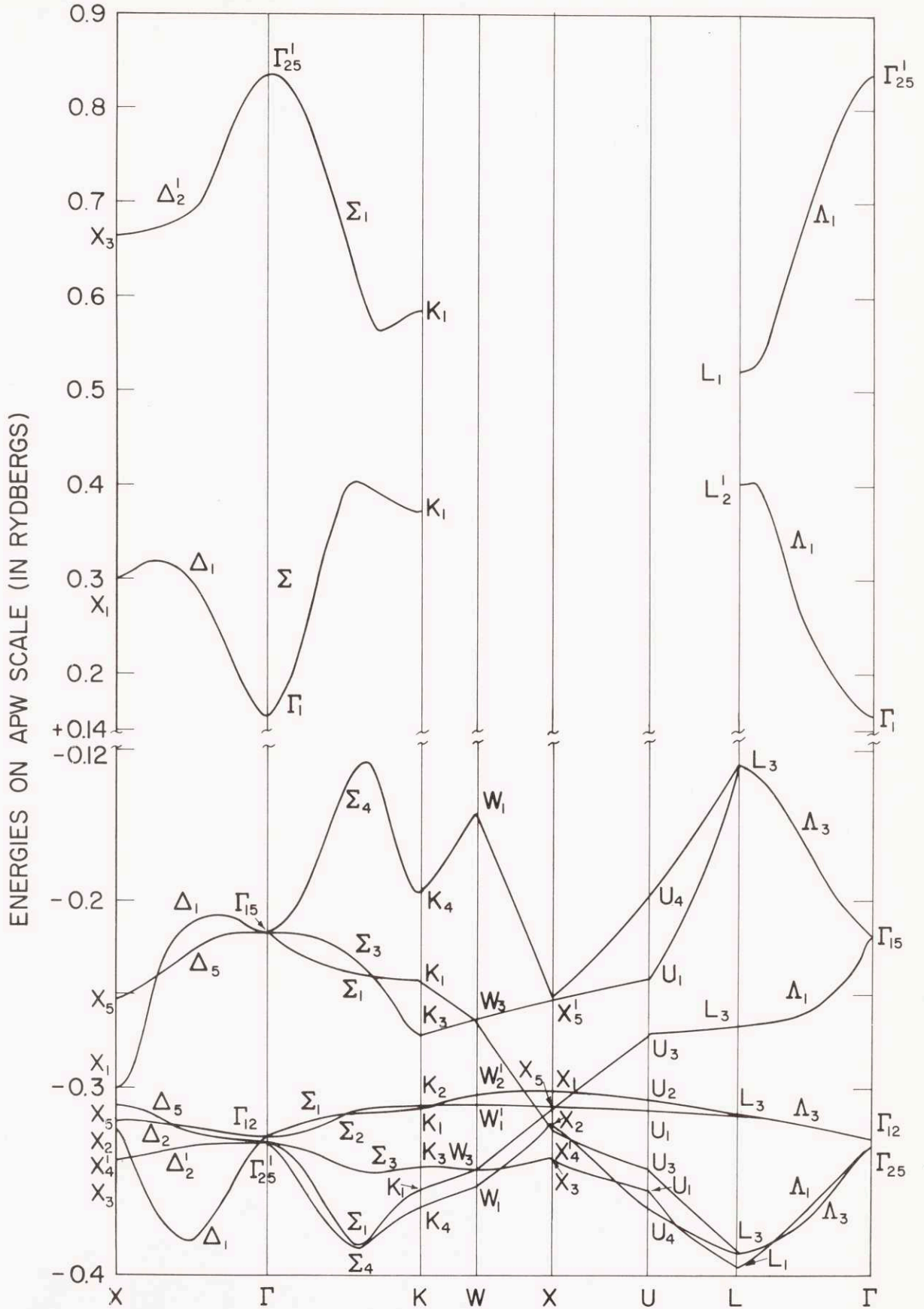
Figure I-5

BAND STRUCTURE OF SILVER BROMIDE
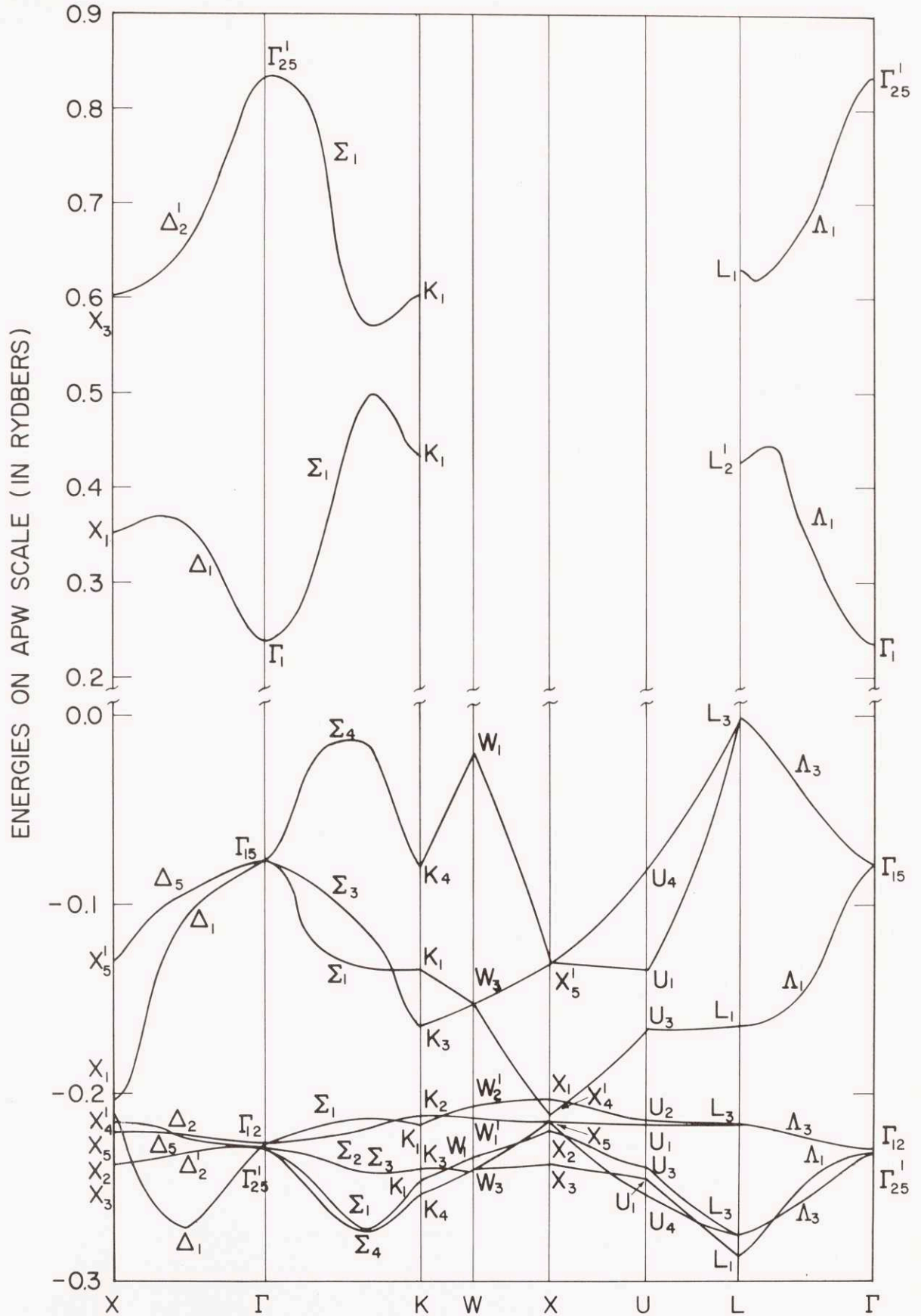
d functions with no mixing of p and d states. At Γ_{15} the eigenfunction is mostly $Cl^-(3p)$ or $Br^-(4p)$ with some $Ag^+(5p)$. The Γ_{12} and Γ_{25} states are almost entirely $Ag^+(4d)$.

As one departs from Γ along any of the three symmetry directions, the bands exhibit a strong p-d mixing.

In the (100) or Δ direction, the p-d mixing is zero at Γ, increases until $\vec{k} = \frac{\pi}{a} (1,0,0)$, and then decreases to zero at the point X (the point group at X is D_{4h} and includes the inversion operation). Along the (110) or Σ direction, the mixing is greatest at the point $\vec{k} = \frac{\pi}{a} (1,1,0)$. Because of transformation properties listed in Table 1-1, the $Ag^+(4d)$ function located at the origin and the $Cl^-(3p)$ (or $Br^-(4p)$) function located at $\frac{a}{2} (0,1,0)$ both have even parity at the point L. Consequently, this point is one of greatest p-d mixing along the (111) direction.

As one can see, a superficial understanding of the interactions away from Γ can be partially obtained from our APW calculation. However, because of the complexity of the details of an APW calculation it becomes increasingly more difficult to obtain additional information about these interactions. In order to better understand the nature of the bands, in Chapter II we illustrate a fitting procedure based on the use of tight binding wave functions. As we will see, the detailed nature of the various interactions involved become quite evident, even with a very crude fitting.

Before proceeding to Chapter II, we mention that when spin is

introduced in the Hamiltonian, direct optical transitions are allowed between all bands except at some points where the wave functions are parity eigenstates (Γ, X, and L); electric dipole transitions are allowed only between states of opposite parity. Also, indirect or phonon-assisted transitions from the uppermost valence bands to the conduction band are allowed. Details regarding both types of transition are given in Appendix Four.

Finally, we mention that the APW bands for AgCl and AgBr in figures I-4 and I-5 are approximately consistent with all experiments known to the author. A more detailed comparison of the bands and experimental results will be given in Chapter III.

Chapter II

Band Fitting by Tight Binding Method

II-1. Introduction

In this chapter we shall show how the APW bands calculated in
Chapter I may be described by analytic functions with a parametric fit
of the bands. This fitting technique has been described in detail by
Slater and Koster.[6] In this method we begin with orthogonalized, Bloch-
like, tight binding wave functions. The usual integrals of the Hamil-
tonian between Bloch functions are regarded as disposable constants
used to fit the bands. These constants appear as the integral between
functions on the same ionic site as well as first, second, and higher
nearest neighbors. Naturally one can fit the APW bands to any desired
accuracy if a complete set of basis functions is used and if one in-
cludes integrals involving functions on ions that are widely separated
in the crystal.

The philosophy of the interpolation scheme employed here will not
be that of obtaining an exact fit for all bands. But rather, we try
to obtain a reasonable fitting for the upper valence bands using a re-
stricted basis set (only functions of p and d symmetry), and including
only as many interactions (i.e. disposable parameters) as necessary
to approximate the APW bands. The value of fitting the bands in this
way is that one can understand the basic structure of the APW bands
without a great deal of numerical labor.

Since the bands for AgCl and AgBr have a very similar structure (see Figures I-4 and I-5), only the fitting of the AgCl bands will be described here. Fortunately, Slater and Koster have discussed the tight binding interpolation scheme extensively, and in the treatment of the AgCl fitting we will use the results of their work.

II-2. AgCl fit.

One starts with a set of normalized basis functions $\phi_1(\vec{r})$, ..., $\phi_n(\vec{r})$ that are orthogonal even when the functions are located on different centers in the crystal. That is, if the vectors $\vec{R}_\ell$ ($\vec{R}_\ell = \ell_1\hat{i} + \ell_2\hat{j} + \ell_3\hat{k}$) denote ionic sites in the crystal, then

$$\int \phi_i^*(\vec{r}-\vec{R}_\ell)\phi_j(\vec{r}-\vec{R}_{\ell'})\,dv = \delta_{ij}\delta_{\ell\ell'} \qquad (II-1)$$

From our functions ϕ_i, we construct normalized Bloch functions

$$\psi_{i,\vec{k}}(\vec{r}) = \frac{1}{\sqrt{N}}\sum_{\vec{R}_\ell} e^{i\vec{k}\cdot\vec{R}_\ell}\phi_i(\vec{r}-\vec{R}_\ell) \qquad (II-2)$$

(N = number of unit cells)

The wave function for an electron in the crystal is then written as

$$\Psi = \sum_{i=1}^{n} a_i\psi_i$$

and the n x n secular equation is obtained in the usual way. The

matrix elements are

$$H_{ij}(\vec{k}) = \sum_{\vec{R}_\ell} e^{i\vec{k}\cdot\vec{R}_\ell} E_{ij}(\ell_1,\ell_2,\ell_3) \tag{II-3}$$

where

$$E_{ij}(\ell_1,\ell_2,\ell_3) = \int \phi_i^*(\vec{r}) H \phi_j(\vec{r} - \ell_1\hat{i} - \ell_2\hat{j} - \ell_3\hat{k})dv \tag{II-4}$$

For AgCl (with the silver ion located at the origin) we have silver ions at

$$\vec{R}_S = \frac{a}{2}(s_1\hat{i} + s_2\hat{j} + s_3\hat{k}) \qquad s_1+s_2+s_3 = \text{even integer}$$

and chlorine ions at

$$\vec{R}_C = \frac{a}{2}(c_1\hat{i} + c_2\hat{j} + c_3\hat{k}) \qquad c_1+c_2+c_3 = \text{odd integer}$$

Our basis functions are

$$
\begin{aligned}
\phi_1 &= f(r)xy \\
\phi_2 &= f(r)xz \\
\phi_3 &= f(r)yz \\
\phi_4 &= f(r)\sqrt{3}(x^2-y^2) \\
\phi_5 &= f(r)(3z^2-r^2)
\end{aligned}
\qquad \text{five Ag}^+ \text{ 4d functions}
\tag{II-5}
$$

$$
\begin{aligned}
\phi_6 &= i\,g(r)\,x \\
\phi_7 &= i\,g(r)\,y \\
\phi_8 &= i\,g(r)\,z
\end{aligned}
\qquad \text{three Cl}^- \text{ 3p functions}
$$

and our Bloch functions ψ_i are

$$\psi_i = \begin{cases} \dfrac{1}{\sqrt{N}} \displaystyle\sum_{\vec{R}_s} e^{i\vec{k}\cdot\vec{R}_s} \, \phi_i(\vec{r} - \vec{R}_s) & i = 1,2,3,4,5 \\ \\ \dfrac{1}{\sqrt{N}} \displaystyle\sum_{\vec{R}_c} e^{i\vec{k}\cdot\vec{R}_c} \, \phi_i(\vec{r} - \vec{R}_c) & i = 6,7,8 \end{cases} \tag{II-6}$$

Thus our final matrix elements in equations II-3 and II-4 may be described as resulting from d-d interactions (both functions on silver sites), p-p interactions (both functions on chlorine sites), and p-d interactions (one function on a chlorine site, the other on a silver site).

Using the abbreviations $\xi = \dfrac{k_x a}{2}$, $\eta = \dfrac{k_y a}{2}$, $\zeta = \dfrac{k_z a}{2}$ the matrix elements (equation II-3) as derived by Slater and Koster are given in Table II-1.*

To start the fitting procedure, we begin with $\vec{k}$ in the (001) direction since many of the matrix elements in Table II-1 vanish when $\xi = \eta = 0$. In addition, we observe that many matrix elements are identical to each other, and we obtain the Hamiltonian matrix:

_____

* Slater and Koster do not list all the matrix elements since many are related by cyclical permutations of coordinates.

Table II-1

d-d

$H_{11} = E_{11}(000) + 4E_{11}(110)\cos\xi\cos\eta + 4E_{11}(011)\cos\zeta(\cos\xi + \cos\eta)$

$H_{22} = E_{11}(000) + 4E_{11}(110)\cos\xi\cos\zeta + 4E_{11}(011)\cos\eta(\cos\xi + \cos\zeta)$

$H_{33} = E_{11}(000) + 4E_{11}(110)\cos\eta\cos\zeta + 4E_{11}(011)\cos\xi(\cos\eta + \cos\zeta)$

$H_{44} = E_{55}(000) + 3E_{55}(110)\cos\zeta(\cos\xi + \cos\eta) + 4E_{44}(110)\left[\cos\xi\cos\eta + \frac{1}{4}\cos\xi\cos\zeta + \frac{1}{4}\cos\eta\cos\zeta\right]$

$H_{55} = E_{55}(000) + 4E_{55}(110)\left[\cos\xi\cos\eta + \frac{1}{4}\cos\xi\cos\zeta + \frac{1}{4}\cos\eta\cos\zeta\right] + 3E_{44}(110)(\cos\xi + \cos\eta)\cos\zeta$

$H_{12} = -4E_{12}(011)\sin\eta\sin\zeta$

$H_{13} = -4E_{12}(011)\sin\xi\sin\zeta$

$H_{14} = 0$

$H_{15} = -4E_{15}(110)\sin\xi\sin\eta$

$H_{23} = -4E_{12}(011)\sin\xi\sin\eta$

$H_{24} = 2\sqrt{3}E_{15}(110)\sin\xi\sin\zeta$

$H_{25} = 2E_{15}(110)\sin\xi\sin\zeta$

$H_{34} = -2\sqrt{3}E_{15}(110)\sin\eta\sin\zeta$

$H_{35} = 2E_{15}(110)\sin\eta\sin\zeta$

$H_{45} = \sqrt{3}E_{55}(110)\cos\zeta(\cos\xi - \cos\eta) - \sqrt{3}E_{44}(110)\cos\zeta(\cos\xi - \cos\eta)$

Table II-1 (continued)

p-d

$H_{61} = 2E_{61}(010)\sin\eta$ $H_{71} = 2E_{61}(010)\sin\xi$ $H_{81} = 0$

$H_{62} = 2E_{61}(010)\sin\zeta$ $H_{72} = 0$ $H_{82} = 2E_{61}(010)\sin\xi$

$H_{63} = 0$ $H_{73} = 2E_{61}(010)\sin\zeta$ $H_{83} = 2E_{61}(010)\sin\eta$

$H_{64} = \sqrt{3}\,E_{85}(001)\sin\xi$ $H_{74} = -\sqrt{3}\,E_{85}(001)\sin\eta$ $H_{84} = 0$

$H_{65} = -E_{85}(001)\sin\xi$ $H_{75} = -E_{85}(001)\sin\eta$ $H_{85} = 2E_{85}(001)\sin\zeta$

p-p

$H_{66} = E_{66}(000) + 4E_{66}(110)\cos\xi(\cos\eta + \cos\zeta) + 4E_{66}(011)\cos\eta\cos\zeta$

$H_{77} = E_{66}(000) + 4E_{66}(110)\cos\eta(\cos\xi + \cos\zeta) + 4E_{66}(011)\cos\xi\cos\zeta$

$H_{88} = E_{66}(000) + 4E_{66}(110)\cos\zeta(\cos\eta + \cos\xi) + 4E_{66}(011)\cos\eta\cos\xi$

$H_{67} = -4E_{67}(110)\sin\xi\sin\eta$

$H_{68} = -4E_{67}(110)\sin\xi\sin\zeta$

$H_{78} = -4E_{67}(110)\sin\eta\sin\zeta$

$$
H(00\zeta) = \begin{pmatrix}
H_{11} & 0 & 0 & 0 & 0 & 0 & 0 & 0 \\
0 & H_{22} & 0 & 0 & 0 & H_{62} & 0 & 0 \\
0 & 0 & H_{22} & 0 & 0 & 0 & H_{62} & 0 \\
0 & 0 & 0 & H_{44} & 0 & 0 & 0 & 0 \\
0 & 0 & 0 & 0 & H_{55} & 0 & 0 & H_{85} \\
0 & H_{62} & 0 & 0 & 0 & H_{66} & 0 & 0 \\
0 & 0 & H_{62} & 0 & 0 & 0 & H_{66} & 0 \\
0 & 0 & 0 & 0 & H_{85} & 0 & 0 & H_{88}
\end{pmatrix} \qquad (II\text{-}7)
$$

By comparing our basis functions $\phi_1, \ldots \phi_8$ with basis functions for the group of Δ (group C_{4v}) and observing that Δ_5 is a doubly degenerate state, we easily find the bands in the Δ direction are given by

Δ_2': energy, $\epsilon = H_{11}(00\zeta)$

Δ_2: $\epsilon = H_{44}(00\zeta)$

Δ_1: $\det \begin{pmatrix} H_{55}-\epsilon & H_{85} \\ H_{85} & H_{88}-\epsilon \end{pmatrix} = 0, \quad \epsilon = \dfrac{(H_{55}+H_{88})}{2} \pm \dfrac{H_{55}-H_{88}}{2}\sqrt{1 + \dfrac{4H_{88}^2}{(H_{55}-H_{88})^2}}$

Δ_5: $\det \begin{pmatrix} H_{22}-\epsilon & H_{62} \\ H_{62} & H_{66}-\epsilon \end{pmatrix} = 0,$ both roots occurring twice

$\epsilon = (\dfrac{H_{55}+H_{66}}{2}) \pm \dfrac{H_{22}-H_{66}}{2}\sqrt{1 + \dfrac{4H_{62}^2}{(H_{22}-H_{66})^2}}$

where $\quad H_{11}(00\zeta) = E_{11}(000) + 4E_{11}(110) + 8\,E_{11}(011)\cos\zeta$

$\quad H_{44}(00\zeta) = E_{55}(000) + 4E_{44}(110) + [6\,E_{55}(110) + 2E_{44}(110)]\cos\zeta$

$\quad H_{22}(00\zeta) = E_{11}(000) + 4E_{11}(110)\cos\zeta + 4E_{11}(011)(1 + \cos\zeta)$

$$H_{55}(00\zeta) = E_{55}(000) + 4E_{55}(110) \left[1 + \tfrac{1}{2}\cos\zeta\right] + 6E_{44}(110)\cos\zeta$$

$$H_{66}(00\zeta) = E_{66}(000) + 4E_{66}(110)\,(1 + \cos\zeta) + 4E_{66}(011)\cos\zeta$$

$$H_{88}(00\zeta) = E_{66}(000) + 8E_{66}(110)\ \cos\zeta \qquad + 4E_{66}(011)$$

$$H_{62}(00\zeta) = 2E_{62}(010)\sin\zeta$$

$$H_{85}(00\zeta) = 2E_{85}(001)\sin\zeta$$

The diagonal matrix elements are determined by fitting at Γ and
X (where the off-diagonal elements vanish). Thus we determine the
E_{ii}'s along the bands

$$
\begin{aligned}
\Gamma'_{25} &- \Delta_2 - X_3\\
\Gamma_{12} &- \Delta_2 - X_2\\
\Gamma_{15} &- \Delta_1 - X'_4\\
\Gamma'_{25} &- \Delta_1 - X_1\\
\Gamma_{15} &- \Delta_5 - X'_5\\
\Gamma'_{25} &- \Delta_5 - X_5
\end{aligned}
\qquad\qquad (\text{II-8})
$$

The fitting for Δ_2 and Δ'_2 turns out to be quite accurate. How-
ever, the fit for Δ_1 and Δ_5 at points between Γ and X is poor because
the p-d matrix elements are non zero. In fact, the Δ_1 bands are not
even fit properly at X; since without the p-d interaction we have bands
$\Gamma_{15} - \Delta_1 - X'_4$ and $\Gamma_{25} - \Delta_1 - X_1$ whereas the APW bands are $\Gamma_{15} - \Delta_1 - X_1$
and $\Gamma'_{25} - \Delta_1 - X'_4$.

To include the p-d interaction, we fit at the point $\vec{k} = \dfrac{\pi}{a}\,(001)$

(or $\zeta = \pi/2$) where the off diagonal elements H_{62} and H_{85} are largest.

However, because our bands in reality cannot be exactly described only

in terms of a p-d interaction, the values of the parameters $E_{61}(010)$ and

$E_{85}(001)$ will depend on which Δ_1 or Δ_5 band we fit. More precisely

to fit along $\Gamma'_{25} - \Delta_5 - X_5$ we obtain $E_{61}(010) = .0133765$; along

$\Gamma_{15} - \Delta_5 - X'_5$, $E_{61}(010) = .0149219$. Similarly along $\Gamma_{12} - \Delta_1 - X'_4$

and $\Gamma_{15} - \Delta_1 - X_1$ we obtain $E_{85}(001)$ equal to $.041647$ and $.0385722$

respectively. In Figures II-1 and II-2 we illustrate these fitted

bands with and without the p-d interaction. For an "overall fit"

the average values of $E_{61}(010)_{avg} = .014092$ and $E_{85}(001)_{average} =$

$.0401096$.

In the (110) or Σ direction ($\xi = \eta$, $\zeta = 0$) the Hamiltonian

matrix is:

$$H(\xi,\xi,0) = \begin{bmatrix} H_{11} & 0 & 0 & 0 & H_{15} & H_{61} & H_{61} & 0 \\ 0 & H_{22} & H_{23} & 0 & 0 & 0 & 0 & H_{61} \\ 0 & H_{23} & H_{22} & 0 & 0 & 0 & 0 & H_{61} \\ 0 & 0 & 0 & H_{44} & 0 & H_{65} & H_{65} & 0 \\ H_{15} & 0 & 0 & 0 & H_{55} & H_{65} & H_{65} & 0 \\ H_{61} & 0 & 0 & H_{65} & H_{65} & H_{66} & H_{67} & 0 \\ H_{61} & 0 & 0 & H_{65} & H_{65} & H_{67} & H_{66} & 0 \\ 0 & H_{61} & H_{61} & 0 & 0 & 0 & 0 & H_{88} \end{bmatrix} \quad (II-9)$$

By direct substitution, one may verify that eigenvectors of the

matrix II-9 are:

Figure II-1 TIGHT BINDING FIT OF THE BANDS $\Gamma_{15}-\Delta_5-X_5'$ AND $\Gamma_{25}'-\Delta_5-X_5$

Figure II-2 TIGHT BINDING FIT OF THE BANDS $\Gamma_{15}-\Delta_1-X_1$ AND $\Gamma_{12}-\Delta_1-X_4'$
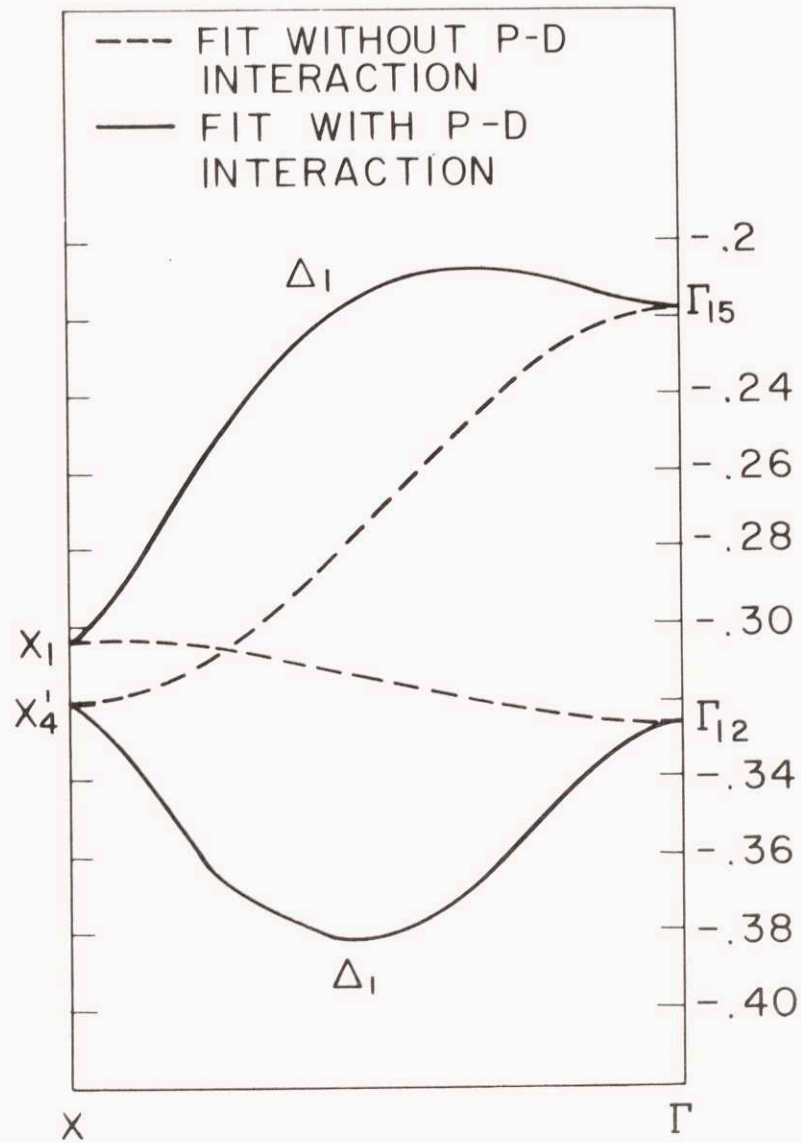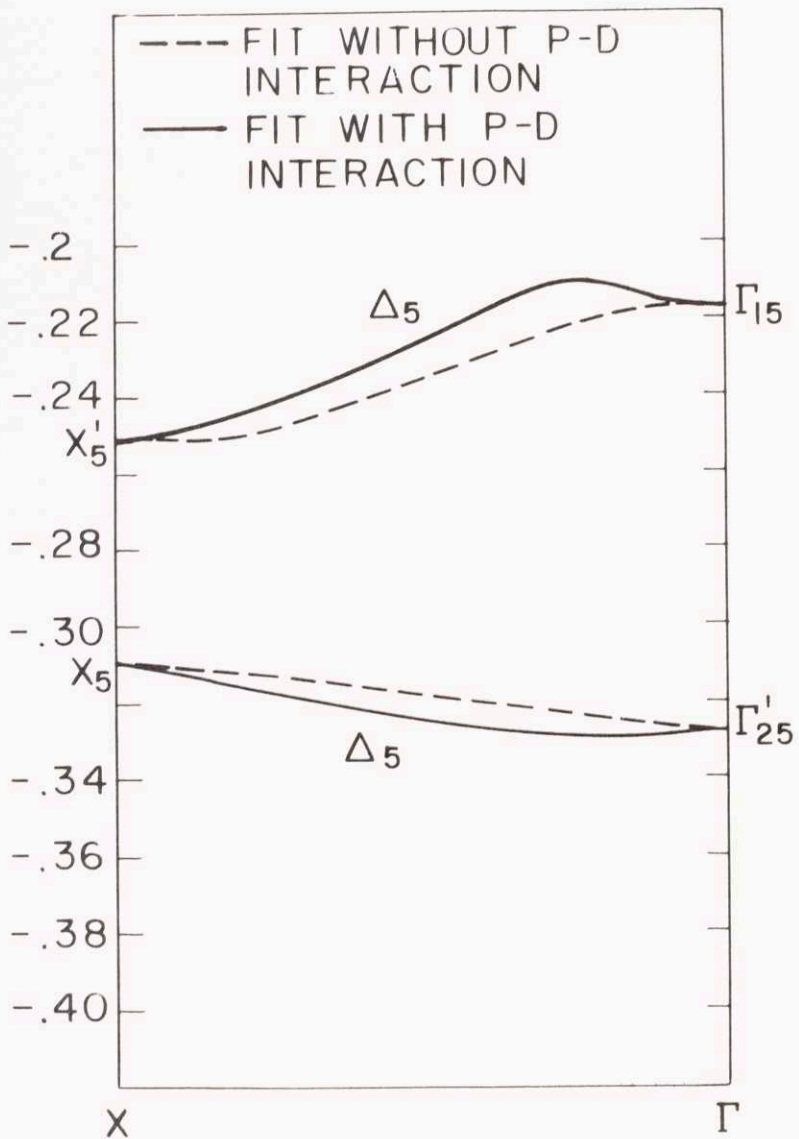
$$v_1 = \begin{bmatrix} v_{11} \\ 0 \\ 0 \\ 0 \\ v_{15} \\ v_{16} \\ v_{16} \\ 0 \end{bmatrix} \quad v_2 = \begin{bmatrix} 0 \\ v_{22} \\ -v_{22} \\ 0 \\ 0 \\ 0 \\ 0 \\ 0 \end{bmatrix} \quad v_3 = \begin{bmatrix} 0 \\ v_{32} \\ v_{32} \\ 0 \\ 0 \\ 0 \\ 0 \\ v_{38} \end{bmatrix} \quad v_4 = \begin{bmatrix} 0 \\ 0 \\ 0 \\ v_{44} \\ 0 \\ v_{46} \\ -v_{46} \\ 0 \end{bmatrix} \quad \text{(II-10)}$$

i.e. $Hv_i = \epsilon_i v_i$

Comparing these eigenvectors with basis functions for the group of Σ (group C_{3v}), we find that the eigenvector v_i corresponds to the irreducible representation Σ_i. Since there are three independent coefficients for vector v_1, we will have three distinct eigenvalues corresponding to symmetry Σ_1. Similarly, we have one Σ_2 band, two Σ_3 bands, and two Σ_4 bands arising from our $Cl^-(3p)$ and Ag^+ (4d) functions.

The corresponding secular equations are:

for Σ_1 bands:

$$\det \begin{bmatrix} H_{11}-\epsilon & H_{15} & 2H_{61} \\ H_{15} & H_{55}-\epsilon & 2H_{65} \\ 2H_{61} & 2H_{65} & 2(H_{66}+H_{77}-\epsilon) \end{bmatrix} = 0 \quad \text{(II-11-a)}$$

for Σ_2: $\epsilon = H_{22}-H_{23}$ (II-11-b)

for Σ_3:

$$\det \begin{bmatrix} 2(H_{22}+H_{23}-\epsilon) & 2H_{61} \\ 2H_{61} & H_{88}-\epsilon \end{bmatrix} = 0 \qquad (\text{II-11-c})$$

for Σ_4:

$$\det \begin{bmatrix} H_{44}-\epsilon & -2\sqrt{3}H_{65} \\ -2\sqrt{3}H_{65} & 2(H_{66}-H_{67}-\epsilon) \end{bmatrix} = 0 \qquad (\text{II-11-d})$$

In the Σ direction we again determine the off diagonal matrix elements where the p-d interaction is largest, i.e. at $\zeta = \pi/2$ or $k = \pi/a(1,1,0)$. The matrix element $H_{23} = -4E_{12}(011)$ can be found from a fit of the band $\Gamma'_{25} - \Sigma_2 - K_2$ (equation II-11-b) or by fitting either of the Σ_3 bands, $\Gamma_{15} - \Sigma_3 - K_3$ or $\Gamma'_{25} - \Sigma_3 - K_3$. However, we again encounter the same problems found in fitting the Δ direction; namely that the three Σ bands cannot all be fit with any single value of $E_{12}(011)$. For simplicity, we determine $E_{12}(011)$ along the $\Gamma'_{25} - \Sigma_2 - K_2$ band, and obtain $E_{12}(011) = .0009562$.

The matrix element $H_{67} = -4E_{67}(011)$ is determined by fitting either of the Σ_4 bands $\Gamma_{15} - \Sigma_4 - K_4$ or $\Gamma_{12} - \Sigma_4 - K_4$. Once more, a single value of $E_{67}(011)$ will not fit both bands. Since the Σ_4 band arising from Γ_{15} is the highest in the valence band (note: when relativistic effects and other perturbations are included, the L_3 state will lie slightly higher), we fit along $\Gamma_{15} - \Sigma_4 - K_4$ at the point $\vec{k} = \frac{\pi}{a}(1,1,0)$ or $\eta = \pi/2$. From equation II-11-d we obtain $E_{67}(011) = .0205815$.

In a similar manner we determine $H_{15} = -4E_{15}(110)$ from any one

of the three Σ_1 bands. As in our previous calculations, a fitting
along these three bands cannot be accomplished with any single value
of $E_{15}(110)$. The average value is $E_{15}(110)_{average} = .0109872$.

Our fitting in the Δ and Σ directions has determined all matrix
elements up to nearest neighbor interactions. To this extent we
have also determined the bands in the (111) direction. A summary of
the parameters is given in Table II-2, and in Table II-3 we compare
the APW and fitted valence bands for the Δ, Λ, and Σ directions.

Table II-2

Parameters for fitting APW bands

$$E_{11}(000) = -.320425$$

$$E_{11}(110) = -.00295625$$

$$E_{11}(011) = .000656250$$

$$E_{55}(000) = -.315162$$

$$E_{55}(110) = -.00003438$$

$$E_{44}(110) = -.00182188$$

$$E_{12}(011) = .0009562$$

$$E_{15}(110) = -.0109872$$

$$E_{66}(000) = -.2606$$

$$E_{66}(011) = -.002125$$

$$E_{66}(110) = .0063625$$

$$E_{67}(110) = .0205815$$

$$E_{61}(010) = .0140492$$

$$E_{85}(001) = .0401096$$

Table II-3

"p" bands

4k	symmetry	APW energy	Fitted energy
0,0,0	Γ_{15}	-.2182	-.2182
0,2,0	Δ_1	-.2091	-.2056
0,4,0	Δ_1	-.2116	-.2087
0,6,0	Δ_1	-.2466	-.2496
0,8,0	X_1	-.3042	-.3042
0,2,0	Δ_5	-.2192	-.2194
0,4,0	Δ_5	-.2255	-.2265
0,6,0	Δ_5	-.2422	-.2415
0,8,0	X_5'	-.2521	-.2521
2,2,0	Σ_1	-.2360	-.2509
4,4,0	Σ_1	-.2394	-.2667
6,6,0	K_1	-.2419	-.2634
2,2,0	Σ_3	-.2195	-.2214
4,4,0	Σ_3	-.2354	-.2415
6,6,0	K_3	-.2724	-.2788
2,2,0	Σ_4	-.1779	-.1641
4,4,0	Σ_4	-.1270	-.1270
6,6,0	Σ_4	-.1993	-.1826

Table II-3 (continued)

4k	symmetry	APW energy	Fitted energy
2,2,2	Λ_1	-.2591	-.2849
	Λ_3	-.1794	-.1665
4,4,4	L_1	-.2668	-.2759
	L_3	-.1281	-.1270

"d" bands

4k	symmetry	APW energy	Fitted energy
0,0,0,	Γ_{12}	-.3263	-.3263
0,2,0	Δ_1	-.3550	-.3505
0,4,0	Δ_1	-.3835	-.3757
0,6,0	Δ_1	-.3689	-.3630
0,8,0	X_4'	-.3200	-.3200
0,2,0	Δ_2	-.3250	-.3252
0,4,0	Δ_2	-.3224	-.3225
0,6,0	Δ_2	-.3198	-.3197
0,8,0	X_2	-.3186	-.3186
0,0,0	Γ_{25}'	-.3270	-.3270
0,2,0	Δ_2'	-.3283	-.3285
0,4,0	Δ_2'	-.3323	-.3323
0,6,0	Δ_2'	-.3361	-.3360
0,8,0	X_3	-.3375	-.3375

Table II-3 (continued)

4k	Symmetry	APW energy	Fitted energy
0,2,0	Δ_5	-.3271	-.3281
0,4,0	Δ_5	-.3257	-.3264
0,6,0	Δ_5	-.3159	-.3169
0,8,0	X_5	-.3086	-.3086
2,2,0	Σ_1	-.3484	-.3701
4,4,0	Σ_1	-.3835	-.4214
6,6,0	K_1	-.3543	-.3733
2,2,0	Σ_1	-.3182	-.3017
4,4,0	Σ_1	-.3119	-.2904
6,6,0	K_1	-.3133	-.3018
2,2,0	Σ_2	-.3234	-.3237
4,4,0	Σ_2	-.3116	-.3166
6,6,0	K_2	-.3105	-.3107
2,2,0	Σ_3	-.3343	-.3350
4,4,0	Σ_3	-.3452	-.3433
6,6,0	K_3	-.3406	-.3366
2,2,0	Σ_4	-.3611	-.3522
4,4,0	Σ_4	-.3847	-.3665
6,6,0	K_4	-.3623	-.3522

Table II-3 (continued)

4k	Symmetry	APW energy	Fitted energy
2,2,2	Λ_1	-.3519	-.3645
	Λ_3	-.3622	-.3731
	Λ_3	-.3185	-.3012
4,4,4	L_1	-.3946	-.4510
	L_3	-.3891	-.4072
	L_3	-.3137	-.2759

As Table II-3 indicates, our simplified fitting is not too bad quantitatively, especially for the higher valence bands. For this reason we may conclude that this higher band may be understood on the basis of a single p-d interaction. However, since the greatest discrepancies are found at the bottom of the "d" bands (especially along the $\Gamma_{12} - \Sigma_4 - K_4$ and $\Gamma_{12} - \Lambda_1 - L_1$ bands), we may safely conclude that a good fitting here would necessitate the use of additional core wave functions in the basis set.

Chapter III
Calculation of Perturbation Effects

III-1. Introduction.

In considering the effects of perturbations on our APW bands, we will be primarily concerned with the states Γ_{15} and L_3 at the top of the valence band. The reason for focusing our attention on these states is that two important experimentally obtained results are the magnitudes of the direct band gap at $\vec{k} = 0$, E_g, and the indirect band gap, E_{ig}. The value for E_g is given by the difference of the energies of the Γ_1 (conduction band) and Γ_{15} states. The indirect gap is the difference of the energies of the Γ_1 state and the highest valence band state, where ever that may be. The experimental values for these quantities are:[7,8]

	E_{ig}	E_g
AgCl	3.25 ev	5.13 ev
AgBr	2.68 ev	4.29 ev

There may be some question about whether or not these values correspond exactly to transitions between electronic bands or from an electronic valence band to an exciton band at Γ_1. However, for the purposes of the present discussion we need not be concerned with this detail. The important point is that the APW bands given in Chapter I were fit so that the APW value for E_g would agree with experiment. Unfortunately, even after fitting the APW bands to agree with E_g, the APW

values for E_{ig} are:

for AgCl E_{ig} = 3.84 ev.

for AgBr E_{ig} = 3.24 ev.

Thus, for both crystals the calculated value of the indirect band gap is too large by approximately .5 ev.

It turns out that after considering some of the deviations of the APW potential used from the actual crystalline potential, the discrepancy in E_{ig} can be resolved. But before discussing the various perturbations, we first return to the definitions of the two band gaps. In the early APW calculations the value of V_0 was set so that the difference of the Γ_1 and Γ_{15} states equalled E_g. Unfortunately, this straightforward definition will lead to confusion when we consider spin-orbit coupling which splits the Γ_{15} state, so we redefine E_g as follows:

E_g = energy difference of lowest conduction band and highest valence band at $\vec{k} = 0$.

Similarly,

E_{ig} = energy difference of lowest conduction band and highest valence band state.

Since the original APW bands were calculated on the basis of fitting E_g, we continue to let E_g be fit even after the perturbations have been applied. This can be done in effect by ignoring the conduction band entirely and studying the difference of the highest valence

band state and the highest valence band state at $\vec{k} = 0$. Let us call this difference Δ.

Thus for our APW calculations, the quantity $\Delta = E_g - E_{ig}$ is too small for both AgCl and AgBr.

The perturbations that we will study are the effect of the cubic field inside an APW sphere, and relativistic effects - the mass velocity shift and spin-orbit coupling.

Calculations will be made by first-order perturbation theory. Second order contributions are small (and will be neglected) because the states of interest are widely separated in energy from any states of like symmetry.

III-2. Cubic field perturbation.

Since the APW method assumes a spherically symmetric potential inside each sphere, any effects of the actual cubic field potential enter the APW calculation only through the constant potential in the region between spheres. Thus, the APW cubic field splittings are ne-cessarily smaller than the correct splittings; and in this section we will study the effect of the non-spherical cubic field inside spheres.

About an ionic site the cubic field may be written as

$$V(\vec{r}) = \pm \left\{ \frac{2\alpha}{a/2} + (3.58)\frac{2a_0}{a/2} \left(\frac{r}{a/2}\right)^4 \left(-\frac{3}{2} + \frac{5}{2} \frac{x^4+y^4+z^4}{r^4}\right) + \begin{array}{l} \text{terms involving} \\ \text{higher powers of } r \end{array} \right\}$$

where α = Madelung constant   for $r < a/2$

a_0 = Bohr radius

+ sign about silver sites

- sign about chlorine sites

(III-1)

The constant Madelung potential, $\frac{2\alpha}{a/2}$, has already been included in the APW calculation. We now consider the second and higher terms.

The cubic field will affect $\underline{d}$ functions(only through the second term in III-1) but leave p like functions unchanged. Therefore, the Γ_{15}' state (p like) will not be affected by the cubic field, but at the point L_3 (containing a large amount of $\underline{d}$ in the wave function) the cubic field will shift our APW bands. Thus, we must consider only the term $V' = (2)(3.58)(\frac{a_0}{a/2})(\frac{r}{a/2})^4(-\frac{3}{2} + \frac{5}{2}\frac{x^4+y^4+z^4}{r^4})$ and its effect on the $\underline{d}$ like portion of the wave function at Σ_4 and L_3.

For a given point $\vec{k}$ in the Brillouin zone we have $\underline{n}$ orthogonal functions $\phi_{\vec{k}}^{(1)}(\vec{r})$, ... $\phi_{\vec{k}}^{(n)}(\vec{r})$ (n = degeneracy of the band) which are eigenfunctions of the unperturbed APW Hamiltonian, H_O. These functions have the form

$$\phi_{\vec{k}}^{(i)}(\vec{r}) = \frac{1}{\sqrt{Q(\vec{k})}}\begin{cases} e^{i\vec{K}\cdot\vec{R}_c}\sum_{l=0}^{L_{max}}\sum_{m=-l}^{l} C_{lm}^{(i)}(\vec{k}) \frac{U_{lc}(r_c)}{U_{lc}(R_{sc})}Y_{lm}(\theta_i,\Phi_c) & \begin{matrix}\text{within}\\\text{chlorine}\\\text{spheres}\end{matrix} \\[3ex] e^{i\vec{k}\cdot\vec{R}_s}\sum_{l=0}^{L_{max}}\sum_{m=-l}^{l} S_{lm}^{(i)}(\vec{k}) \frac{U_{ls}(r_s)}{U_{ls}(R_{ss})}Y_{lm}(\theta_s,\phi_s) & \begin{matrix}\text{within}\\\text{silver}\\\text{spheres}\end{matrix} \\[3ex] \text{plane wave outside spheres} \end{cases}$$

(III-2)

where $\vec{R}_c$ = chlorine ionic site

$\vec{R}_s$ = silver ionic site

$\vec{r}_c = \vec{r} - \vec{R}_c$, $\vec{r}_s = \vec{r} - \vec{R}_s$, $r_c = |\vec{r}_c|$, $r_s = |\vec{r}_s|$

(θ_c, ϕ_c) are spherical angles about center $\vec{R}_c$

(θ_s, ϕ_s) are spherical angles about center $\vec{R}_s$

$C_{\ell m}^{(i)}(\vec{k})$ and $S_{\ell m}^{(i)}(\vec{k})$ are the coefficients of chlorine and silver respectively for the spherical harmonics in the ith function tabulated in Appendix Two.

$\dfrac{U_{\ell c}(r_c)}{r_c}$ = chlorine radial wave function for a given ℓ value

$\dfrac{U_{\ell c}(R_{sc})}{R_{sc}}$ = chlorine radial wave function for a given ℓ value evaluated at the chlorine sphere radius.

$\dfrac{U_{\ell s}(r_s)}{r_s}$ = silver radial wave function for a given ℓ value

$\dfrac{U_{\ell s}(R_{ss})}{R_{ss}}$ = silver radial wave function for a given ℓ value evaluated at the silver sphere radius

$Q(\vec{k})$ is a normalization constant and is independent of i.

We will also need the quantities

$$q_{\ell c}(\vec{k}) = \frac{1}{Q(\vec{k})} \sum_{m=-\ell}^{\ell} \left| C_{\ell m}^{(i)}(\vec{k}) \right|^2 \; \frac{\displaystyle\int_0^{R_{sc}} U_{\ell c}^2(r_c) dr_c}{U_{\ell c}^2(R_{sc})}$$

(III-3)

and

$$q_{\ell s}(\vec{k}) = \frac{1}{Q(\vec{k})} \sum_{m=-\ell}^{\ell} \left| S_{\ell m}^{(i)}(\vec{k}) \right|^2 \; \frac{\displaystyle\int_0^{R_{ss}} U_{\ell s}(r_s) dr_s}{U_{\ell s}^2(R_{ss})}$$

which are the amounts of charge (normalized to unity) associated with a particular ℓ value within the chlorine and silver spheres respectively. Note that the q_ℓ's are independent of $\underline{i}$.

The above notation is written for AgCl. For AgBr, simply replace the letter $\underline{C}$ by the letter $\underline{B}$ everywhere.

The first order energy shift due to the cubic field perturbation for the L_3 state is given by

$$\Delta E(\vec{k}) = \int_o^{R_s} \phi^{*(i)}_{\vec{k}}(\vec{r}_s) V'(\vec{r}_s) \phi^{(i)}_{\vec{k}}(\vec{r}_s) dv_s \qquad (III\text{-}4)$$

where we must integrate over the silver sphere, and the integral is independent of $\underline{i}$.

Let $\qquad V'(\vec{r}_s) = \eta(r_s) V(\theta_s, \phi_s) \qquad (III\text{-}5)$

where $\qquad \eta(r_s) = (3.58) \dfrac{2a_0}{a/2} \left(\dfrac{r_s}{a/2} \right)^4$

and $\qquad V(\theta_s, \phi_s) = 1-5[\sin^2\theta_s \cos^2\theta_s + \sin^4\theta_s \sin^2\phi_s \cos^2\phi_s]$

then after substituting equations III-2, III-3, and III-5 into III-4 we obtain

$$\Delta E(\vec{k}) = \frac{q_{2s}}{\sum\limits_{m=-2}^{2} |S_{2m}^{(1)}|^2} \left\{ \iint \left(\sum_{m=-2}^{2} S_{2m}^{*(1)}(\vec{k}) Y_{2m}^{*}(\theta_s,\phi_s) \right) V(\theta_s,\phi_s) \left(\sum_{m=-2}^{2} S_{2m}^{(1)}(\vec{k}) Y_{2m}(\theta_s,\phi_s) \right) d\Omega_s \quad X \right.$$

(III-6)

$$X \quad \frac{\int_0^{R_{ss}} U_{2s}^2(r) \eta(r_s) dr_s}{\int_0^{R_{ss}} U_{2s}^2(r_s) dr_s} \left. \right\}$$

and finally

$$\Delta E(\vec{k}) = q_{2s} \frac{\left[\frac{12}{21} (S_{22}^{(1)}(\vec{k}))^2 - \frac{16}{21} (R_e S_{21}^{(1)}(\vec{k}))^2 \right]}{\sum\limits_{m=-2}^{2} |S_{2m}^{(1)}(\vec{k})|^2} \quad X \quad 3.58 \frac{a_0}{a/2} \quad < \left(\frac{r_s^4}{a/2} \right)^4 >$$

(III-7)

here $\quad R_e S_{21}^{(1)}(\vec{k}) = $ Real part of $S_{21}^{(1)}(\vec{k})$

and $\quad < \left(\frac{r_s}{a/2} \right)^4 > = $ average value of $\left(\frac{r_s^4}{a/2} \right)^4$ within silver sphere

$$= \frac{\int_0^{R_{ss}} U_{2s}^2(r_s) \left(\frac{r_s}{a/2} \right)^4 dr_s}{\int_0^{R_{ss}} U_{2s}^2(r_s) dr_s}$$

After substituting the values of q_{2s} (given in Appendix One), the values of the S'_{2m}'s (given in Appendix Two), and performing the radial integrations we obtain the cubic field shifts given in Table III-1.

Table III-1

	AgCl	AgBr	
$\Delta E \quad = $	.00576	.00337	at L_3

Note that the additional cubic field within the APW spheres has the effect of raising the L_3 state, or, equivalently, increasing $\Delta = E_g - E_{ig}$. The effect is smaller in AgBr because the lattice constant is larger (i.e., the strength of the cubic field is smaller in AgBr).

III-3. Mass-velocity perturbation.

The mass-velocity perturbation may be approximated by a spherically symmetric operator about each site in the crystal. Since the electron's speed is largest for core states and smallest far from ionic sites, we ignore the mass-velocity effect for the plane waves between APW spheres, and restrict ourselves to calculating the first order correction to a given energy level by considering only the portion of the wave function within spheres.

Because the mass-velocity perturbation, V', is spherically symmetric about a given site, when the integral of V' between the APW functions (given in III-2) is calculated, all cross product terms of different ℓ and m values vanish (because of the orthogonality of the spherical harmonics) and one finally obtains

$$\Delta E_{\text{mass-vel.}}^{(\vec{k})} = \sum_{\ell=0}^{L\,\max\,=\,12} \left(q_{\ell c}(\vec{k}) v_{\ell c} + q_{\ell s}(\vec{k}) v_{\ell s} \right) \qquad (III\text{-}8)$$

where the ν's are the ionic mass-velocity parameters defined by

$$v_{\ell c} = \frac{\int_0^{R_{sc}} U_{\ell c}^2(r_c) V'(r_c) dr_c}{\int_0^{R_{ss}} U_{\ell c}^2(r_c) dr_c} \qquad (III-9)$$

$$v_{\ell s} = \frac{\int_0^{R_{ss}} U_{\ell s}^2 r_s V'(r_s) dr_s}{\int_0^{R_{ss}} U_{\ell s}^2(r_s) dr_s}$$

We must now determine the mass-velocity parameters given in equations III-9. For a first estimate we can use the free-ion parameter since the radial wave functions within APW spheres for the free ions and the crystal are substantially the same, especially near the nucleus where the mass-velocity effect is largest.

For the free ions, Herman and Skillman calculated the mass-velocity shift by first order perturbation theory, averaging the mass-velocity operator $V' = -\alpha^2(E - V)^2$ over the free-ion wave function. However, a more accurate calculation has been performed by Waber[9] who solved the Dirac equation for the energies of the two possible $\underline{j}$ values of a given electron. By taking the appropriate weighted average of Waber's two eigenvalues, one obtains the energy for an electron with all relativistic effects included with the exception of spin-orbit coupling.

In Table III-2 below we compare the Herman-Skillman and Waber calculations for $Cl^-(3p)$, $Br^-(4p)$, and $Ag^+(4d)$ ionic eigenvalues.

Table III-2

	H-S (non-relativistic)	H-S(including mass-vel.)	Waber(rel)	Waber - H-S (mass-vel.)
$Cl^-(3p)$	- .19094587	- .19794587	- .1906440	+.00030187
$Br^-(4p)$	- .18183391	- .21283391	- .1807204	+.00104187
$Ag^+(4d)$	-1.5682048	-1.6152048	-1.5082592	+.0599456

(Note: the Herman-Skillman mass-velocity energy was found by
interpolation from their tables which list only even
Z energies).

Waber's eigenvalues are higher than those of Herman-Skillman for
every case shown. This may be explained by the fact that the mass-
velocity operator in reality produces two effects for a valence
electron:

1. It lowers the eigenvalue because the mass-velocity operator
   is always negative.

2. It raises the eigenvalue because the core electrons are
   drawn closer to the nucleus, producing a stronger inner
   shielding of the nucleus.

The Herman-Skillman calculation ignores the second effect which, as Waber's
calculation indicates, is actually greater in magnitude than the
first.

It is interesting to note that Waber's eigenvalues are very

close to the Herman-Skillman non-relativistic energies. Therefore, in our perturbation calculation, we may approximate the mass-velocity parameter (to be substituted into equation III-8) by the difference of the Waber and Herman-Skillman (non-relativistic) levels given in column four of Table III-2. Thus,

$$
\begin{array}{lll}
\text{for} & \text{Cl}^-(3p) & \nu_{1C} = .00030 \\
& & \\
\text{for} & \text{Br}^-(4p) & \nu_{1B} = .00104 \\
& & \\
\text{for} & \text{Ag}^+(4d) & \nu_{2S} = .05995
\end{array}
\qquad (\text{III-10})
$$

After substituting the mass-velocity parameter (equation III-10) and the appropriate q_ℓ's into equation III-8, we obtain the shifts in the bands at Γ_{15} and L_3. The results are given in Table III-3.

Table III-3
Mass-velocity Shifts

	Γ_{15}	L_3
AgCl	.0002	.0399
AgBr	.0009	.0269

III-4. Spin-orbit coupling.

In this section we will calculate spin-orbit effects at our main points of interest, namely Γ_{15} and L_3 at the top of the valence band. Since the spin-orbit parameters for the mixture of ionic states that we are concerned with (i.e. $\text{Cl}^-(3p)$, $\text{Br}^-(4p)$, $\text{Ag}^+(4d)$ and $\text{Ag}^+(5p)$) all are very small compared to the crystal field splitting (at Γ_{15} and L_3), we may expect that a perturbation treatment of spin-orbit

coupling will be valid.

To compute spin-orbit energies, we must add spin to our original spin independent functions $(\phi_{\vec{k}}^{(1)}(\vec{r}), \ldots \phi_{\vec{k}}^{(n)}(\vec{r}))$ given in equation III-2.

Let $\quad \psi_{\vec{k}}^{(1)}(\vec{r}) = \phi_{\vec{k}}^{(1)}(\vec{r})\alpha, \ \psi_{\vec{k}}^{(2)}(\vec{r}) = \phi_{\vec{k}}^{(2)}(\vec{r})\alpha, \ \ldots, \psi_{\vec{k}}^{(n)}(\vec{r}) = \phi_{\vec{k}}^{(n)}(\vec{r})\alpha$

$$(III-11)$$

$$\psi_{\vec{k}}^{(n+1)}(\vec{r}) = \phi_{\vec{k}}^{(1)}(\vec{r})\beta, \ \ldots \qquad\qquad \psi_{\vec{k}}^{(2n)}(\vec{r}) = \phi_{\vec{k}}^{(n)}(\vec{r})\beta$$

(α and β are the usual spinors, i.e. $\alpha = \begin{pmatrix} 1 \\ 0 \end{pmatrix}$ $\beta = \begin{pmatrix} 0 \\ 1 \end{pmatrix}$)

These 2n functions form a basis for a <u>2n</u> dimensional representation of the double group at the point $\vec{k}$. In general, this <u>2n</u> dimensional representation will be reducible and may be decomposed into a sum of irreducible representations of the double group. In Appendix Four we give a brief discussion of the irreducible representations of the double group for the valence bands in AgCl and AgBr. A schematic drawing of these bands with spin included is shown in figure A4-1.

The spin-orbit operator is

$$H_{so} = \xi(r)\vec{l} \cdot \vec{\sigma} \qquad\qquad (III-12)$$

where $\quad \xi(r) = \dfrac{\alpha^2}{2} \dfrac{1}{r} \dfrac{dV}{dr}$

α = fine structure constant

and $\quad \vec{l} \cdot \vec{\sigma} = l_x\sigma_x + l_y\sigma_y + l_z\sigma_z$

$$= \begin{bmatrix} l_z & l_- \\ l_+ & -l_z \end{bmatrix}$$

(l_+ and l_- are the usual raising and lowering operators)

When we calculate matrix elements of the spin-orbit operator between our 2n functions $\psi_{\vec{k}}^{(i)}(\vec{r})$ (equation III-11) we first note that all diagonal elements vanish (i.e. $(H_{so})_{ii} = 0$). The reason for this is that the wave functions $\psi_{\vec{k}}^{(i)}(\vec{r})$ are simple products of a Bloch orbital function times a spinor. Consequently, the matrix element

$$(H_{so})_{ii} = \langle \psi_{\vec{k}}^{(i)}(\vec{r}) | H_{so} | \psi_{\vec{k}}^{(i)}(\vec{r}) \rangle$$

where

$$= \sum_{j=x,y,z} [\langle \phi_{\vec{k}}^{(i)}(\vec{r}) | \xi(r) l_j | \phi_{\vec{k}}^{(i)}(\vec{r}) \rangle \langle s_i | \sigma_j | s_i] \rangle \qquad s_i = \begin{cases} \alpha & i=1, \ n \\ \beta & i = n+1, \\ & 2n \end{cases}$$

is a sum of three terms, each of which factors into a product of the matrix element of a component of the orbital angular momentum between Bloch functions (modified only by a radial operator), and a matrix element of the same component of the spin angular mcmentum between spinors.

Since the crystal Hamiltonian is invariant under inversion, we have $\phi_{\vec{k}}^{*(i)}(\vec{r}) = \phi_{-\vec{k}}^{(i)}(\vec{r}) = \phi_{\vec{k}}^{(i)}(-\vec{r})$. Using the fact that $l_j = (-i\vec{r} \times \vec{\nabla})_j$, the matrix element is:

$$\langle \phi_{\vec{k}}^{(i)}(\vec{r}) | \xi(r) l_j | \phi_{\vec{k}}^{(i)}(\vec{r}) \rangle = \int \phi_{\vec{k}}^{*(i)}(\vec{r}) [\xi(r) l_j] \phi_{\vec{k}}^{(i)}(\vec{r}) dv$$

$$= \int \phi_{-\vec{k}}^{(i)}(\vec{r}) [\xi(r) l_j] \phi_{-\vec{k}}^{(i)*}(\vec{r}) dv$$

$$= \int \phi_{\vec{k}}^{(i)}(\vec{r}) [\xi(r) l_j] \phi_{\vec{k}}^{(i)*}(\vec{r}) dv$$

$$= - \int \phi_{\vec{k}}^{(i)}(\vec{r}) [\xi(r)l_j]^* \phi_{\vec{k}}^{(i)*}(\vec{r}) dv$$

$$= - < \phi_{\vec{k}}^{(i)}(\vec{r}) | \xi(r)l_j | \phi_{\vec{k}}^{(i)}(\vec{r}) >^*$$

But this matrix element must be real; hence it is zero.

The fact that the first order matrix elements vanish has important consequences as far as the spin-orbit bands are concerned. Specifically, a band that is non degenerate without spin will be shifted only in second order by an amount proportional to $\lambda^2/\Delta E$ where λ is of the order of the spin orbit parameters, and ΔE the difference in energy of a neighboring band of similar symmetry (under the double group). Thus for the Σ_4 band at the top of the valence band (labeled Σ_5 in the double group), the shift is of order $\lambda^2/\Delta E$ which is definitely negligible. Consequently, we must calculate only the splittings at Γ_{15} and L_3 since these states are degenerate without spin.

The non-diagonal matrix elements of the spin-orbit operator are: for $i \neq j$

$$(H_{so})_{ij} = < \psi_{\vec{k}}^{(i)}(\vec{r}) | H_{so} | \psi_{\vec{k}}^{(j)}(\vec{r}) >$$

$$= \sum_{n,\ell} \sum_{m=-\ell}^{\ell} \sum_{m'=-\ell}^{\ell} \frac{C_{\ell m}^{*(i)}(\vec{k}) C_{\ell m'}^{(j)}(\vec{k})}{|C_{\ell m}^{(i)}(\vec{k})|^2} q_{\ell c}(\vec{k}) \zeta_{n\ell}^{(c)} (\vec{\ell} \cdot \vec{\sigma})_{\ell m, \ell m'}^{ij}$$

(III-13)

$$+ \sum_{n,\ell} \sum_{m=-\ell}^{\ell} \sum_{m'=-\ell}^{\ell} \frac{S_{\ell m}^{*(i)}(\vec{k}) S_{\ell m'}^{(j)}(\vec{k})}{|S_{\ell m}^{(i)}(\vec{k})|^2} q_{\ell s}(\vec{k}) \zeta_{n\ell}^{(s)} (\vec{\ell} \cdot \vec{\sigma})_{\ell m, \ell m'}^{ij} \}$$

where $(\vec{\ell} \cdot \vec{\sigma})_{\ell m, \ell m'}^{ij} = < Y_{\ell m} s_i | \; \vec{\ell} \cdot \vec{\sigma} | Y_{\ell m} s_j >$

$$\zeta_{n\ell}^{(c)} = \frac{\frac{1}{2} \int_0^{R_{sc}} U_{\ell s}^2(r_s) \xi(r_c) dr_c}{\int_0^{R_{sc}} U_{\ell c}^2(r_c) dr_c}$$

$$\zeta_{n\ell}^{(s)} = \frac{\frac{1}{2} \int_0^{R_{ss}} U_{\ell s}^2(r_s) \xi(r_s) dr_s}{\int_0^{R_{ss}} U_{\ell s}^2(r_s) \xi(r_s) dr_s}$$

Note that the summation on n,ℓ in equation III-13 must be included if there is any appreciable mixing of core states in our valence band wave functions.

Splitting at Γ_{15}

As figure A4-1 indicates, the Γ_{15} state is split into a Γ_8^- (four fold degenerate) and a Γ_6^- (doubly degenerate) state, the Γ_8^- level lies highest. Since Γ_{15} is predominantly p-like (mostly $Cl^-(3p)$ or $Br^-(4p)$ with a small amount of $Ag^+(5p)$), the splitting resembles the free ion $j_{\frac{3}{2}} - j_{\frac{1}{2}}$ splitting in that the fourfold degenerate $j_{\frac{3}{2}}$ ionic level lies above the doubly degenerate $j_{\frac{1}{2}}$ ionic level.

The matrix elements (III-13) at Γ_{15} are:

$$
(H_{so})_{ij} = \left\{ \sum_{m=-1}^{1} \sum_{m'=-1}^{1} \left[\frac{C_{lm}^{*(i)} C_{lm'}^{(j)}}{\left| C_{lm}^{(i)} \right|^2} \, q_{1c} \, \zeta_{3P}^{(c)} \right]_{at \; \Gamma_{15}} (\vec{l} \cdot \vec{\sigma})_{lm,lm'}^{ij} \right.
$$

$$
\left. + \sum_{m=-1}^{1} \sum_{m'=-1}^{1} \left[\frac{S_{lm}^{*(j)} S_{lm'}^{(j)}}{\left| S_{lm}^{(i)} \right|^2} \, q_{1s} \, \zeta_{5P}^{(s)} \right]_{at \; \Gamma_{15}} (\vec{l} \cdot \vec{\sigma})_{lm,lm'}^{ij} \right\}
$$

After substituting the coefficients given in Appendix Two, we ob-
tain the spin-orbit matrix:

$$
H_{so} = \lambda
\begin{bmatrix}
0 & -i & 0 & 0 & 0 & 1 \\
i & 0 & 0 & 0 & 0 & -i \\
0 & 0 & 0 & -1 & i & 0 \\
0 & 0 & -1 & 0 & i & 0 \\
0 & 0 & -i & -i & 0 & 0 \\
1 & i & 0 & 0 & 0 & 0
\end{bmatrix}
\quad at \; \Gamma_{15}.
\qquad (III-14)
$$

where $\lambda = q_{1c} \zeta_{3p}^{(c)} + q_{1s} \zeta_{5p}^{(s)}$

By rearranging rows and columns, the secular determinant factors:

$$
\det \left| H_{so} - \epsilon 1 \right| =
\begin{bmatrix}
-\epsilon & -i\lambda & \lambda & 0 & 0 & 0 \\
i\lambda & -\epsilon & -i\lambda & 0 & 0 & 0 \\
\lambda & +i\lambda & -\epsilon & 0 & 0 & 0 \\
0 & 0 & 0 & -\epsilon & -i\lambda & \lambda \\
0 & 0 & 0 & i\lambda & -\epsilon & -i\lambda \\
0 & 0 & 0 & \lambda & i\lambda & -\epsilon
\end{bmatrix}
= 0
$$

with roots $\qquad \epsilon = \begin{cases} +\lambda & \text{occuring 4 times} \\ -2\lambda & \text{occuring 2 times} \end{cases}$ $\qquad$ (III-15)

We approximate the one electron spin-orbit parameters by their free ion values. Thus, substituting

Cl^- (3p): $\qquad \zeta_{3p}^{(c)} = .0030$

$\qquad\qquad\qquad\qquad\qquad\qquad$ from Waber's $\qquad$ (III-16)
$\qquad\qquad\qquad\qquad\qquad\qquad$ relativistic
Br^- (4p): $\qquad \zeta_{4p}^{(B)} = .0122$ $\qquad$ solutions

Ag^+ (5p): $\qquad \zeta_{5p}^{(s)} \simeq .0105$ $\qquad$ from Atomic Energy Levels.*

into III-15 we find that the Γ_{15} level is split into the two levels: $+\epsilon$, -2ϵ where

$$\epsilon = \begin{cases} .0027 & AgCl \\ .0110 & AgBr \end{cases} \qquad (III-16)$$

Splitting at L_3

The L_3 state will be split into a (doubly degenerate) L_6^+ state and singly degenerate L_4^+ and L_5^+ states, as shown in figure A4-1. The L_4^+ and L_5^+ states are degenerate with each other because of time reversal symmetry; therefore L_3 will be split into only two levels by the spin-orbit interaction.

The wave function at L_3 is composed mostly of Cl^-(3p) or Br^-(4p)

---

* Atomic Energy Levels, Vol. III, circular 467, U.S. Dept. of Commerce.

and $Ag^+(5d)$ ionic-like function. After using equation III-13 to determine the matrix elements, we obtain the spin-orbit matrix

$$H_{so} = \frac{\lambda}{\sqrt{3}} \begin{bmatrix} 0 & i & 0 & \sqrt{2}\omega \\ -i & 0 & -\sqrt{2}\omega & 0 \\ 0 & -\sqrt{2}\omega^* & 0 & -i \\ -\sqrt{2}\omega^* & 0 & i & 0 \end{bmatrix} \quad \text{at } L_3 \qquad (III-17)$$

where $\omega = e^{i\,\pi/4}$, and

$$\lambda = \begin{cases} q_{1C}\zeta_{3p}^{(c)} - (K)_{AgCl}\,q_{2s}\zeta_{4d}^{(s)} & \text{for AgCl} \\ q_{1B}\zeta_{4p}^{(B)} - (K)_{AgBr}\,q_{2s}\zeta_{4d}^{(s)} & \text{for AgBr} \end{cases} \qquad (III-18)$$

The constant K is defined by

$$K = \sqrt{3}\left\{ \frac{(S_{22}^{*(1)}S_{22}^{(2)} - S_{2-2}^{*(1)}S_{2-2}^{2}) + (S_{21}^{*(1)}S_{21}^{(2)} - S_{2-1}^{*(1)}S_{2-1}^{(2)})}{\sum_{m=-2}^{2}\left| S_{2m}^{(1)} \right|^{2}} \right\}_{\text{at } L_3} \qquad (III-19)$$

for either crystal. The eigenvalues of the spin-orbit matrix at L_3 are $\mathcal{E} = \pm\lambda$.

It is interesting to note that the form of the splitting at L_3 is quite different from that at Γ_{15}. First of all, at L_3 the individual contributions of the two ions are of opposite sign, which will tend to reduce the size of the actual band splittings. Secondly, the

angular dependence of the d portion of the wave function in the crystal will be distorted from that of the free ion by the cubic field. For this reason the constant K appears in equation III-18, and is then a measure of the cubic field strength in the crystal. Substituting the values of the $S_{2m}^{(i)}$ (given in Appendix Two) in equation III-19, we find that

$$(K)_{AgCl} = .67$$

$$(K)_{AgBr} = .83$$

$$(III-20)$$

which agrees with our previous reasoning, since the lattice spacing for AgBr is larger than that of AgCl (i.e., the cubic field strength is smaller).

Because our four spin-dependent functions transform as a basis for a reducible representation of the double group at L_3, the preceding analysis has only determined the energy splitting and gives no information about the symmetry labels of the split levels. In order to determine whether the L_6^+ or L_4^+ and L_5^+ levels is highest, we must apply projection operators to the eigenfunctions of the spin-orbit matrix (equation III-17).

Details about the use of projection operators in this case are given in Appendix Five. There it is shown that the vector

$$\Psi = \begin{pmatrix} 3/2 \\ b \\ -3/2\, \omega^* \\ b\omega^* \end{pmatrix} \qquad \text{where } b = \sqrt{\tfrac{3}{2}} - \sqrt{\tfrac{3}{2}}\, i \\ \omega = e^{i\,\pi/4}$$

$$(III-21)$$

is an eigenvector of the spin-orbit matrix (III-17) with symmetry L_4^+ and eigenvalue $\epsilon = + \lambda$. Consequently the L_5^+ state also has energy $\epsilon = + \lambda$ and the L_6^+ state is associated with the level $\epsilon = - \lambda$.

Using the free ion spin orbit parameters obtained from Waber's calculation (for $Ag^+(4d)$ $\zeta_{4d}^{(s)} = .00935$) we obtain

$$\epsilon = \begin{cases} -.0032 & AgCl \\ +.0029 & AgBr \end{cases}$$

or equivalently

<div align="center">

Table III-4

	L_4^+	L_5^+	L_6^+
AgCl	-.0032	-.0032	+.0032
AgBr	.0029	.0029	-.0029

</div>

Thus, in AgCl the L_6^+ state lies highest, in AgBr the L_4^+ and L_5^+ states are highest.

III-5. Summary of Perturbations and final Results.

The results of the three perturbations are summarized in tables III-5 and III-6 for AgCl and AgBr respectively.

<div align="center">

Table III-5 - AgCl

</div>

APW state	cubic field	mass vel.	spin orbit
Γ_{15}	0	.0002	Γ_8^-: .0027 Γ_6^-: -.0054
L_3	.0058	.0039	L_6^+: .0032 L_4^+, L_5^+: -.0032

Table III-6   AgBr

APW state	cubic field	mass-vel.	spin-orbit
Γ_{15}	0	.0009	Γ_8^-: .0110
			Γ_6^-: -.0220
L_3	.0033	.-269	L_4^+, L_5^+: .0029
			L_6^+: -.0029

By referring to Tables III-5 and III-6 we see that for both crystals the L_3 state (using single group notation) is the highest point in the valence band after all perturbations have been applied. Schematic drawings (not to scale) of the perturbation effects for the Γ_{15} and L_3 states are shown in figures III-1 and III-2 for AgCl and AgBr respectively.

As we mentioned previously, the quantity Δ will be used to compare our results with experiment. From Tables III-5 and III-6 we find:

	$(\Delta)_{APW}$	$(\Delta)_{APW}$ + perturbation	Δ experimental = $E_g - E_{ig}$
AgCl	1.220 ev	1.843 ev	1.880 ev.
AgBr	1.049 ev	1.336 ev	1.61 ev.

In other words, after fitting our bands gap, E_g to the

Figure III-1

Perturbation Effects in AgCl

$$\Delta = L_3 - \Gamma_{15}$$
$$= .0901$$

$$\Delta = L_6^+ - \Gamma_8^- = .1361$$
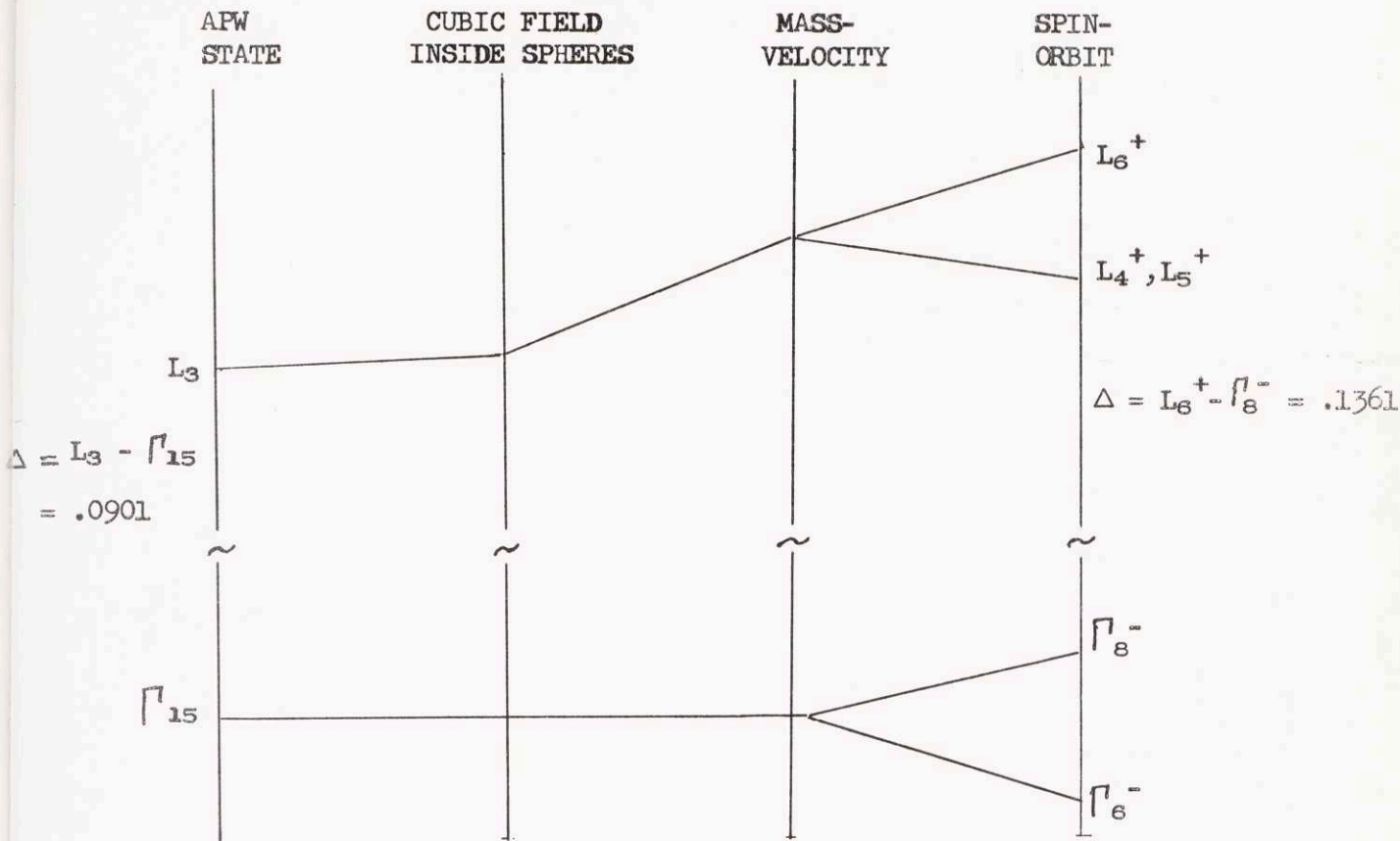
Figure III-2

Perturbation Effects in AgBr

$$\Delta = L_3 - \Gamma_{15}$$
$$= 0.775$$

$$\Delta = L_4^+ - \Gamma_{15} = .0987$$
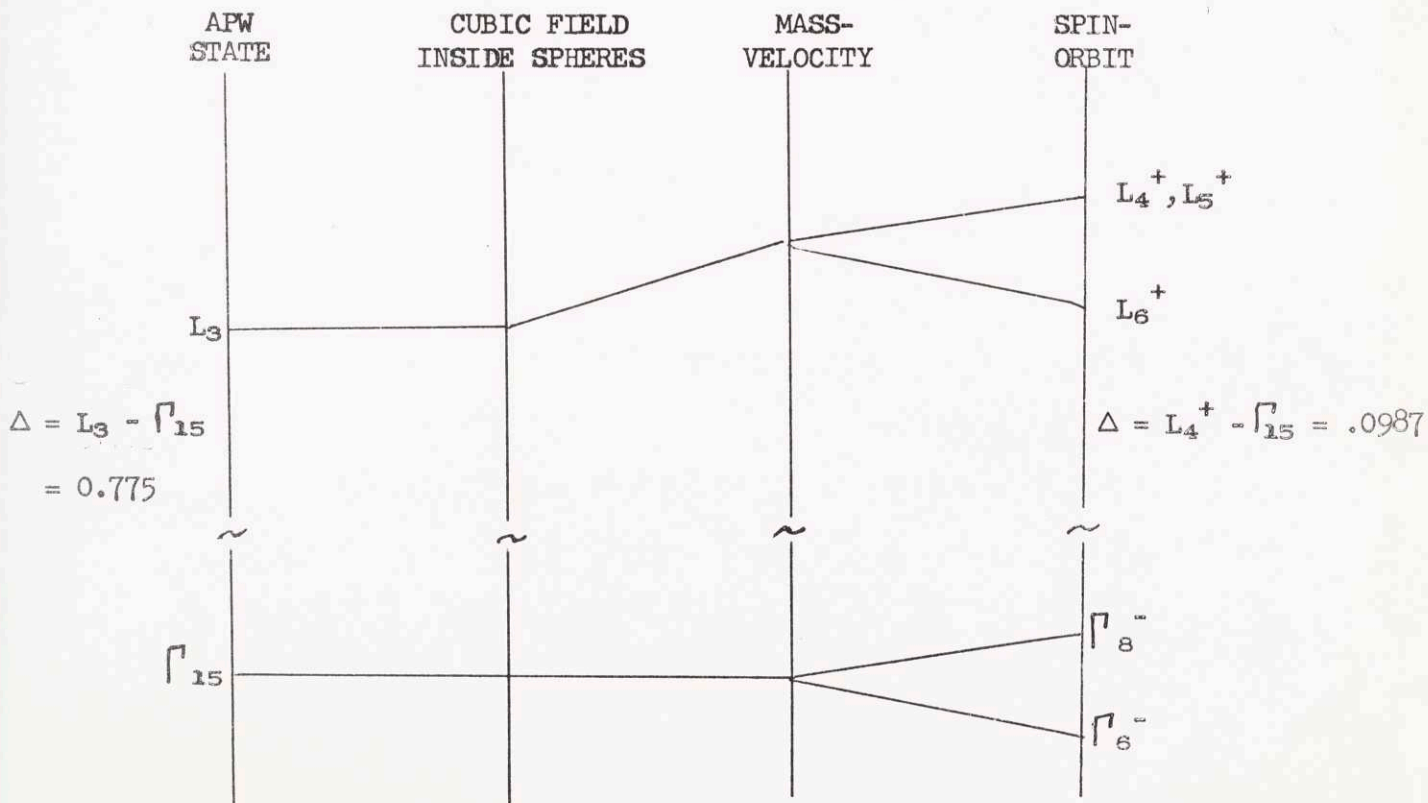
experimental values we obtain the indirect gap $E_{ig} = E_g - \Delta$, :

	$(E_{ig})_{calc.}$	$(E_{ig})_{experimental}$
AgCl	3.29 ev.	3.25 ev.
AgBr	2.95 ev.	2.68 ev.

At this point it should be mentioned that the values for E_{ig} given above are threshold energies found from optical absorption measurements and really do not correspond to transitions between electron states in the crystal, but transitions involving exciton formation. To determine E_{ig} for electronic transitions from the valence band to the conduction band one must take into account the binding energy of the exciton. However, not only is the binding energy of the exciton known only approximately, but, in addition, surface effects may further distort the exciton levels.[10] Thus, because we can only obtain crude approximations for the exciton binding energies, the true value of E_{ig} must be considered somewhat uncertain. A reasonable estimate of the exciton binding energy is a few tenths of an electron volt; consequently, the corrected sizes of the indirect band gaps are: $E_{ig} = 3.4$ ev in AgCl and $E_{ig} = 2.9$ ev. in AgBr.

We may conclude that the APW bands calculated after varying one parameter, V_0, certainly are in fairly good agreement with experimental facts. Moreover, even though the effects of some of the major perturbations have been calculated only approximately, at least the

correction terms tend to decrease the size of discrepancies between the APW calculation and experimental results. Because of the uncertainty in the true value of the indirect band gap, a precise comparison of the difference between the calculations and experiments is impossible, but the discrepancies are only of the order of one or two tenths of an electron volt (i.e. the error in the calculation of the indirect band gap is 5% of the size of the gap).

Appendix One - Numerical Details of APW Calculations

Cube edge, $a = 10.46$ atomic units

Madelung potential, $V_M = \pm \dfrac{2\alpha}{a/2} = \pm \dfrac{4\alpha}{a}$ where $\alpha = 1.747558$

$$V_M = \pm\ 0.668282217$$

sphere radii are $(Rs)_{Ag}^+ = 2.60$ a.u., $(Rs)_{C\ell}^- = 2.63$ a.u.

ionicities are: $Ag^\pm$: +1; C_ℓ^- : -1.

$Vo = -.579357$

TABLE A1-1

Numerical potential used to obtain energy bands for silver-chloride.

Potential used is tabular value - V_{Shift}, where $V_{Shift} = V_M - V_O$.

For chlorine $V_{Shift} = 1.088925$, for silver $V_{Shift} = 1.247639$.

r	Silver Potential	r	Chlorine Potential
.0012266	76221.36230	.0017216	19660.72876
.0024533	37901.89258	.0034432	9785.44580
.0036799	25127.27856	.0051648	6493.29266
.0049065	18739.46582	.0068864	4846.98915
.0061332	14906.69385	.0086080	3859.03900
.0073598	12351.62756	.0103296	3200.31854
.0085864	10526.80750	.0120512	2729.74609
.0098131	9158.50818	.0137728	2376.78986
.0110397	8094.61035	.0154944	2102.25638
.0122663	7243.84009	.0172160	1882.62376
.0134930	6548.09686	.0189376	1702.93207
.0147196	5968.63867	.0206591	1553.20404
.0159462	5478.63605	.0223807	1426.53362
.0171729	5058.93311	.0241023	1317.98093
.0183995	4695.46661	.0258239	1223.92776
.0196261	4377.69415	.0275455	1141.65770
.0208528	4097.54822	.0292671	1069.09547
.0220794	3848.75784	.0309887	1004.62495
.0233060	3626.36865	.0327103	946.97129
.0245327	3426.41632	.0344319	895.11147
.0269858	3081.58112	.0378751	805.61683
.0294392	2794.85745	.0413183	731.14745
.0318925	2552.82355	.0447615	668.23425

TABLE A1-1 (continued)

r	Silver Potential	r	Chlorine Potential
.0343457	2345.89508	.0482047	614.40343
.0367990	2167.04453	.0516479	567.83854
.0392523	2011.00258	.0550910	527.17647
.0417055	1873.73729	.0585342	491.37437
.0441588	1752.11154	.0619774	459.62084
.0466121	1643.64845	.0654206	431.27509
.0490653	1546.36067	.0688638	405.82449
.0515186	1458.63741	.0723070	382.85398
.0539719	1379.16191	.0757502	362.02409
.0564251	1306.84669	.0791934	343.05443
.0588784	1240.78227	.0826366	325.71142
.0613317	1180.20766	.0860798	309.79902
.0637849	1124.47839	.0895230	295.15143
.0662382	1073.04678	.0929661	281.62753
.0686916	1025.44504	.0964093	269.10643
.0711447	981.27003	.0998525	257.48383
.0735980	940.17476	.1032957	246.67001
.0785045	866.04665	.1101821	227.16421
.0834111	801.06423	.1170685	210.07030
.0883176	743.68162	.1239549	194.98497
.0932241	692.68025	.1308412	181.58945
.0981307	647.08877	.1377276	169.62877
.1030372	606.12086	.1446140	158.89489
.1079437	569.13486	.1515004	149.21728
.1128503	535.60062	.1583868	140.45524
.1177568	505.07705	.1652731	132.49141
.1226633	477.19402	.1721595	125.22519
.1275699	451.64007	.1790459	118.57200
.1324764	428.15045	.1859323	112.46151
.1373829	406.49860	.1928187	106.83187
.1422895	386.48938	.1997050	101.63052
.1471960	367.95464	.2065914	96.81260
.1521025	350.74837	.2134778	92.33908
.1570091	334.74313	.2203642	88.17616
.1619156	319.82697	.2272506	84.29381
.1668221	305.90114	.2341370	80.66610
.1717287	292.87850	.2410233	77.27049
.1815417	269.23887	.2548961	71.09732
.1913548	248.37656	.2685689	65.63782
.2011679	229.86310	.2823416	60.78361
.2109809	213.34915	.2961144	56.44670
.2207940	198.54753	.3098871	52.55494
.2306071	185.22248	.3236599	49.04890
.2404201	173.17849	.3374327	45.87858

TABLE A1-1 (continued)

r	Silver Potential	r	Chlorine Potential
.2502332	162.25272	.3512054	43.00202
.2600463	152.30886	.3649782	40.38354
.2698593	143.23164	.3787510	37.99268
.2796724	134.92279	.3925237	35.80338
.2894854	127.29818	.4062965	33.79306
.2992985	120.28530	.4200692	31.94224
.3091116	113.82079	.4338420	30.23386
.3189247	107.84921	.4476148	28.65329
.3287377	102.32167	.4613875	27.18762
.3385508	97.19559	.4751603	25.82556
.3483636	92.43244	.4889330	24.55715
.3581769	87.99859	.5027058	23.37371
.3679900	83.86405	.5164786	22.26756
.3876161	76.38983	.5440241	20.26105
.4072422	69.82642	.5715696	18.49180
.4268684	64.02853	.5991151	16.92400
.4464945	58.87959	.6266607	15.52915
.4661206	54.28586	.6542062	14.28434
.4857468	50.17156	.6817517	13.17073
.5053729	46.47497	.7092972	12.17265
.5249990	43.14483	.7368428	11.27655
.5445252	40.13803	.7643883	10.47059
.5642513	37.41732	.7919338	9.74412
.5838774	34.94994	.8194793	9.08754
.603506	32.70666	.8470249	8.49222
.623197	30.66144	.8745704	7.95046
.6427558	28.79105	.9021159	7.45551
.6623820	27.07522	.9296614	7.00155
.6820081	25.49625	.9572069	6.58357
.7016342	24.03903	.9847525	6.19735
.7212604	22.69058	1.0122980	5.83934
.7408865	21.43989	1.0398435	5.50651
.7605126	20.27743	1.0673890	5.19632
.7997649	18.18641	1.1224801	4.63556
.8390172	16.36429	1.1775711	4.14314
.8782694	14.77029	1.2326622	3.70856
.9175217	13.37152	1.2877532	3.32358
.9567739	12.14109	1.3428443	2.98155
.9960262	11.05633	1.3979353	2.67698
1.0352785	10.09807	1.4530264	2.40524
1.0745307	9.24980	1.5081174	2.16237
1.1137830	8.49735	1.5632085	1.94496
1.1530353	7.82847	1.6182995	1.75004
1.1922875	7.23257	1.6733906	1.57503

TABLE A1-1 (continued)

r	Silver Potential	r	Chlorine Potential
1.2315398	6.70046	1.7286816	1.41766
1.2707921	6.22421	1.7835726	1.27595
1.3100443	5.79693	1.8386637	1.14816
1.3492966	5.41267	1.8937547	1.03276
1.3885489	5.06624	1.9488458	0.92838
1.4278011	4.75313	2.0039368	0.83384
1.4670534	4.46946	2.0590279	0.74809
1.5063056	4.21182	2.1141189	0.67020
1.5455579	3.97723	2.1692100	0.59935
1.6240624	3.56758	2.2793921	0.47604
1.7025670	3.22318	2.3895742	0.37320
1.7810715	2.93102	2.4997562	0.28701
1.8595760	2.68105	2.6099384	0.21447
1.9380805	2.46545	2.7201204	0.15317
2.0165851	2.27804	2.8303025	0.10120
2.0950896	2.11428	2.9404846	0.05704
2.1735941	1.97005	3.0506667	0.01946
2.2520986	1.84213		
2.3306032	1.72804		
2.4091077	1.66037		
2.4876122	1.60797		
2.5661168	1.55878		
2.6446213	1.51250		
2.7231258	1.46890		
2.8016303	1.42774		
2.8801349	1.38882		
2.9586394	1.35197		
2.0371439	1.31702		

TABLE A1-2

Starting Values for Silver Potential

$R_1 = 0.00122663$ $R_2 = 0.00245325$

ℓ	$P_\ell(R_1)$	$P_\ell(R_2)$
0	0.108829744E-02	0.191204511E-02
1	0.141955070E-05	0.535101919E-05
2	0.177585952E-08	0.136673540E-07
3	0.219954081E-11	0.341918737E-10
4	0.271363884E-14	0.848564327E-13
5	0.334140100E-17	0.209769309E-15
6	0.410985142E-20	0.517412595E-18
7	0.505156033E-23	0.127448827E-20
8	0.620621569E-26	0.313646004E-23
9	0.762236707E-29	0.771380305E-26
10	0.935949534E-32	0.189626046E-28
11	0.114905238E-34	0.465991966E-31
12	0.141048819E-37	0.114483923E-33

Starting Values for Chlorine Potential

$R_1 = 0.00172158$ $R_2 = 0.00344319$

ℓ	$P_\ell(R_1)$	$P_\ell(R_2)$
0	0.162221357E-02	0.305117846E-02
1	0.287813716E-05	0.111776300E-04
2	0.500395164E-08	0.392577983E-07
3	0.865691431E-11	0.136499569E-09
4	0.149472073E-13	0.472736463E-12
5	0.257829472E-16	0.163401678E-14
6	0.444491304E-19	0.564171329E-17
7	0.766025417E-22	0.194654733E-19
8	0.131984435E-24	0.671303995E-22
9	0.227369450E-27	0.231437661E-24
10	0.391643129E-30	0.797714740E-27
11	0.674544670E-33	0.274906747E-29
12	0.116172016E-35	0.947250791E-32

TABLE A1-3

Silver Chloride Energy Band States and Charge Densities

Here we list the values of $\epsilon(\vec{k})$ calculated by the APW method ($\vec{k}$ is given in units of $\frac{\pi}{a}$). Also, for points of major interest in the valence band the "charge density" within each sphere and between spheres is given. This "charge density" within a given sphere is the total amount of charge in that sphere which can be associated with a particular ℓ value. The charge between spheres is labeled "plane wave". Finally, only the dominant contributions to the charge density are tabulated below even though the calculations were performed for $\ell = 0,\dots, 12$.

LOWEST CONDUCTION BAND

4k	Symmetry	APW Energy (in Rydbergs)
0,0,0	Γ_1	.1569
0,2,0	Δ_1	.2200
0,4,0	Δ_1	.3029
0,6,0	Δ_1	.3199
0,8,0	X_1	.3005
2,2,0	Σ_1	.2599
4,4,0	Σ_1	.4063
6,6,0	K_1	.3723
2,2,2	Λ_1	.2791
4,4,4	$L_2{}'$	.4088

TABLE A1-3 (continued)

SECOND LOWEST CONDUCTION BAND

4k	Symmetry	APW Energy (in Rydbergs)
0,0,0	Γ_{25}'	.8351
0,4,0	Δ_2'	.6871
0,8,0	X_3	.6625
6,6,0	K_1	.5864
4,4,4	L_1	.5202

TABLE A1-3 (continued)

"p" bands

4k	Symmetry	APW Energy	Plane Wave Charge	Charge In Chlorine Sphere	Charge In Silver Sphere
0,0,0	Γ_{15}	-.2182	.068	.897, $\ell = 1$	.023, $\ell = 1$
0,2,0	Δ_1	-.2091			
0,4,0	Δ_1	-.2116	.113	.019, $\ell = 0$ .482, $\ell = 1$ .003, $\ell = 2$	.048, $\ell = 0$ .003, $\ell = 1$ .328, $\ell = 2$
0,6,0	Δ_1	-.2466			
0,8,0	X_1	-.3042	.019	.024, $\ell = 1$ .001, $\ell = 2$	.953, $\ell = 2$
0,2,0	Δ_5	-.2192			
0,4,0	Δ_5	-.2255	.072	.818, $\ell = 1$	.018, $\ell = 1$ .085, $\ell = 2$
0,6,0	Δ_5	-.2422			
0,8,0	X_5'	-.2521	.110	.858, $\ell = 1$	.027, $\ell = 1$
2,2,0	Σ_1	-.2360			
4,4,0	Σ_1	-.2394	.088	.009, $\ell = 0$ .415, $\ell = 1$ .007, $\ell = 2$	.049, $\ell = 0$ .429, $\ell = 2$
6,6,0	K_1	-.2419	.085	.006, $\ell = 0$ .514, $\ell = 1$ .004, $\ell = 2$	.029, $\ell = 0$ .010, $\ell = 1$ .349, $\ell = 2$
2,2,0	Σ_3	-.2195			
4,4,0	Σ_3	-.2354	.075	.690, $\ell = 1$	.022, $\ell = 1$ .209, $\ell = 2$
6,6,0	K_3	-.2724	.086	.481, $\ell = 1$	.025, $\ell = 1$ .405, $\ell = 2$
2,2,0	Σ_4	-.1779			
4,4,0	Σ_4	-.1271	.027	.321, $\ell = 1$	.648, $\ell = 2$

TABLE A1-3 (continued)

$4k$	Symmetry	APW Energy	Plane Wave Charge	Charge In Chlorine Sphere	Charge In Silver Sphere
6,6,0	K_4	-.1993	.065	.671, $l=1$ .006, $l=2$	.015, $l=1$ .039, $l=2$
4,8,0	W_1	-.1547			
	W_3	-.2644			
2,2,2	Λ_1	-.2591			
	Λ_3	-.1794			
4,4,4	L_1	-.2668	.062	.334, $l=1$	.042, $l=0$ .560, $l=2$
	L_3	-.1281	.019	.314, $l=1$	.666, $l=2$
			d bands		
0,0,0	Γ_{12}	-.3263	.029	.019, $l=2$	.952, $l=2$
0,2,0	Δ_1	-.3550			
0,4,0	Δ_1	-.3835	.084	.336, $l=1$	.012, $l=0$ .002, $l=1$ .563, $l=2$
0,6,0	Δ_1	-.3689			
0,8,0	X_4'	-.3200	.186	.764, $l=1$	.049, $l=1$
0,2,0	Δ_2	-.3250			
0,4,0	Δ_2	-.3224	.025	.018, $l=2$	.956, $l=2$
0,6,0	Δ_2	-.3198			
0,8,0	X_2	-.3186	.002	.016, $l=2$	.960, $l=2$
0,0,0	Γ_{25}'	-.3270	.046	.007, $l=2$	.947, $l=2$
0,2,0	Δ_2'	-.3283			
0,4,0	Δ_2'	-.3323	.055	.008, $l=2$	.936, $l=2$
0,6,0	Δ_2'	-.3361			

TABLE Al-3 (continued)

4k	Symmetry	APW Energy	Plane Wave Charge	Charge In Chlorine Sphere	Charge In Silver Sphere
0,8,0	X_3	-.3375	.065	.010, $l = 2$	.925, $l = 2$
0,2,0	Δ_5	-.3271			
0,4,0	Δ_5	-.3257	.051	.090, $l = 1$ .002, $l = 2$	.002, $l = 1$ .853, $l = 2$
0,6,0	Δ_5	-.3159			
0,8,0	X_5	-.3086	.026		.973, $l = 2$
2,2,0	Σ_1	-.3484			
4,4,0	Σ_1	-.3835	.115	.367, $l = 1$	.027, $l = 0$ .488, $l = 2$
6,6,0	K_1	-.3543	.100	.279, $l = 0$	.011, $l = 0$ .006, $l = 1$ .596, $l = 2$
2,2,0	Σ_1	-.3182			
4,4,0	Σ_1	-.3119	.028	.003, $l = 0$ .001, $l = 1$ .003, $l = 2$	.962, $l = 2$
6,6,0	K_1	-.3133	.035	.034, $l = 1$	.915, $l = 2$
2,2,0	Σ_2	-.3234			
4,4,0	Σ_2	-.3116	.035	.002, $l = 2$	.961, $l = 2$
6,6,0	K_2	-.3105	.029		.970, $l = 2$
2,2,0	Σ_3	-.3343			
4,4,0	Σ_3	-.3452	.088	.192, $l = 1$ .003, $l = 2$	.008, $l = 1$ .708, $l = 2$
6,6,0	K_3	-.3406	.115	.337, $l = 1$	.020, $l = 1$ .526, $l = 2$
2,2,0	Σ_4	-.3611			
4,4,0	Σ_4	-.3847	.058	.258, $l = 1$	.653, $l = 2$

TABLE A1-3 (continued)

4k	Symmetry	APW Energy	Plane Wave Charge	Charge In Chlorine Sphere	Charge In Silver Sphere
6,6,0	K_4	-.3623	.055	.260, $\ell = 1$	.004, $\ell = 1$ .075, $\ell = 2$
4,8,0	W_1	-.3534			
	W_2'	-.3078			
	W_1'	-.3083			
	W_3	-.3427			
2,2,2	Λ_1	-.3519			
	Λ_3	-.3622			
	Λ_3	-.3185			
4,4,4	L_1	-.3946	.167	.412, $\ell = 1$	.047, $\ell = 0$ .372, $\ell = 2$
	L_3	-.3891	.063	.282, $\ell = 1$	.653, $\ell = 2$
	L_3	-.3137	.029	.002, $\ell = 1$	.967, $\ell = 2$

AgBr Calculation

Cube edge, $a = 10.926$ atomic units

Madelung potential, $V_M = \pm \dfrac{2\alpha}{a/2} = \pm \dfrac{4\alpha}{a} = \pm .654423576$

Sphere radii are: $(Rs)_{Ag}^{+} = 2.6105$ a.u.

$(Rs)_{Br}^{-} = 2.8525$

ionicities are: $Ag^{+} : +1$; $Br^{-} : -1$

$Vo = .69465$

TABLE A1-4

Numerical potential used to obtain energy bands for silver-bromide.

Potential used is tabular value $- V_{Shift}$, where $V_{Shift} = V_M - V_O$.

For bromine $V_{Shift} = .0402300$, for silver $V_{Shift} = 1.34907000$

r	Silver Potential	r	Bromine Potential
0.001226619	76221.2714844	0.001353279	51458.8803711
0.002453253	37901.7529297	0.002706580	25593.8713379
0.003679894	25127.2478027	0.004059874	16971.2055664
0.004906528	18739.4462891	0.005413160	12659.3913574
0.006133154	14906.6660156	0.006766446	10072.1009521
0.007359788	12351.5981445	0.008119840	8347.1942139
0.008586422	10526.7927246	0.009473041	7115.1671753
0.009813063	9158.4963379	0.010826327	6191.2527466
0.011039697	8094.5987549	0.012179621	5472.7929077
0.012266323	7243.8256226	0.013532907	4898.1845093
0.013492957	6548.0795288	0.014886208	4428.2191772
0.014719598	5968.6193848	0.016239487	4036.7518005
0.015946232	5478.6204834	0.017592788	3705.6761475
0.017172866	5058.9168091	0.018946074	3422.0620728
0.018399492	4695.4506836	0.020299368	3176.4215088
0.019626126	4377.6776733	0.021652654	2961.6369934
0.020852767	4097.5325317	0.023005955	2772.2655640
0.022079401	3848.7419739	0.024359249	2604.0711670
0.023306035	3626.3529358	0.025712535	2453.7120667
0.024532661	3426.4010315	0.027065821	2318.5105896
0.026985936	3081.5674438	0.029772416	2085.3107605
0.029439196	2794.8447266	0.032478996	1891.3712006

TABLE A1-4 (continued)

r	Silver Potential	r	Bromine Potential
0.031892464	2552.8117676	0.035185583	1727.6218262
0.034345739	2345.8832703	0.037892163	1587.5860748
0.036798999	2167.0331116	0.040598743	1466.5140076
0.039252259	2010.9913025	0.043305330	1360.8458099
0.041705534	1873.7269135	0.046011910	1267.8590851
0.044158794	1752.1028290	0.048718490	1185.4371948
0.046612062	1643.6396179	0.051425077	1111.9107056
0.049065337	1546.3517151	0.054131657	1045.9430542
0.051518597	1458.6299896	0.056838252	986.4518738
0.053971872	1379.1561584	0.059544832	932.5508575
0.056425132	1306.8414307	0.062251419	883.5079498
0.058878407	1240.7777557	0.064957999	838.7114868
0.061331667	1180.2032928	0.067665479	797.6473007
0.063784935	1124.4744720	0.070371166	759.8796921
0.066238210	1073.0437775	0.073077746	725.0369415
0.068691470	1025.4428406	0.075784326	692.8004532
0.071144730	981.2686539	0.078490913	662.8954239
0.073598005	940.1729889	0.081197943	635.0838013
0.078504533	866.0449371	0.086610660	584.9391479
0.083411068	801.0629425	0.092023835	540.9999084
0.088317603	743.6798782	0.097437002	502.2084160
0.093224138	692.6789466	0.102850169	467.7335472
0.098130681	647.0874100	0.108263329	436.9139366
0.103037201	606.1197433	0.113676496	409.2166367
0.107943736	569.1331253	0.119089663	384.2070427
0.112850279	535.5987701	0.124502838	361.5272636
0.117756814	505.0748444	0.129916005	340.8795433
0.122663349	477.1917229	0.135329165	322.0150108
0.127569877	451.6385078	0.140742339	304.7227592
0.132476412	428.1489754	0.146155499	288.8235130
0.137382947	406.4972382	0.151568659	274.1633911
0.142289475	386.4880676	0.156981841	260.6103592
0.147196017	367.9537277	0.162394993	248.0500317
0.152102545	350.7477188	0.167808175	236.3829498
0.157009087	334.7429733	0.173221335	225.5222321
0.161915623	319.8269997	0.178634502	215.3918247
0.166822158	305.9013290	0.184047677	205.9247189
0.171728693	292.8784409	0.189460844	197.0619106
0.181541756	269.2388268	0.200287171	180.9469128
0.191354819	248.3766289	0.211113505	166.6930752
0.201167889	229.8634224	0.221939839	154.0190144
0.210980959	213.3494549	0.232766174	142.6975994
0.220794030	198.5481701	0.243592501	132.5428543
0.230607100	185.2233200	0.254418835	123.4003258
0.240420163	173.1795063	0.265245177	115.1403875
0.250233233	162.2538338	0.276071511	107.6528263
0.260046303	152.3100491	0.286897846	100.8437424
0.269859366	143.2328358	0.297724180	94.6324692

TABLE A1-4 (continued)

r	Silver Potential	r	Bromine Potential
0.279672429	134.9241047	0.308550514	88.9495497
0.289485507	127.2996359	0.319376834	83.7352304
0.299298570	120.2867231	0.330203183	78.9379807
0.309111640	113.8220320	0.341029510	74.5134745
0.318924710	107.8502293	0.351855852	70.4234180
0.328737773	102.3225965	0.362832186	66.6346397
0.338550851	97.1962032	0.373508506	63.1182976
0.348363914	92.4329672	0.384334855	59.8491740
0.358176984	87.9991198	0.395161182	56.8051538
0.367990054	83.8645573	0.405987523	53.9666767
0.387616195	76.3902225	0.427640185	48.8390660
0.407242328	69.8267384	0.449292853	44.3482490
0.426868461	64.0288830	0.470945530	40.3987737
0.446494602	58.8800192	0.492598191	36.9121356
0.466120735	54.2864919	0.514250860	33.8230796
0.485745875	50.1724153	0.535903521	31.0768130
0.505373001	46.4760094	0.557556190	28.6270983
0.524999142	43.1460447	0.579208858	26.4346728
0.544625267	40.1387682	0.600861527	24.4661427
0.564251415	37.4172416	0.622514196	22.6929793
0.583877549	34.9495497	0.644166857	21.0908067
0.603503682	32.7063808	0.665819533	19.6387401
0.623129822	30.6612298	0.687472194	18.3188715
0.642755955	28.7909672	0.709124871	17.1158204
0.662382089	27.0751970	0.730777532	16.0163610
0.682008237	25.4962490	0.752430201	15.0090995
0.701634370	24.0390699	0.774082877	14.0841998
0.721260510	22.6906250	0.795735531	13.2331501
0.740886644	21.4399514	0.817388214	12.4486718
0.760512777	20.2775328	0.839040875	11.7240320
0.799765050	18.1863356	0.882346220	10.4336432
0.839017332	16.3641756	0.925651558	9.3240875
0.878269605	14.7701148	0.968956888	8.3652444
0.917521879	13.3713899	1.012262210	7.5340976
0.956774138	12.1409519	1.055567548	6.8105917
0.966026412	11.0562338	1.098872870	6.1780844
1.035278693	10.0980246	1.142178223	5.6221419
1.074530959	9.2498018	1.185483560	5.1309130
1.113783240	8.4973800	1.228788882	4.6944700
1.153035477	7.8285376	1.272094220	4.3045799
1.192287773	7.2327107	1.315399557	3.9545009
1.231540024	6.7006694	1.358704895	3.6387040
1.270792305	6.2244602	1.402010232	3.3526863
1.310044587	5.7972141	1.445315555	3.0927294
1.349296853	5.4129696	1.488620907	2.8556974
1.388549149	5.0665382	1.531926244	2.6390250

TABLE A1-4 (continued)

r	Silver Potential	r	Bromine Potential
1.427801400	4.7534295	1.575231582	2.4405118
1.467053682	4.4697595	1.618536904	2.2582954
1.506365963	4.2121184	1.661842242	2.0907371
1.545558214	3.9775616	1.705147594	1.9364346
1.624062777	3.5678524	1.791758269	1.6628587
1.702567324	3.2234192	1.878368914	1.4291870
1.781071872	2.9312140	1.964979589	1.2287914
1.859576404	2.6812400	2.051590264	1.0563051
1.938080952	2.4656413	2.138200939	0.9073308
2.016585499	2.2782515	2.224811614	0.7782427
2.095090032	2.1442354	2.311422259	0.6660390
2.173594564	1.9697405	2.398032933	0.5682079
2.252099127	1.8416888	2.484643608	0.4826654
2.330603629	1.7276102	2.571254253	0.4076546
2.409108192	1.6603654	2.657864958	0.3417047
2.487612754	1.6079673	2.744475633	0.2835761
2.566117257	1.5587752	2.831086248	0.2322267
2.644521849	1.5125036	2.917696983	0.1867669
2.723126352	1.4688998	3.004307598	0.1464482
2.801630914	1.4277398	3.090918303	0.1106344
2.880135506	1.3888235	3.177528977	0.0787765
2.958640009	1.3519725	3.264139622	0.0504112
3.037144601	1.3170265	3.350750357	0.0251396
3.115649104	1.2838416	3.437361002	0.0026110

TABLE A1-5

Starting Values for Silver Potential

R_1 = .001226619 $\qquad\qquad$ R_2 = .002453253

ℓ	$P_\ell(R_1)$	$P_\ell(R_2)$
0	0.11336545E-02	0.21398334E-02
1	0.13999555E-05	0.54440691E-05
2	0.16957746E-08	0.13312540E-07
3	0.20444263E-11	0.32246228E-10
4	0.24601492E-14	0.77817373E-13
5	0.29576492E-17	0.18744398E-15
6	0.35538675E-20	0.45103516E-18
7	0.42688610E-23	0.10845897E-20
8	0.51265719E-26	0.26069453E-23
9	0.61556672E-29	0.62642142E-26
10	0.73905125E-32	0.15048931E-28
11	0.88723274E-35	0.36147066E-31
12	0.10650562E-37	0.86813138E-34

Starting Values for Bromine Potential

R_1 = .001353279 $\qquad\qquad$ R_2 = .002706580

ℓ	$P_\ell(R_1)$	$P_\ell(R_2)$
0	0.12418757E-02	0.24539369E-02
1	0.16519856E-05	0.69535451E-05
2	0.21638519E-08	0.19069694E-07
3	0.28234833E-11	0.51886594E-10
4	0.36789075E-14	0.14073923E-12
5	0.47897289E-17	0.38115773E-15
6	0.62332861E-20	0.10313664E-17
7	0.81097445E-23	0.27892264E-20
8	0.10549212E-25	0.75404397E-23
9	0.13720781E-28	0.20379768E-25
10	0.17844255E-31	0.55070835E-28
11	0.23205376E-34	0.14879354E-30
12	0.30175614E-37	0.40197628E-33

TABLE A1-6

Silver Bromide Energy Band States and Charge Densities

Here we list the values of $\epsilon(\vec{k})$ calculated by the APW method ($\vec{k}$ is given in units of $\frac{\pi}{a}$). Also, for points of major interest in the valence band the "charge density" within each sphere and between spheres is given. This "charge density" within a given sphere is the total amount of charge in that sphere which can be associated with a particular ℓ value. The charge between spheres is labeled "plane wave". Finally, only the dominant contributions to the charge density are tabulated below even though the calculations were performed for $\ell = 0, \ldots, 12$.

LOWEST CONDUCTION BAND

4k	Symmetry	APW Energy (in Rydbergs)
0,0,0	Γ_1	.2396
0,2,0	Δ_1	.2961
0,4,0	Δ_1	.4000
0,6,0	Δ_1	.3708
0,8,0	X_1	.3552
2,2,0	Σ_1	.3380
4,4,0	Σ_1	.4984
6,6,0	K_1	.4323
2,2,2	Γ_1	.3799
4,4,4	L_2'	.4277

TABLE Al-6 (continued)

SECOND LOWEST CONDUCTION BAND

4k	Symmetry	APW Energy (in Rydbergs)
0,0,0	Γ_{25}'	.8366
0,2,0	Δ_2	.7486
0,4,0	Δ_2	.6663
0,6,0	Δ_2	.6179
0,8,0	X_3	.6020
2,2,0	Σ_1	.7507
4,4,0	Σ_1	.5699
6,6,0	K_1	.6044
4,4,4	L_1	.6300

TABLE A1-6 (continued)

"p" bands

4k	Symmetry	APW Energy	Plane Wave Charge	Charge In Bromine Sphere	Charge In Silver Sphere
0,0,0	Γ_{15}	-.0782	.077	.901, $l = 1$	.014, $l = 1$
0,2,0	Δ_1	-.0893			
0,4,0	Δ_1	-.0995	.153	.031, $l = 0$ .534, $l = 1$	.049, $l = 0$ .224, $l = 1$
0,6,0	Δ_1	-.1430			
0,8,0	X_1	-.2048	.019	.027, $l = 1$	.950, $l = 2$
0,2,0	Δ_5	-.0827			
0,4,0	Δ_5	-.0958	.093	.857, $l = 1$	.021, $l = 1$ .023, $l = 2$
0,6,0	Δ_5	-.1001			
0,8,0	X_5'	-.1247	.131	.834, $l = 1$	.031, $l = 1$
2,2,0	Σ_1	-.1198			
4,4,0	Σ_1	-.1362	.125	.012, $l = 1$ .442, $l = 2$	.058, $l = 1$ .351, $l = 2$
6,6,0	K_1	-.1345	.119	.558, $l = 1$	.038, $l = 0$ .011, $l = 1$ .259, $l = 2$
2,2,0	Σ_3	-.0881			
4,4,0	Σ_3	-.1180	.106	.726, $l = 1$ .001, $l = 2$	.028, $l = 1$ .135, $l = 2$
6,6,0	K_3	-.1652	.134	.544, $l = 1$	.033, $l = 1$ .287, $l = 2$
2,2,0	Σ_4	-.0250			
4,4,0	Σ_4	-.0184	.030	.397, $l = 1$	.571, $l = 2$
6,6,0	K_4	-.0779			
4,8,0	W_1	-.0182			

TABLE A1-6 (continued)

4k	Symmetry	APW Energy	Plane Wave Charge	Charge In Bromine Sphere	Charge In Silver Sphere
	W_3	-.1518			
2,2,2	Λ_1	-.1444			
	Λ_3	-.0500			
4,4,4	L_1	-.1644			
	L_3	-.0007	.043	.515, $\ell = 1$	.440, $\ell = 2$

d bands

4k	Symmetry	APW Energy	Plane Wave Charge	Charge In Bromine Sphere	Charge In Silver Sphere
0,0,0	Γ_{12}	-.2275			
0,2,0	Δ_1	-.2483			
0,4,0	Δ_1	-.2730	.087	.278, $\ell = 1$	.010, $\ell = 0$ .619, $\ell = 2$
0,6,0	Δ_1	-.2601			
0,8,0	X_4'	-.2105	.230	.719, $\ell = 1$	.051, $\ell = 1$
0,2,0	Δ_2	-.2263			
0,4,0	Δ_2	-.2240	.028	.020, $\ell = 2$	.952, $\ell = 2$
0,6,0	Δ_2	-.2216			
0,8,0	X_2	-.2206	.024	.027, $\ell = 1$	.950, $\ell = 2$
0,0,0	Γ_{25}'	-.2282	.050	.008, $\ell = 2$	.941, $\ell = 2$
0,2,0	Δ_2'	-.2294			
0,4,0	Δ_2'	-.2330	.061	.010, $\ell = 2$	.929, $\ell = 2$
0,6,0	Δ_2'	-.2364			
0,8,0	X_3	-.2378	.071	.012, $\ell = 2$	.917, $\ell = 2$
0,2,0	Δ_5	-.2277			
0,4,0	Δ_5	-.2254	.052	.050, $\ell = 1$	.001, $\ell = 1$ .892, $\ell = 2$

TABLE A1-6 (continued)

4k	Symmetry	APW Energy	Plane Wave Charge	Charge In Bromine Sphere	Charge In Silver Sphere
0,6,0	Δ_5	-.2177			
0,8,0	X_5	-.2119	.030		.968, $l = 2$
2,2,0	Σ_1	-.2196			
4,4,0	Σ_1	-.2140	.032		.958, $l = 2$
6,6,0	K_1	-.2154	.035	.011, $l = 0$ .032, $l = 2$	.915, $l = 2$
2,2,0	Σ_1	-.2430			
4,4,0	Σ_1	-.2731	.148	.355, $l = 1$	.032, $l = 0$ .458, $l = 2$
6,6,0	K_1	-.2468	.109	.223, $l = 1$	.008, $l = 0$ .005, $l = 1$ .645, $l = 2$
2,2,0	Σ_2	-.2249			
4,4,0	Σ_2	-.2190	.039	.002, $l = 2$	.956, $l = 2$
6,6,0	K_2	-.2135	.033		.965, $l = 2$
2,2,0	Σ_3	-.2335			
4,4,0	Σ_3	-.2421	.090	.132, $l = 1$ .004, $= 2$	.006, $l = 1$ .766, $l = 2$
6,6,0	K_3	-.2396	.121	.260, $l = 1$ .001, $l = 2$	.016, $l = 1$ .600, $l = 2$
2,2,0	Σ_4	-.2527			
4,4,0	Σ_4	-.2729			
6,6,0	K_4	-.2536			
4,8,0	W_1	-.2334			
	W_2'	-.2068			
	W_1'	-.2116			
	W_3	-.2405			

TABLE A1-6 (continued)

4k	Symmetry	APW Energy	Plane Wave Charge	Charge In Bromine Sphere	Charge In Silver Sphere
2,2,2	Λ_1	-.2468			
	Λ_3	-.2199			
	Λ_3	-.2513			
4,4,4	L_1	-.2872			
	L_3	-.2160	.033	.001, $\ell = 1$	.962, $\ell = 2$
	L_3	-.2761	.063	.226, $\ell = 1$	.708, $\ell = 2$

Appendix Two

Coefficients of the Spherical Harmonics for the Scalar APW Wave Functions

at Γ_{15}

AgCl

$S_{1-1}^{(1)} = iS$	$C_{1-1}^{(1)} = -iC$
$S_{10}^{(1)} = 0$	$C_{10}^{(1)} = 0$
$S_{11}^{(1)} = -iS$	$C_{11}^{(1)} = iC$

where
$S = .69156066$
$C = 1.5125040$

$S_{1-1}^{(2)} = -S$	$C_{1-1}^{(2)} = C$
$S_{10}^{(2)} = 0$	$C_{10}^{(2)} = 0$
$S_{11}^{(2)} = -S$	$C_{11}^{(2)} = C$

$S_{1-1}^{(3)} = 0$	$C_{1-1}^{(3)} = 0$
$S_{10}^{(3)} = i\sqrt{2}S$	$C_{10}^{(3)} = -i\sqrt{2}C$
$S_{11}^{(3)} = 0$	$C_{11}^{(3)} =$

AgBr

$S_{1-1}^{(1)} = iS$	$B_{1-1}^{(1)} = -iB$
$S_{10}^{(1)} = 0$	$B_{10}^{(1)} = 0$
$S_{11}^{(1)} = -iS$	$B_{11}^{(1)} = iB$

where
$S = 5.4092276$
$B = 13.520740$

$S_{1-1}^{(2)} = -S$	$B_{1-1}^{(2)} = B$
$S_{10}^{(2)} = 0$	$B_{10}^{(2)} = 0$
$S_{11}^{(2)} = -S$	$B_{11}^{(2)} = B$

$S_{1-1}^{(3)} = 0$	$B_{1-1}^{(3)} = 0$
$S_{10}^{(3)} = i\sqrt{2}S$	$B_{10}^{(3)} = i\sqrt{2}B$
$S_{11}^{(3)} = 0$	$B_{11}^{(3)} = 0$

at L_3

$$S_{2-2}^{(1)} = -\frac{15}{\sqrt{2}} S$$

$$S_{2-1}^{(1)} = (1-i)\, 3S$$

$$C_{1-1}^{(1)} = -(1 + i)\, \sqrt{3}C$$

AgCl $\quad S_{20}^{(1)} = 0$

$$C_{10}^{(1)} = 0$$

$$S_{21}^{(1)} = -(1 + i)\sqrt{3}S$$

$$C_{11}^{(1)} = (-1 + i)\sqrt{3}C$$

$$S_{22}^{(1)} = \frac{-15}{\sqrt{2}} S$$

where
$$S = .020969772$$
$$C = 1.0860413$$

$$S_{2-2}^{(2)} = -2iS$$

$$S_{2-1}^{(2)} = (1 + i)S$$

$$C_{1-1}^{(2)} = (-1 + i)\, C$$

$$S_{20}^{(2)} = -15S$$

$$C_{10}^{(2)} = -2\sqrt{2}C$$

$$S_{21}^{(2)} = (-1 + i)S$$

$$C_{11}^{(2)} = -(1 + i)C$$

$$S_{22}^{(2)} = 2\, iS$$

$$S_{2-2}^{(1)} = \frac{-12}{\sqrt{2}} S$$

$$S_{2-1}^{(1)} = (1-i)\sqrt{3}S$$

$$B_{1-1}^{(1)} = -(1 + i)\sqrt{3}B$$

AgBr $\quad S_{20}^{(1)} = 0$

$$B_{10}^{(1)} = 0$$

$$S_{21}^{(1)} = -(1 + i)$$

$$B_{11}^{(1)} = (-1 + i)\sqrt{3}B$$

$$S_{22}^{(1)} = \frac{-12}{\sqrt{2}} S$$

where
$$S = .046648408$$
$$B = 1.0447396$$

$$S_{2-2}^{(2)} = -2iS$$

$$S_{2-1}^{(2)} = (1 + i)S$$

$$S_{20}^{(2)} = -12S$$

$$S_{21}^{(2)} = (-1 + i)S$$

$$S_{22}^{(2)} = 2iS$$

$$B_{1-1}^{(2)} = (-1 + i)B$$

$$B_{10}^{(2)} = -2\sqrt{2}B$$

$$B_{11}^{(2)} = -(1 + i)B$$

Appendix Three - Operations of the Cubic Group, O_h.

The operations of the cubic group listed here are those defined by

Slater in "Quantum Theory of Molecules and Solids, Volume One".

$R_1 \; \psi(x,y,z) = \psi(x,y,z)$

$R_2 \; \psi(x,y,z) = \psi(x,-y,-z)$

$R_3 \; \psi(x,y,z) = \psi(-x,y,z)$

$R_4 \; \psi(x,y,z) = \psi(-x,-y,z)$

$R_5 \; \psi(x,y,z) = \psi(y,z,x)$

$R_6 \; \psi(x,y,z) = \psi(-y,z,-x)$

$R_7 \; \psi(x,y,z) = \psi(-y,-z,x)$

$R_8 \; \psi(x,y,z) = \psi(y,-z,-x)$

$R_9 \; \psi(x,y,z) = \psi(z,x,y)$

$R_{10} \; \psi(x,y,z) = \psi(-z,-x,y)$

$R_{11} \; \psi(x,y,z) = \psi(z,-x,-y)$

$R_{12} \; \psi(x,y,z) = \psi(-z,x,-y)$

$R_{13} \; \psi(x,y,z) = \psi(-x,z,-y)$

$R_{14} \; \psi(x,y,z) = \psi(-x,-z,y)$

$R_{15} \; \psi(x,y,z) = \psi(-z,-y,x)$

$R_{16} \; \psi(x,y,z) = (z,-y,-x)$

$R_{17} \; \psi(x,y,z) = \psi(y,-x,-z)$

$R_{18} \; \psi(x,y,z) = \psi(-y,x,-z)$

$R_{19} \; \psi(x,y,z) = \psi(x,z,y)$

$R_{20} \; \psi(x,y,z) = \psi(x,-z,-y)$

$R_{21} \; \psi(x,y,z) = \psi(z,y,x)$

$R_{22} \; \psi(x,y,z) = \psi(-z,y,-x)$

$R_{23} \; \psi(x,y,z) = \psi(y,x,z)$

$R_{24} \; \psi(x,y,z) = \psi(-y,-x,z)$

$R_{25} \; \psi(x,y,z) = \psi(-x,-y,-z)$

$R_{26} \; \psi(x,y,z) = \psi(-x,y,z)$

$R_{27} \; \psi(x,y,z) = \psi(x,-y,-z)$

$R_{28} \; \psi(x,y,z) = \psi(x,y,-z)$

$R_{29} \; \psi(x,y,z) = \psi(-y,-z,-x)$

$R_{30} \; \psi(x,y,z) = \psi(y,-z,x)$

$R_{31} \; \psi(x,y,z) = \psi(y,z,x)$

$R_{32} \; \psi(x,y,z) = \psi(-y,z,x)$

$R_{33} \; \psi(x,y,z) = \psi(-z,-x,-y)$

$R_{34} \; \psi(x,y,z) = \psi(z,x,-y)$

$R_{35} \; \psi(x,y,z) = \psi(-z,x,y)$

$R_{36} \; \psi(x,y,z) = \psi(z,-x,y)$

$R_{37} \; \psi(x,y,z) = \psi(x,-z,y)$

$R_{38} \; \psi(x,y,z) = \psi(x,z,-y)$

$R_{39} \; \psi(x,y,z) = \psi(z,y,-x)$

$R_{40} \; \psi(x,y,z) = \psi(-z,y,x)$

$R_{41} \; \psi(x,y,z) = \psi(-y,x,z)$

$R_{42} \; \psi(x,y,z) = \psi(y,-x,z)$

$R_{43} \; \psi(x,y,z) = \psi(-x,-z,-y)$

$R_{44} \; \psi(x,y,z) = \psi(-x,z,y)$

$R_{45} \; \psi(x,y,z) = \psi(-z,-y,-x)$

$R_{46} \; \psi(x,y,z) = \psi(z,-y,x)$

$R_{47} \; \psi(x,y,z) = \psi(-y,-x,-z)$

$R_{48} \; \psi(x,y,z) = \psi(y,x,-z)$

Appendix Four - Interband Transitions

A- IV-1 Introduction

The transition probability for an electronic transition from an initial state $\underline{i}$ to a final state $\underline{f}$ is proportional to $\left|H'_{fi}\right|^2$ where

$$H'_{fi} = \int \psi^*_{\vec{K}_f} H' \psi_{\vec{K}_i} \, dv \qquad (A4-1)$$

Here $\psi_{\vec{K}_f}$ and $\psi_{\vec{K}_i}$ are the final and initial Bloch wave functions for the electron in the cyrstal. H' is the interaction that mixes the two states.

For direct optical transitions, H' is the electric dipole operator

$$H' = \frac{-ieh}{mc} \vec{A} \cdot \vec{\nabla} \, .$$

Writing the vector potential in the form

$$\vec{A} = \vec{Ao} \, e^{i \, \vec{K} \cdot \vec{r}} \qquad (\vec{Ao} = \text{constant vector in the direction of polarization})$$

we obtain

$$H' = \frac{-ieh}{mc} e^{i \, \vec{k} \cdot \vec{r}} \, \vec{Ao} \cdot \vec{\nabla} \qquad (A4-2)$$

which has the form of a Bloch wave.

The interaction for the scattering of an electron by a phonon is

$$(A4-3) \qquad H' = \vec{u} \cdot \vec{\nabla} V(\vec{r}) \qquad \text{where} \qquad \vec{u} = \text{lattice displacement} = \vec{\epsilon} \, e^{i \, \vec{k} \cdot \vec{r}}$$

$$V(\vec{r}) = \text{crystalline potential}$$

and also has the Bloch form.

Thus for either type of transition, the matrix element is

$$H'_{f_i} = \int \psi^*_{\vec{k}_f} H'_{\vec{k}} \psi_{\vec{k}_i} \, dv \qquad (A4\text{-}4)$$

where $H'_{\vec{k}}$ is a Bloch wave. As a consequence of **translational invariance** we have the usual selection rule:

$$-\vec{k}_f + \vec{k} + \vec{k}_i = \begin{cases} 0 \\ \text{or} \\ \text{a vector of the} \\ \text{reciprocal lattice} \end{cases} \qquad (A4\text{-}5)$$

We now discuss the selection rules that follow from the rotational invariance of the crystal.

Let:

$\psi^{(\alpha)}_{\vec{k}_f}$ transform as a basis partner for the αth irreducible represen-
tation of the group of $\vec{k}_f$.

$\psi^{(\beta)}_{\vec{k}_f}$ transform as a basis partner for the βth irreducible represen-
tation of the group of $\vec{k}$.

$\psi^{(\gamma)}_{\vec{k}_f}$ transform as a basis partner for the γth irreducible represen-
tation of the group of $\vec{k}_i$.

Then from group theoretical arguments[11] it may be deduced that the matrix element H'_{f_i} vanishes unless the direct product representation

$$\Gamma^{*(\alpha)} \times \Gamma^{(\beta)} \times \Gamma^{(\gamma)} \qquad (A4\text{-}6)$$

contains the identity representation in its decomposition. Since $\vec{k}_f$, $\vec{k}$, and $\vec{k}_i$ will in general belong to different groups, the direct

product group contains only their common elements. The number of times

that the identity representation is contained in the decomposition of the

direct product is given by

$$\frac{1}{g} \sum_{\ell=1}^{g} \chi^{*(\alpha)}(R_\ell) \chi^{(\beta)}(R_\ell) \chi^{(\gamma)}(R_\ell) \qquad (A4-7)$$

where $R_\ell = \ell^{th}$ common element of the groups $\vec{k}_i$, $\vec{k}$, and $\vec{k}_f$

$\chi^{(\alpha)}(R_\ell)$ = character of the element R_ℓ for the αth irreducible representation. (Similarly for $\chi^{(\beta)}(R_\ell)$ and $\chi^{(\gamma)}(R_\ell)$).

g = number of common elements, R_ℓ.

Note that the order of the factors in either A4-6 or A4-7 is immaterial.

If the sum A4-7 is zero, then the matrix element H'_{fi} vanishes and the

corresponding transition is forbidden. Otherwise the transition is

allowed.

In general, to perform the sum on group elements (equation A4-7),

one must consider the representations of the entire space groups, but

if (as in the present case of the NaCl structure) the space groups do

not contain glide planes or screw displacements (i.e. symmorphic

space groups), only the appropriate point group representations are re-

quired. Thus for the three main symmetry directions we need only the

character tables for the groups O_h (for the point Γ), C_{2v} (for the Σ

direction and the point K), C_{3v} (for the Λ direction), D_{3d} (for the

point L), C_{4v} (for the Δ direction), and D_{4h} (for the point X). The

character tables for these groups are given at the end of this appendix

in tables A4-1 to A4-6. In these tables barred operations correspond to an additional rotation by 2π. After each character table we give the multiplication table for the direct products of the different irreducible representations of that group.

For the groups that contain the inversion operation (O_h, D_{4h}, D_{3d}) the multiplication table is given only for those representations even on inversion. To determine the decomposition of the direct product of $\Gamma_i^{\pm}$ x $\Gamma_j^{\pm}$ (where the plus sign means even on inversion, the minus sign means odd on inversion), we use the rule that the product of two even (or two odd) representations is even; the product of an even representation and an odd representation is odd. For example, from table A4-1 we have: Γ_{12} x Γ_8^+ = Γ_6^+ + Γ_7^+ + Γ_8^+; therefore Γ_{12} x Γ_8^- = Γ_6^- + Γ_7^- + Γ_8^-.

Before proceeding with the calculations, it is important to remember that in general the addition of spin in the Hamiltonian and wave functions will sometimes alter selection rules. For this reason, we consider the problem of determining the selection rules in both cases: first without spin, and then with spin added.

A- IV-2 - Selection Rules Without Spin

(a) Vertical Transitions

For vertical (or direct optical) transitions we have, to excellent approximation, $\vec{k}_f = \vec{k}_i$, or $\vec{k} = 0$ in equation A4-5. Thus one studies the direct product $\Gamma^{(\alpha)}$ x Γ_{15} x $\Gamma^{(\beta)}$ since the interaction (light) behaves like an ordinary vector. Because spin is ignored, we use only

single valued representations in our calculations.

Point Γ (Group O_h).

Here all three vectors belong to the same group. Hence, from the multiplication table A4-1 we have:

transition $\Gamma_1 \longrightarrow \Gamma_{15}$: Γ_1 x Γ_{15} x Γ_{15} = Γ_1 + Γ_2 + Γ_{15} + Γ_{25}'

Contains identity   representation Γ_1 and is therefore <u>allowed</u>

$\Gamma_1 \longrightarrow \Gamma_{12}$: Γ_1 x Γ_{15} x Γ_{12} = Γ_{15} + Γ_{25} $\therefore$ <u>forbidden</u>

$\Gamma_1 \longrightarrow \Gamma_{25}'$: Γ_1 x Γ_{15} x Γ_{25}' = Γ_2' + Γ_{12}' + Γ_{15} + Γ_{25}

$\therefore$ <u>forbidden</u>

$\Gamma_1 \longrightarrow \Gamma_{15}$: Γ_{15} x Γ_{15} x Γ_{15} = Γ_1' + $2\Gamma_2'$ + Γ_{12}' + 3 Γ_{15} + 3 Γ_{25}

$\therefore$ <u>forbidden</u>

$\Gamma_{15} \longrightarrow \Gamma_{25}'$: Γ_{15} x Γ_{15} x Γ_{25}' = Γ_1 + 2 Γ_2 + 3 Γ_{15}' + 3 Γ_{25}'

$\therefore$ <u>allowed</u>

Along Δ (Group C_{4v}

Using equation A4-7 and table A4-2, we find that only the direct products Δ_1 x Γ_{15} and Δ_5 x Γ_{15} contain the identity representation Δ_1. Thus, the transition $\Delta_i \longrightarrow \Delta_j$ is allowed only if Δ_i x Δ_j contains either Δ_1 or Δ_5. From the multiplication table A4-2 we find that the allowed transitions are:

$$\Delta_1 \longrightarrow \Delta_1 \qquad \text{since} \qquad \Delta_1 \times \Delta_1 = \Delta_1$$

$$\Delta_1 \longrightarrow \Delta_5 \qquad " \qquad \Delta_1 \times \Delta_5 = \Delta_5$$

$$\Delta_2 \longrightarrow \Delta_2 \qquad " \qquad \Delta_2 \times \Delta_2 = \Delta_1$$

$$\Delta_2 \longrightarrow \Delta_5 \qquad " \qquad \Delta_2 \times \Delta_5 = \Delta_5$$

$$\Delta_2' \longrightarrow \Delta_2' \qquad " \qquad \Delta_2' \times \Delta_2' = \Delta_1$$

$$\Delta_2' \longrightarrow \Delta_5 \qquad " \qquad \Delta_2' \times \Delta_5 = \Delta_5$$

$$\Delta_5 \longrightarrow \Delta_5 \qquad " \qquad \Delta_5 \times \Delta_5 = \Delta_1 + \Delta_2' + \Delta_2 + \Delta_2'$$

All other direct transitions $\Delta_i \longrightarrow \Delta_j$ are forbidden

At X (Group D_{4h})

From equation A4-7 and Table A4-3 we find that only the direct products $\Gamma_{15} \times X_4'$ and $\Gamma_{15} \times X_5'$ contain the identity representation, X_1. The allowed transitions $X_i \longrightarrow X_j$ must contain either X_4' or X_5' in the direct product $X_i \times X_j$. By inspection of Table A4-3, we obtain:

$$X_1 \longrightarrow X_4'$$
$$X_1 \longrightarrow X_5'$$
$$X_2 \longrightarrow X_5'$$
$$X_3 \longrightarrow X_5' \qquad \Big\} \quad \text{Allowed transitions at X}$$
$$X_4' \longrightarrow X_5$$
$$X_4 \longrightarrow X_5'$$
$$X_5 \longrightarrow X_5'$$

All other direct transitions at X are forbidden

<u>Along Σ and at K (Group C_{2v})</u>

Only the direct products Σ_1 x Γ_{15}, Σ_3 x Γ_{15}, and Σ_4 x Γ_{15} contain the identity representation, Σ_1. Thus, allowed transitions $\Sigma_i \longrightarrow \Sigma_j$ must contain Σ_1, Σ_3 or Σ_4 in the direct product Σ_i x Σ_j. From table A4-4, we have:

$$
\left.
\begin{array}{l}
\Sigma_1 \longrightarrow \Sigma_3 \\
\Sigma_1 \longrightarrow \Sigma_4 \\
\Sigma_2 \longrightarrow \Sigma_2 \\
\Sigma_2 \longrightarrow \Sigma_3 \\
\Sigma_2 \longrightarrow \Sigma_4 \\
\Sigma_3 \longrightarrow \Sigma_3 \\
\Sigma_4 \longrightarrow \Sigma_4
\end{array}
\right\} \text{allowed}
\left\{
\begin{array}{l}
K_1 \longrightarrow K_3 \\
K_1 \longrightarrow K_4 \\
K_2 \longrightarrow K_2 \\
K_2 \longrightarrow K_3 \\
K_2 \longrightarrow K_4 \\
K_3 \longrightarrow K_3 \\
K_4 \longrightarrow K_4
\end{array}
\right.
$$

Also, the only <u>forbidden</u> transitions are:

$$
\left.
\begin{array}{l}
\Sigma_1 \longrightarrow \Sigma_2 \\
\Sigma_3 \longrightarrow \Sigma_4
\end{array}
\right\} \underline{\text{forbidden}}
\left\{
\begin{array}{l}
K_1 \longrightarrow K_2 \\
K_3 \longrightarrow K_4
\end{array}
\right.
$$

<u>Along Λ (Group C_{3v})</u>

Here only the direct product Λ_3 x Γ_{15} contains the identity representation Λ_1. The allowed transitions $\Lambda_i \longrightarrow \Lambda_j$ must contain Λ_3 in the direct product Λ_i x Λ_j. By inspection of table A4-5 we find the allowed transitions are:

$$
\left.
\begin{array}{l}
\Lambda_1 \longrightarrow \Lambda_3 \\
\Lambda_3 \longrightarrow \Lambda_3
\end{array}
\right\} \text{allowed}
$$

but

$$
\Lambda_1 \longrightarrow \Lambda_1 \quad \text{forbidden}
$$

At L (Group D_{3d})

At the point L, only the direct products L'_2 x Γ_{15} and L'_3 x Γ_{15} contain the identity representation L_1. As in the previous cases, the transition $L_i \longrightarrow L_j$ will be allowed only if the direct product L_i x L_j contains L'_2 or L'_3. From table A4-6, we find that the allowed transitions are:

$$
\left.
\begin{aligned}
L_1 &\longrightarrow L'_2 \\
L_1 &\longrightarrow L'_3 \\
L_2 &\longrightarrow L'_3 \\
L_3 &\longrightarrow L'_2 \\
L_3 &\longrightarrow L'_3
\end{aligned}
\right\} \text{ allowed}
$$

(b)   Indirect Transitions

Indirect transitions are the result of an electron being scattered by a phonon from an initial state $\vec{k_i}$, to an intermediate state $\vec{k}$ and then emitting or absorbing a photon to arrive at a final state $\vec{k_f}$. The second step of the process is a direct transition ($\vec{k_f} = \vec{k}$) and governed by the selection rules determined in the previous section. We now study the phonon assisted transitions, i.e. those transitions in which an electron along a particular band is scattered by a phonon either to the point Γ or to the edge of the Brillouin zone.

Yanagawa[12] has shown that the only allowed phonons for an NaCl structure are:

$$
\begin{aligned}
&\Delta_1 \text{ and } \Delta_5 &&\text{in the } \Delta \text{ direction} \\
&\Sigma_1, \Sigma_3, \text{ and } \Sigma_4 &&\text{in the } \Sigma \text{ direction} \\
&\Lambda_1 \text{ and } \Lambda_3 &&\text{in the } \Lambda \text{ direction}
\end{aligned}
$$

In order to determine whether or not an electron-phonon interaction is possible along a particular direction, we again inspect the decomposition of the direct product $\Gamma^{*(\alpha)} \times \Gamma^{(\beta)} \times \Gamma^{(\gamma)}$ and see if it contains the identity representation. However, for the electron-phonon interaction we really have very little work to do. In each direction, one of the allowed phonons has the identity representation for that particular direction. Therefore the representation of the direct product of (electron representation)x(phonon representation) will always contain the irreducible representation of the electron along a given band. Since the symmetry of the electron band must be compatible with that of the associated state at Γ or the zone edge, the decomposition of the direct product will always contain the identity representation. Thus we may conclude that the electron-phonon interaction is allowed for all bands; selection rules for the total indirect transition being those of the "direct" portion of the two step process.

A- IV-3 Transitions when Hamiltonian is spin dependent

   (a) Direct Transitions

   We now consider the transitions when the Hamiltonian is spin depen-
dent because of the addition of spin-orbit coupling. The wave functions
are two component spinors formed from linear combinations of the un-
perturbed APW functions each multiplied by a spinor, α or β (where α
$= \begin{pmatrix} 1 \\ 0 \end{pmatrix}$, $\beta = \begin{pmatrix} 0 \\ 1 \end{pmatrix}$). Defining $D_{1/2}$ as the spinor representation, we find
that the direct product $D_{1/2}$ x $\Gamma^{(\gamma)}$ may be decomposed into a sum of
irreducible representations of the double group.[13] These are:

at Γ :

$$D_{1|2} \times \Gamma_1 = \Gamma_6^+$$

$$D_{1|2} \times \Gamma_2 = \Gamma_7^+$$

$$D_{1|2} \times \Gamma_{12} = \Gamma_8^+$$

$$D_{1|2} \times \Gamma_{15}' = \Gamma_6^+ + \Gamma_8^+$$

$$D_{1|2} \times \Gamma_{25}' = \Gamma_7^+ + \Gamma_8^+$$

$$D_{1|2} \times \Gamma_1' = \Gamma_6^-$$

$$D_{1|2} \times \Gamma_2' = \Gamma_7^-$$

$$D_{1|2} \times \Gamma_{12}' = \Gamma_8^-$$

$$D_{1|2} \times \Gamma_{15} = \Gamma_6^- + \Gamma_8^-$$

$$D_{1|2} \times \Gamma_{25} = \Gamma_7^- + \Gamma_8^-$$

   + means that the representation has even parity

   - means that the representation has odd parity

<u>along Δ:</u>

$$D_{1/2} \ \times \ \Delta_1 \ = \ \Delta_6$$

$$D_{1/2} \ \times \ \Delta'_1 \ = \ \Delta_6$$

$$D_{1/2} \ \times \ \Delta_2 \ = \ \Delta_7$$

$$D_{1/2} \ \times \ \Delta'_2 \ = \ \Delta_7$$

$$D_{1/2} \ \times \ \Delta_5 \ = \ \Delta_6 \ + \ \Delta_7$$

<u>at X:</u>

$$D_{1/2} \ \times \ X_1 \ = \ X_6^{+} \qquad D_{1/2} \ \times \ X_1 \ = \ X_6^{-}$$

$$D_{1/2} \ \times \ X_2 \ = \ X_7^{+} \qquad D_{1/2} \ \times \ X_2' \ = \ X_7^{-}$$

$$D_{1/2} \ \times \ X_3 \ = \ X_7^{+} \qquad D_{1/2} \ \times \ X_3' \ = \ X_7^{-}$$

$$D_{1/2} \ \times \ X_4 \ = \ X_6^{+} \qquad D_{1/2} \ \times \ X_4' \ = \ X_6^{-}$$

$$D_{1/2} \ \times \ X_5 \ = \ X_6^{+} + X_7^{+} \qquad D_{1/2} \ \times \ X_5' \ = \ X_6^{-} + X_7^{-}$$

<u>along Σ and at K:</u>

$$D_{1/2} \ \times \ \Sigma_1 \ = \ \Sigma_5 \qquad D_{1/2} \ \times \ K_1 \ = \ K_5$$

$$D_{1/2} \ \times \ \Sigma_2 \ = \ \Sigma_5 \qquad D_{1/2} \ \times \ K_2 \ = \ K_5$$

$$D_{1/2} \ \times \ \Sigma_3 \ = \ \Sigma_5 \qquad D_{1/2} \ \times \ K_3 \ = \ K_5$$

$$D_{1/2} \ \times \ \Sigma_4 \ = \ \Sigma_5 \qquad D_{1/2} \ \times \ K_4 \ = \ K_5$$

<u>along Λ:</u>

$$D_{1/2} \ \times \ \Lambda_1 \ = \ \Lambda_6$$

$$D_{1/2} \ \times \ \Lambda_2 \ = \ \Lambda_6$$

$$D_{1/2} \ \times \ \Lambda_3 \ = \ \Lambda_4 \ + \ \Lambda_5 \ + \ \Lambda_6$$

<u>at L:</u>

$$D_1|_2 \ \times \ L_1 \ = \ L_6^+ \qquad\qquad D_1|_2 \ \times \ L_1' \ = \ L_6^-$$

$$D_1|_2 \ \times \ L_2 \ = \ L_6^+ \qquad\qquad D_1|_2 \ \times \ L_2' \ = \ L_6^-$$

$$D_1|_2 \ \times \ L_3 \ = \ L_4^+ + L_5^+ + L_6^+ \qquad D_1|_2 \ \times \ L_3' \ = \ L_4^- + L_5^- + L_6^-$$

The APW bands will be altered when spin-orbit coupling is included in the Hamiltonian. At some points in the Brillouin zone, an unperturbed band will be split into several distinct bands; in some cases the original APW states are only shifted slightly because of the spin-orbit interaction. The upper valence and lower conduction bands (for AgCl) with and without spin orbit coupling included are sketched in Figure A4-1 for the three symmetry directions. Note that the drawing is not to scale and the spin orbit splittings have been greatly magnified.

The addition of spin-orbit coupling has reduced the number of possible symmetries in our bands. Consequently, since more bands have like symmetry, there is a great deal more mixing of states than before. We now show that because of this additional mixing of states, almost all direct transitions are allowed. The only forbidden direct transitions are those between states of the same parity (at the points Γ, X, and L which are parity eigenstates) and the transition $\Gamma_6^\pm \longrightarrow \Gamma_7^\mp$. at Γ.

The representations at Γ are $\Gamma_6^\pm$, $\Gamma_7^\pm$, $\Gamma_8^\pm$. Since the parity of the electric dipole interaction is odd, we can have non-zero matrix elements only between states of opposite parity.

The direct products $\Gamma_i^\pm$ x $\Gamma_j^\mp$ (i, j = 6, 7, 8) may be decomposed into the irreducible representations of the single group (see Table A4-1). In order that the transition $\Gamma_i^\pm \longrightarrow \Gamma_j^\mp$ be allowed, this decomposition of this direct product must contain the representation Γ_{15} since the interaction has symmetry Γ_{15}. From Table A4-1 we find that;

UPPER VALENCE AND LOWEST CONDUCTION BANDS WITH AND WITHOUT SPIN-ORBIT INTERACTION

WITHOUT SPIN

WITH SPIN-ORBIT
INCLUDED
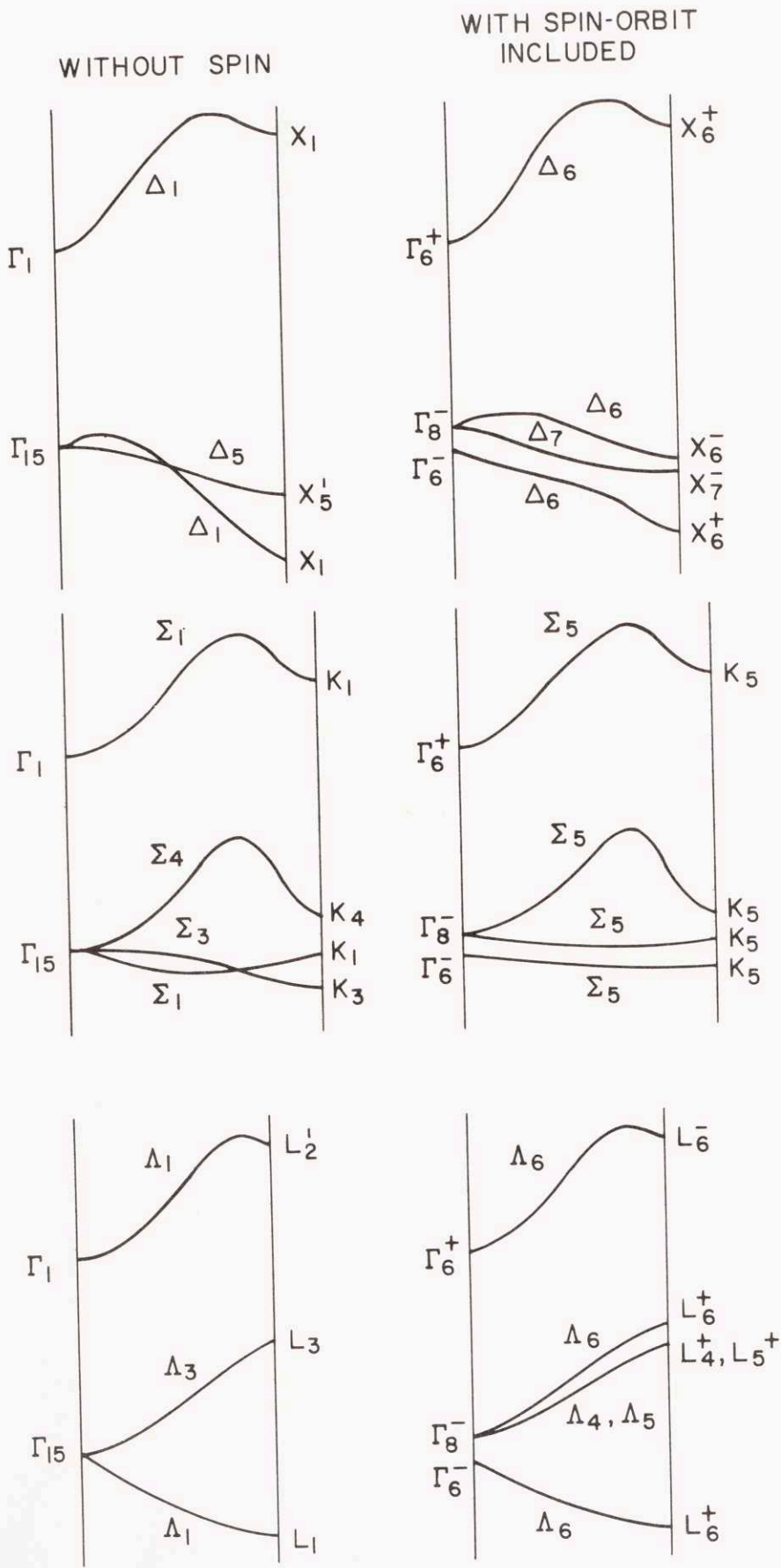
$$\Gamma_6^{\pm} \times \Gamma_6^{\mp} = \Gamma_1' + \Gamma_{15} \qquad \text{allowed}$$

$$\Gamma_6^{\pm} \times \Gamma_7^{\mp} = \Gamma_2' + \Gamma_{25} \qquad \text{forbidden}$$

$$\Gamma_6^{\pm} \times \Gamma_8^{\mp} = \Gamma_{12}' + \Gamma_{15} + \Gamma_{25} \qquad \text{allowed}$$

$$\Gamma_7^{\pm} \times \Gamma_7^{\mp} = \Gamma_1' + \Gamma_{15} \qquad \text{allowed}$$

$$\Gamma_7^{\pm} \times \Gamma_8^{\mp} = \Gamma_{12}' + \Gamma_{15} + \Gamma_{25} \qquad \text{allowed}$$

$$\Gamma_8^{\pm} \times \Gamma_8^{\mp} = \Gamma_1' + \Gamma_2' + 2\Gamma_{15} + 2\Gamma_{25} \qquad \text{allowed}$$

along Δ

Here the possible symmetries are now Δ_6 and Δ_7. Since the direct products $\Delta_6 \times \Delta_6$, $\Delta_6 \times \Delta_7$ and $\Delta_7 \times \Delta_7$ all contain Δ_1 or Δ_5, every transition is allowed.

at X.

The decomposition of the direct product $X_i^{\pm} \times X_j^{\mp}$ must contain either X_4' or X_5'. From Table A4-3, we see that the direct products $X_6^{\pm} \times X_6^{\mp}$, $X_6^{\pm} \times X_7^{\mp}$, $X_7^{\pm} \times X_7^{\mp}$ all contain X_4' or X_5' and therefore every parity allowed transition is possible.

along Σ and K

Here the only possible symmetry is Σ_5 (or K_5). Since $\Sigma_5 \times \Sigma_5 = \Sigma_1 + \Sigma_2 + \Sigma_3 + \Sigma_4$, all transitions are allowed.

along Λ

The allowed symmetries are Λ_4, Λ_5, and Λ_6, and the decomposition of the direct products $\Lambda_i \times \Lambda_j$ (i,j = 4, 5, 6) must contain either Λ_1 or Λ_3. From Table A4-5, the allowed transitions are:

$$\left.\begin{array}{l}\Lambda_4 \longrightarrow \Lambda_5 \\ \Lambda_4 \longrightarrow \Lambda_6 \\ \Lambda_5 \longrightarrow \Lambda_6 \\ \Lambda_6 \longrightarrow \Lambda_6\end{array}\right\} \text{ allowed}$$

and

$$\left.\begin{array}{l}\Lambda_4 \longrightarrow \Lambda_4 \\ \Lambda_5 \longrightarrow \Lambda_5\end{array}\right\} \text{ forbidden}$$

Note that in the absence of a magnetic field, Λ_4 and Λ_5 are degenerate bands. Therefore, in this case all direct transitions between bands with distinct eigenvalues are possible.

at L.

The symmetries of bands with distinct energies are $L_4^{\pm}$ (or $L_5^{\pm}$) and $L_6^{\pm}$. Since the direct products $L_6^{\pm} \times L_6^{\mp}$, $L_4^{\pm} \times L_6^{\mp}$ and $L_5^{\pm} \times L_6^{\mp}$ all contain L_3', every transition between distinct states of opposite parity is allowed.

In order to see more clearly how the addition of spin-orbit coupling changes some of the selection rules for direct transitions, we study a particular case in detail: the transition $\Sigma_3 \longrightarrow \Sigma_4$. As we have seen, without spin this transition is forbidden; with spin-orbit coupling the transition is allowed. For simplicity, in this example, we ignore all other bands.

Let the unperturbed (spin-independent) Hamiltonian be $H^{(o)}$ with eigenfunctions $\varphi_3^{(o)}$ and $\varphi_4^{(o)}$ (transforming like Σ_3 and Σ_4, respectively) and eigenvalues $\epsilon_3^{(o)}$ and $\epsilon_4^{(o)}$. Call the eigenfunctions under

the double group $\psi_3{}^{(0)}$ and $\psi_4{}^{(0)}$ before the spin-orbit perturbation is introduced (note that there are really two eigenfunctions for each band, but because each band is doubly degenerate we only use one function for each band). When spin-orbit coupling is added to the Hamiltonian, we find that the diagonal matrix elements $\left\langle \psi_i{}^{(0)} \middle| H_{so} \middle| \psi_i{}^{(0)} \right\rangle$ vanish (proven in Chapter III), and the off diagonal elements $\left\langle \psi_i{}^{(0)} \middle| H_{so} \middle| \psi_j{}^{(0)} \right\rangle$ are proportional to a spin orbit parameter λ. For $\left| \epsilon_3{}^{(0)} - \epsilon_4{}^{(0)} \right| \gg \lambda$, the energies of the bands will be:

$$\epsilon_3 \simeq \epsilon_3{}^{(0)} - \frac{\lambda^2}{\epsilon_3{}^{(0)} - \epsilon_4{}^{(0)}}$$

$$\epsilon_2{}^{(0)} \simeq \epsilon_2{}^{(0)} + \frac{\lambda^2}{\epsilon_3{}^{(0)} - \epsilon_4{}^{(0)}}$$

and the wave functions become (to first order in λ):

$$\psi_3 = \psi_3{}^{(0)} + \frac{\lambda}{\epsilon_3{}^{(0)} - \epsilon_4{}^{(0)}} \psi_4{}^{(0)}$$

$$\psi_4 = \psi_4{}^{(0)} + \frac{\lambda}{\epsilon_4{}^{(0)} - \epsilon_3{}^{(0)}} \psi_3{}^{(0)}$$

The matrix element for a direct transition from band three to band four is

$$H'_{34} = \left\langle \psi_4 \middle| H' \middle| \psi_3 \right\rangle$$

$$= \frac{\lambda}{\epsilon_4{}^{(0)} - \epsilon_3{}^{(0)}} \left[\left\langle \psi_3{}^{(0)} \middle| H' \middle| \psi_3{}^{(0)} \right\rangle - \left\langle \psi_4{}^{(0)} \middle| H' \middle| \psi_4{}^{(0)} \right\rangle \right]$$

since the matrix elements $< \psi_3^{(o)} | H' | \psi_4^{(o)} >$ vanish by symmetry. Thus the
transition probability for the transition will be proportional to

$$\left(\frac{\lambda}{\epsilon_3^{(o)} - \epsilon_4^{(o)}} \right)^2$$

and therefore the corresponding intensity will

be much less than that of a transition allowed without spin (assuming
that the density of states is the same).

(b) Indirect Transitions with Spin

Since the addition of spin in the Hamiltonian serves to bring about
more mixing of the unperturbed functions, the matrix elements for the
electron-phonon interaction can only increase when spin is added. Be-
cause all such interactions were permissible without spin, the transitions
are still allowed. In fact, the arguments that were given for the spin-
independent situation may be applied here without any changes.

TABLE A4-1

CHARACTER TABLE FOR GROUP O_h

	E	$\bar{E}$	$8C_3$	$\overline{8C_3}$	$\begin{matrix}3C_4^2\\\overline{3C_4^2}\end{matrix}$	$6C_4$	$\overline{6C_4}$	$\begin{matrix}6C_2\\\overline{6C_2}\end{matrix}$	J	$\bar{J}$	$8JC_3$	$\overline{8JC_3}$	$\begin{matrix}3JC_4^2\\\overline{3JC_4^2}\end{matrix}$	$6JC_4$	$\overline{6JC_4}$	$\begin{matrix}6JC_2\\\overline{6JC_2}\end{matrix}$
Γ_1	1	1	1	1	1	1	1	1	1	1	1	1	1	1	1	1
Γ_2	1	1	1	1	1	-1	-1	-1	1	1	1	1	1	-1	-1	-1
Γ_{12}	2	2	-1	-1	2	0	0	0	2	2	-1	-1	2	0	0	0
Γ_{15}'	3	3	0	0	-1	1	1	-1	3	3	0	0	-1	1	1	-1
Γ_{25}'	3	3	0	0	-1	-1	-1	1	3	3	0	0	-1	-1	-1	1
Γ_1'	1	1	1	1	1	1	1	1	-1	-1	-1	-1	-1	-1	-1	-1
Γ_2'	1	1	1	1	1	-1	-1	-1	-1	-1	-1	-1	-1	1	1	1
Γ_{12}'	2	2	-1	-1	2	0	0	0	-2	-2	1	1	-2	0	0	0
Γ_{15}	3	3	0	0	-1	1	1	-1	-3	-3	0	0	1	-1	-1	1
Γ_{25}	3	3	0	0	-1	-1	-1	1	-3	-3	0	0	1	1	1	-1
$\Gamma_6^{\pm}$	2	-2	1	-1	0	$\sqrt{2}$	$-\sqrt{2}$	0	±2	∓2	±1	∓1	0	$\pm\sqrt{2}$	$\mp\sqrt{2}$	0
$\Gamma_7^{\pm}$	2	-2	1	-1	0	$-\sqrt{2}$	$\sqrt{2}$	0	±2	∓2	±1	∓1	0	$\mp\sqrt{2}$	$\pm\sqrt{2}$	0
$\Gamma_8^{\pm}$	4	-4	-1	1	0	0	0	0	±4	∓4	∓1	±1	0	0	0	0

MULTIPLICATION TABLE FOR EVEN REPRESENTATIONS

	Γ_1	Γ_2	Γ_{12}	Γ_{15}	Γ_{25}	Γ_6^+	Γ_7^+	Γ_8^+
Γ_1	Γ_1	Γ_2	Γ_{12}	Γ_{15}'	Γ_{25}'	Γ_6^+	Γ_6^+	Γ_8^+
Γ_2		Γ_1	Γ_{12}	Γ_{25}'	Γ_{15}'	Γ_7^+	Γ_6^+	Γ_8^+
Γ_{12}			$\Gamma_1 + \Gamma_2 + \Gamma_{12}$	$\Gamma_{15}' + \Gamma_{25}'$	$\Gamma_{15}' + \Gamma_{25}$	Γ_8^+	Γ_8^+	$\Gamma_6^+ + \Gamma_7^+ + \Gamma_8^+$
Γ_{15}'				$\Gamma_1 + \Gamma_{12} + \Gamma_{15}' + \Gamma_{25}'$	$\Gamma_2 + \Gamma_{12} + \Gamma_{15}' + \Gamma_{25}'$	$\Gamma_6^+ + \Gamma_8^+$	$\Gamma_7^+ + \Gamma_8^+$	$\Gamma_6^+ + \Gamma_7^+ + \Gamma_8^+$
Γ_{25}'					$\Gamma_1 + \Gamma_{12} + \Gamma_{15}' + \Gamma_{25}'$	$\Gamma_7^+ + \Gamma_8^+$	$\Gamma_6^+ + \Gamma_8^+$	$\Gamma_6^+ + \Gamma_7^+ + 2\Gamma_8^+$
Γ_6^+						$\Gamma_1 + \Gamma_{15}'$	$\Gamma_2 + \Gamma_{25}'$	$\Gamma_{12} + \Gamma_{15}' + \Gamma_{25}'$
Γ_7^+							$\Gamma_1 + \Gamma_{15}'$	$\Gamma_{12} + \Gamma_{15}' + \Gamma_{25}'$
Γ_8^+								$\Gamma_1 + \Gamma_2 + \Gamma_{12} + \Gamma_{15}' + 2\Gamma_{25}'$

TABLE A4-2

CHARACTER TABLE FOR GROUP C_{4v}

	E	$\overline{E}$	$2C_4$	$\overline{2C_4}$	$\dfrac{C_2}{\overline{C_2}}$	$2\,\sigma_v$ $2\,\overline{\sigma_v}$	$2\,\dfrac{\sigma_d}{\overline{\sigma_d}}$
Δ_1	1	1	1	1	1	1	1
Δ'_1	1	1	1	1	1	-1	-1
Δ_2	1	1	-1	-1	1	1	-1
Δ'_2	1	1	-1	-1	1	-1	1
Δ_5	2	2	0	0	-2	0	0
Δ_6	2	-2	$\sqrt{2}$	$-\sqrt{2}$	0	0	0
Δ_7	2	-2	$-\sqrt{2}$	$\sqrt{2}$	0	0	0

MULTIPLICATION TABLE

	Δ_1	Δ'_1	Δ_2	Δ'_2	Δ_5	Δ_6	Δ_7
Δ_1	Δ_1	Δ'_1	Δ_2	Δ'_2	Δ_5	Δ_6	Δ_7
Δ'_1		Δ_1	Δ'_2	Δ_2	Δ_5	Δ_6	Δ_7
Δ_2			Δ_1	Δ'_1	Δ_5	Δ_7	Δ_6
Δ'_2				Δ_1	Δ_5	Δ_7	Δ_6
Δ_5					$\Delta_1 + \Delta_5$ $+ \Delta_2 + \Delta'_2$	$\Delta_6 + \Delta_7$	$\Delta_6 + \Delta_7$
Δ_6						$\Delta_1 + \Delta'_1 + \Delta_5$	$\Delta_2 + \Delta'_2 + \Delta_5$
Δ_7							$\Delta_1 + \Delta'_1 + \Delta_5$

TABLE A4-3

CHARACTER TABLE FOR GROUP D_{4h}

	E	Ē	$2C_4$	$2\overline{C_4}$	C_2 / $\overline{C_2}$	$2C_2'$ / $2\overline{C_2'}$	$2C_2''$ / $2\overline{C_2''}$	J	J̄	$2S_4$	$2\overline{S_4}$	σ_h / $\overline{\sigma_h}$	$2\sigma_v$ / $2\overline{\sigma_v}$	$2\sigma_d$ / $2\overline{\sigma_d}$
X_1	1	1	1	1	1	1	1	1	1	1	1	1	1	1
X_2	1	1	1	1	1	-1	-1	1	1	1	1	1	-1	-1
X_3	1	1	-1	-1	1	1	-1	1	1	-1	-1	1	1	-1
X_4	1	1	-1	1	1	-1	1	1	1	-1	-1	1	-1	1
X_5	2	2	0	0	-2	0	0	2	2	0	0	-2	0	0
X'_1	1	1	1	1	1	1	1	-1	-1	-1	-1	-1	-1	-1
X'_2	1	1	1	1	1	-1	-1	-1	-1	-1	-1	-1	1	1
X'_3	1	1	-1	-1	1	1	-1	-1	-1	1	1	-1	-1	1
X'_4	1	1	-1	1	1	-1	1	-1	-1	1	1	-1	1	-1
X'_5	2	2	0	0	-2	0	0	-2	-2	0	0	2	0	0
$X_6^{\pm}$	2	-2	$\sqrt{2}$	$-\sqrt{2}$	0	0	0	± 2	∓ 2	$\pm\sqrt{2}$	$\mp\sqrt{2}$	0	0	0
$X_7^{\pm}$	2	-2	$-\sqrt{2}$	$\sqrt{2}$	0	0	0	± 2	∓ 2	$\mp\sqrt{2}$	$\pm\sqrt{2}$	0	0	0

MULTIPLICATION TABLE FOR EVEN REPRESENTATIONS

	X_1	X_2	X_3	X_4	X_5	X_6^{+}	X_7^{+}
X_1	X_1	X_2	X_3	X_4	X_5	X_6^{+}	X_7^{+}
X_2		X_1	X_4	X_3	X_5	X_6	X_7
X_3			X_1	X_2	X_5	X_7	X_6
X_4				X_1	X_5	X_7	X_6
X_5					$X_1 + X_2 + X_3 + X_4$	$X_6 + X_7$	$X_6 + X_7$
X_6^{+}						$X_1 + X_2 + X_5$	$X_3 + X_4 + X_5$
X_7^{+}							$X_1 + X_2 + X_5$

TABLE A4-4

CHARACTER TABLE FOR GROUP C_{2v}

	E	$\overline{E}$	$\dfrac{C_2}{\overline{C_2}}$	$\dfrac{JC_4^2}{\overline{JC_4^2}}$	$\dfrac{JC_2}{\overline{JC_2}}$
Σ_1	1	1	1	1	1
Σ_2	1	1	1	-1	-1
Σ_3	1	1	-1	-1	1
Σ_4	1	1	-1	1	-1
Σ_5	2	-2	0	0	0

MULTIPLICATION TABLE

	Σ_1	Σ_2	Σ_3	Σ_4	Σ_5
Σ_1	Σ_1	Σ_2	Σ_3	Σ_4	Σ_5
Σ_2		Σ_1	Σ_4	Σ_3	Σ_5
Σ_3			Σ_1	Σ_2	Σ_5
Σ_4				Σ_4	Σ_5
Σ_5					$\Sigma_1 + \Sigma_2 + \Sigma_3 + \Sigma_4 + \Sigma_5$

TABLE A4-5

CHARACTER TABLE FOR GROUP C₃ᵥ

	E	$\bar{E}$	$2C_3$	$\overline{2C_3}$	$3\overline{\sigma_v}$	$3\overline{\sigma_v}$
Λ_1	1	1	1	1	1	1
Λ_2	1	1	1	1	-1	-1
Λ_3	2	2	-1	-1	0	0
Λ_4	1	-1	-1	1	i	$-i$
Λ_5	1	-1	-1	1	$-i$	i
Λ_6	2	-2	1	-1	0	0

MULTIPLICATION TABLE

	Λ_1	Λ_2	Λ_3	Λ_4	Λ_5	Λ_6
Λ_1	Λ_1	Λ_2	Λ_3	Λ_4	Λ_5	Λ_6
Λ_2		Λ_1	Λ_3	Λ_5	Λ_4	Λ_6
Λ_3			$\Lambda_1 + \Lambda_2 + \Lambda_3$	Λ_6	Λ_6	$\Lambda_4 + \Lambda_5 + \Lambda_6$
Λ_4				Λ_2	Λ_1	Λ_3
Λ_5					Λ_2	Λ_3
Λ_6						$\Lambda_1 + \Lambda_2 + \Lambda_3$

TABLE A4-6

CHARACTER TABLE FOR GROUP D_{3d}

	E	$\bar{E}$	$2C_3$	$\overline{2C_3}$	$3C_2$	$\overline{3C_2}$	J	$\bar{J}$	$2JC_3$	$\overline{2JC_3}$	$3JC_2$	JC_2
L_1	1	1	1	1	1	1	1	1	1	1	1	1
L_2	1	1	1	1	-1	-1	1	1	1	1	-1	-1
L_3	2	2	-1	-1	0	0	2	2	-1	-1	0	0
L'_1	1	1	1	1	1	1	-1	-1	-1	-1	-1	-1
L'_2	1	1	1	1	-1	-1	-1	-1	-1	-1	1	1
L'_3	2	2	-1	-1	0	0	-2	-2	1	1	0	0
$L_4^{\pm}$	1	-1	-1	1	i	$-i$	± 1	∓ 1	∓ 1	± 1	$\pm i$	$\mp i$
$L_5^{\pm}$	1	-1	-1	1	$-i$	i	± 1	∓ 1	∓ 1	± 1	$\mp i$	$\pm i$
$L_6^{\pm}$	2	-2	1	-1	0	0	± 2	∓ 2	± 1	∓ 1	0	0

MULTIPLICATION TABLE FOR EVEN REPRESENTATIONS

	L_1	L_2	L_3	L_4^{+}	L_5^{+}	L_6^{+}
L_1	L_1	L_2	L_3	L_4^{+}	L_5^{+}	L_6^{+}
L_2		L_1	L_3	L_5^{+}	L_4^{+}	L_6^{+}
L_3			$L_1 + L_2 + L_3$	L_6^{+}	L_6^{+}	$L_4^{+} + L_5^{+} + L_6^{+}$
L_4^{+}				L_2	L_1	L_3
L_5^{+}					L_2	L_3
L_1^{+}						$L_1 + L_2 + L_3$

Appendix Five - Use of Projection Operators to Classify Spin Eigenstates

As mentioned in Chapter III, at the point L_3 the spin-orbit matrix is:

$$H_{so} = \begin{bmatrix} 0 & i & 0 & \sqrt{2}\omega \\ -i & 0 & -\sqrt{2}\omega & 0 \\ 0 & -\sqrt{2}\omega^* & 0 & -i \\ \sqrt{2}\omega^* & 0 & i & 0 \end{bmatrix} \qquad \text{(A5-1)}$$

$$\text{Where } \omega = e^{i\frac{\pi}{4}}$$

This matrix has four eigenvalues: λ, λ, $-\lambda$, $-\lambda$. One pair of these eigenvalues must correspond to the degenerate states L_4^+ and L_5^+; the other pair is associated with the doubly degenerate state L_6^+.

One could determine the eigenvectors for these states by applying projection operators to the four functions
($\psi_1 = \varphi_1\alpha$, $\psi_2 = \varphi_2\alpha$, $\psi_3 = \varphi_1\beta$, $\psi_4 = \varphi_2\beta$) that form a basis for the product representation of space and spin at L. However, it is unnecessary to use projection operators for all three states L_4^+, L_5^+, and L_6^+ because once the eigenvalue for any one state, say L_4^+, is determined, the eigenvalues for the other two states are known.

A projection operator for the αth irreducible representation is defined as:

$$P_{ij}^{(\alpha)} = \sum_R \left[\Gamma_{ij}(R) \right]^* R \qquad \text{(A5-2)}$$

here the summation is over the elements R in the group, and i, j = 1, ..., n_α

where n_α = dimension of the αth irreducible representation.

Thus, for a given value of j, the n_α functions $P_{ij}^{(\alpha)} \psi$ (where ψ is any arbitrary function) transform as a basis set for the αth irreducible representation of the group.

The double group at L (group D_{3d}) contains $2 \times 12 = 24$ operations. Six of these operations are R_1, R_5, R_9, R_{19}, R_{21}, and R_{23} (see Appendix Three). To each of these operations we add the inversion, which makes a total of twelve operations. Finally, because of spin, to each of these twelve operations, we apply an additional rotation of 2π which gives us a final total of 24 operations in all.

Now let us determine the projection operator for the representation L_4^+. Since this is a one dimensional representation the projection operator applied to a function, ψ, is

$$P\psi = \sum_R \chi^*(R)R\psi$$

But L_4^+ is even on inversion, so that adding this operation gives nothing new. Similarly, because spinors and the characters of the double-valued representations go into their negative upon rotations through 2π, these additional twelve operations may be ignored. Thus the final form of the projection operator for L_4^+ is

$$(A5-3) \qquad P = \sum_R \chi^*(R)R \qquad \text{(sum on only six elements: } R_1, R_5, R_9, R_{19}, R_{21}, R_{23})$$

The characters $\chi(R)$ for the representation L_4^+ are:

	R_1	R_5	R_9	R_{19}	R_{21}	R_{23}
L_4^+	1	-1	-1	i	i	i

$$\chi(JR_i) = \chi(R_i) \qquad J = \text{inversion}$$

$$\chi(\overline{R_i}) = -\chi(R_i)$$

To determine the effect of an operation on a spinor we use the matrices found by Slater.[14] The matrices for the spatial functions are generated by the APW wave functions at L_3. These matrices are given in Table A5-1.

TABLE A5-1

Basis functions for spinor operations are $S_1 = \alpha$, $S_2 = \beta$.

Basis functions for spatial operations are the APW functions φ_1 and φ_2 at L_3.

	Spinor Matrices	Spatial Matrices
R_1	$\begin{pmatrix} 1 & 0 \\ 0 & 1 \end{pmatrix}$	$\begin{pmatrix} 1 & 0 \\ 0 & 1 \end{pmatrix}$
R_5	$\begin{pmatrix} \dfrac{\omega^*}{\sqrt{2}} & \dfrac{-\omega}{\sqrt{2}} \\[2ex] \dfrac{\omega^*}{\sqrt{2}} & \dfrac{\omega}{\sqrt{2}} \end{pmatrix}$	$\begin{pmatrix} \dfrac{-1}{2} & \dfrac{\sqrt{3}}{2} \\[2ex] \dfrac{-\sqrt{3}}{2} & -1/2 \end{pmatrix}$
R_9	$\begin{pmatrix} \dfrac{\omega}{\sqrt{2}} & \dfrac{\omega}{\sqrt{2}} \\[2ex] \dfrac{-\omega^*}{\sqrt{2}} & \dfrac{\omega^*}{\sqrt{2}} \end{pmatrix}$	$\begin{pmatrix} \dfrac{-1}{2} & \dfrac{-\sqrt{3}}{2} \\[2ex] \dfrac{\sqrt{3}}{2} & -\dfrac{1}{2} \end{pmatrix}$
R_{19}	$\begin{pmatrix} \dfrac{-i}{\sqrt{2}} & \dfrac{1}{\sqrt{2}} \\[2ex] \dfrac{-1}{\sqrt{2}} & \dfrac{i}{\sqrt{2}} \end{pmatrix}$	$\begin{pmatrix} \dfrac{1}{2} & \dfrac{-\sqrt{3}}{2} \\[2ex] \dfrac{-\sqrt{3}}{2} & \dfrac{1}{2} \end{pmatrix}$
R_{21}	$\begin{pmatrix} \dfrac{i}{2} & \dfrac{-i}{\sqrt{2}} \\[2ex] \dfrac{i}{\sqrt{2}} & \dfrac{-i}{\sqrt{2}} \end{pmatrix}$	$\begin{pmatrix} \dfrac{1}{2} & \dfrac{\sqrt{3}}{2} \\[2ex] \dfrac{\sqrt{3}}{2} & -\dfrac{1}{2} \end{pmatrix}$
R_{23}	$\begin{pmatrix} 0 & -\omega^* \\ \omega & 0 \end{pmatrix}$	$\begin{pmatrix} -1 & 0 \\ 0 & 1 \end{pmatrix}$

where $\omega = e^{i\,\pi/4}$

The matrices in Table A5-1 are defined by

$$Rf_i = \sum_j \Gamma_{ji}(R) f_j \text{ where } f_i = i^{th} \text{ basis function}$$

For example, consider operation R_5:

<u>Spinors</u>

$$R_5\alpha = \frac{\omega^*\alpha}{\sqrt{2}} + \frac{\omega^*}{\sqrt{2}}\beta$$

$$R_5\beta = \frac{-\omega}{\sqrt{2}}\alpha + \frac{\omega}{\sqrt{2}}\beta$$

<u>Space</u>

$$R_5\varphi_1 = -\frac{1}{2}\varphi_1 - \frac{\sqrt{3}}{2}\varphi_2$$

$$R_5\varphi_2 = \frac{\sqrt{3}}{2}\varphi_1 - \frac{1}{2}\varphi_2$$

thus

$$R_5(\varphi_1\alpha) = (R_5\varphi_1)\cdot(R_5\alpha)$$

$$= \left(-\frac{1}{2}\varphi_1 - \frac{\sqrt{3}}{2}\varphi_2\right)\cdot\left(\frac{\omega^*\alpha}{\sqrt{2}} + \frac{\omega^*}{\sqrt{2}}\beta\right)$$

$$= \frac{-\omega^*}{2\sqrt{2}}\varphi_1\alpha - \frac{\sqrt{3}}{2\sqrt{2}}\varphi_2\alpha \quad \frac{-\omega^*}{2\sqrt{2}}\varphi_1\beta - \frac{\sqrt{3}}{2\sqrt{2}}\omega^*\varphi_2\beta$$

After performing these calculations for all six operations, and using equation A5-3 with the character table for L_4^+, we find that

$$P(\varphi_1\alpha) = P\psi_1 = \frac{3}{2}\psi_1 + b\psi_2 - \frac{3}{2}\omega^*\psi_3 + b\omega^*\psi_4 = \overline{\Psi}$$

$$P(\varphi_2\alpha) = P\psi_2 = \frac{3}{2}b^*\overline{\Psi}$$

$$P(\varphi_1\beta) = P\psi_3 = -\omega\overline{\Psi}$$

$$P(\varphi_2\beta) = P\psi_4 = b^*\overline{\Psi}$$

$$\text{where } b = \sqrt{\frac{3}{2}} - \sqrt{\frac{3}{2}}\ i$$

Thus, application of the projection operator for L_4^+ on any of our original functions ψ_1, ψ_2, ψ_3, ψ_4 gives us only one new function (within a constant factor). This is because the irreducible representation L_4^+ is one dimensional. The column vector corresponding to $\overline{\Psi}$

$$\begin{pmatrix} 3/2 \\ b \\ \frac{-3}{2}\omega^* \\ b\omega^* \end{pmatrix}$$

is an eigenvector of the spin orbit matrix (equation A5-1) with eigenvalue $+\lambda$. Since L_4^+ and L_5^+ are degenerate by time reversal, L_5^+ also has energy $+\lambda$. Consequently the doubly degenerate state L_6^+ has energy $-\lambda$.

As a check on our results, we can apply the time reversal operator

$$K = -i\,\sigma y\; Ko$$

$$\text{where}\quad \sigma y = \begin{pmatrix} 0 & -i \\ i & 0 \end{pmatrix}$$

$$Ko = \text{complex conjugation}$$

to our eigenfunction for L_4^+. The new function $K\bar{\psi}$ is the eigenfunction for L_5^+. We find that

$$K\,\bar{\psi} = \begin{pmatrix} \frac{3}{2}\,\omega \\ -b^*\omega \\ 3/2 \\ b^* \end{pmatrix}$$

is an eigenvector of the spin-orbit matrix with eigenvalue $+\lambda$ as required. We also verify that $\bar{\psi}$ and $K\bar{\psi}$ are orthogonal since they transform as basis functions for different irreducible representations:

$$(\bar{\psi},\ K\bar{\psi}) = \left[\frac{3}{2},\ b^*,\ -\frac{3}{2}\,\omega^*,\ b^*\omega \right] \begin{pmatrix} \frac{3}{2}\,\omega \\ -b^*\omega \\ \frac{3}{2} \\ b^* \end{pmatrix} = \frac{9}{4}\,\omega\ -b^{*2}\,\omega\ -\frac{9}{4}\,\omega + b^{*2}\,\omega$$

$$= 0$$

References

1. J. C. Slater, Phys. Rev., 51, 846 (1937).

2. J. H. Wood, Phys. Rev., 126, 517 (1962).

3. A. C. Switendick, M. I. T. Solid-State and Molecular Theory Group Quarterly Progress Report No. 49, July 15, 1962.

4. F. Herman and S. Skillman, Atomic Structure Calculations, Prentice-Hall, Inc. (1963).

5. A. C. Switendick, Doctoral Thesis M. I. T. (1963).

6. J. C. Slater and G. F. Koster, Phys. Rev., 94, 1498 (1954).

7. F. C. Brown, J. of Phys. Chem., 66, 2368 (1962).

8. Y. Okamoto, Nachrichten der Akadamie der Wissenschaften in Göttingen, 275 (1956).

9. J. Waber (Private Communication).

10. F. C. Brown, Op. Cit.

11. J. Zak, J. of Math. Phys., 3, 1278 (1962).

12. S. Yanagawa, Prog. of Theor. Phys., 10, 83 (1953).

13. R. J. Elliott, Phys. Rev., 96, 260, 280 (1954).

14. J. C. Slater, M. I. T. Solid-State and Molecular Theory Group Quarterly Progress Report No. 49, July 15, 1963.

Biographical Sketch

The author was born at Lakewood, New Jersey on March 8, 1938. He attended the public schools there, graduating from Lakewood High School in June of 1955. He majored in physics at M. I. T. and received the degree of Bachelor of Science in June of 1959. In the Fall of 1959 he entered the Graduate School of M. I. T. and began his graduate study.